6-1990

Linear free energy correlations of the effect of substituents on the cinnamaldehyde-bisulfite reaction

Susanne M. Hoff
Union College - Schenectady, NY

Recommended Citation

Hoff, Susanne M., "Linear free energy correlations of the effect of substituents on the cinnamaldehyde-bisulfite reaction" (1990). *Honors Theses*. 2029.
https://digitalworks.union.edu/theses/2029

LINEAR FREE ENERGY CORRELATIONS OF THE EFFECT OF SUBSTITUENTS ON THE CINNAMALDEHYDE-BISULFITE REACTION

by

Susanne M. Hoff

* * * * * * * * * * * * *

Submitted in partial fulfillment
of the requirements for
Honors in the Department of Chemistry

Union College

June, 1990

ABSTRACT

HOFF, SUSANNE Linear Free Energy Correlations of the Effect of Substituents on the Cinnamaldehyde-Bisulfite Reaction. Department of Chemistry, June 1990.

This thesis was primarily concerned with the correlation of the kinetics and equilibrium of the cinnamaldehyde-bisulfite reaction with the effect of ortho, meta, and para substituents. The cinnamaldehyde-bisulfite reaction is seen below:

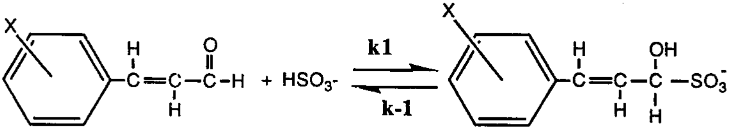

where X=p-NMe$_2$, p-MeO, p-Me, H, p-Cl, p-Br, p-NO$_2$, m-NO$_2$, m-Br, o-NO$_2$, and o-MeO.

The cinnamaldehydes were synthesized via a crossed aldol condensation reaction between acetaldehyde and the corresponding substituted benzaldehyde. The equilibrium constant and second order rate constant for the cinnamaldehyde-bisulfite reaction were determined through UV-visible spectroscopy.

The equilibrim and kinetics data was then correlated by Hammet's equation (log $K/KH=\rho\sigma°$) for the meta and para derivatives. In order to correlate the ortho derivatives, new σ values were derived using a least squares maniupulation of NMR ^{13}C chemical shifts.

ACKNOWLEGEMENT

As I finally finish this monster of a thesis, I would like to thank a few people and express a few wishes for some:

Professor Hull---without whom none of this would have been possible
Professor Werner and Professor Anderson---for encouraging me to pursue a graduate degree
Lee---for the "top ten"
J.C., Ed, Chris, and Lee---"Congratulations! You're done!"
Lynette, Gene, Chris, and Joe---"Good Luck and THANKS!"
Gene---see you at Berkeley
Marie--for all her help
John and Lisa---for support when I was really down

I would also like to acknowlege Dow Chemical Co. for a summer grant.

TABLE OF CONTENTS

Abstract---i

Table of Tables---iv

Table of Figures---v

Table of Spectra--x

Introduction--1

Experimental--15

Results---28

Discussion---54

References--84

Appendix A--86

Appendix B--106

Appendix C--136

TABLE OF TABLES

Rate and equilibrium constants for the reaction of bisulfite with substituted acetophenones---7

Summary of the results of LeTarte and Nicosia---8

Acetaldehyde used in synthesis of cinnamaldehydes--- 18

λmax, [Cinnmaldehyde], and [HSO3-] for Keq determination--- 25

Concentrations of bisulfite for kinetics runs--- 27

Ratio of cinnamaldehyde to benzaldehyde in synthesis--- 28

Physical data for synthesized cinnamaldehyde--- 29

C-13 NMR chemical shifts, ∂--- 36

Determination of the extinction coefficient of the p-nitro-cinnmaldehyde-bisulfite addtion product--- 41

Determination of the extinction coefficient of the o-nitro-cinnamaldehyde-bisulfite addtion product--- 42

Summary of equilibrium constants, Keq--- 45

[Cinnamaldehyde], [HSO3-], and k'--- 46

Summary of rate constants, k1 and k--- 52

Summary of equilibrium, kinetics, NMR, and σ data---53

Correlations matrix for meta and para substituents---58

Sources of various σ-values--- 59

Correlations matrix for all substiutuents including ortho---70

σ_{SH} values---73

ρ and R^2 values for correlations involving σ_{SH} values---79

TABLE OF FIGURES

1/A versus [HSO3-] for p-methoxycinnamaldehyde 40

1/A versus [HSO3-] for p-nitrocinnamaldehyde 40

A versus [ONC] for o-nitrocinnamaldehyde 43

A_2 versus C_2 for the bisulfite adduct of o-nitrocinnamaldehyde 43

1/A versus [HSO3-] for o-nitrocinnamaldehyde 43

ln[A-Ainf.] versus time, [HSO3-]=1.36e-3 M, for methoxycinnamaldehyde 47

ln[A-Ainf.] versus time, [HSO3-]=1.09e-3 M, for p-methoxycinnamaldehyde 47

ln[A-Ainf.] versus time, [HSO3-]=8.15e-4 M, for p-methoxycinnamaldehyde 47

ln[A-Ainf.] versus time, [HSO3-]=1.22e-3 M, for p-methoxycinnamaldehyde 48

ln[A-Ainf.] versus time, [HSO3-]=9.50e-4 M, for p-methoxycinnamaldehyde 48

ln[A-Ainf.] versus time, [HSO3-]=2.17e-3 M, for p-methoxycinnamaldehyde 48

k' versus [HSO3-] for p-methoxycinnamaldehyde 49

k' versus [HSO3-] for p-nitrocinnamaldehyde 49

log k/kH versus log K/KH 60

log K/KH versus σ° 60

log k/kH versus σ° 60

Resonance structures for cinnamaldehyde stabilization by an electron-donating group (p-MeO) 61

Proposed first transition state for the nucleophilic attack of bisulfite on cinnamaldehyde 62

Mechanism of the cinnamaldehyde-bisulfite reaction 63

log K/KH versus ∂C-∂CH 65

log k/kH versus ∂C-∂CH 65

Resonance structures of p-nitrocinnamaldehyde 66

∂C versus σ° 67

∂D versus $\sigma+$ 67

∂D-∂C versus $\sigma+$ 67

log K/KH versus σ_{SH} 74

log k/kH versus σ_{SH} 74

log K/KH versus σ_{SH} for the ionization of benzoic acids 76

log K/KH versus σ_{SH} for the ionization of *trans*-cinnamic acids 76

log K/KH versus σ_{SH} for the ionization of phenylacetic acids 76

log K/KH versus σ_{SH} for the ionization of phenoxyacetic acids 78

log k/kH versus σ_{SH} for the hydrolysis of phenylacetates 78

Potential energy diagram for the cinnamaldehyde-bisulfite reaction 80

Potential energy diagram for acid dissociation 81

1/A versus [HSO3-] for p-methylcinnamaldehyde 87

1/A versus [HSO3-] for m-nitrocinnamaldehyde 87

1/A versus [HSO3-] for p-bromocinnamaldehyde 87

1/A versus [HSO3-] for p-chlorocinnamaldehyde 88

1/A versus [HSO3-] for m-bromocinnamaldehyde---------------------------------88

1/A versus [HSO3-] for o-methoxycinnmaldehyde-------------------------------- 88

ln[A-Ainf.] versus time, [HSO3-]=8.45e-5 M, for
p-nitrocinnamaldehyde-- 89

ln[A-Ainf.] versus time, [HSO3-]=2.81e-4 M, for
p-nitrocinnamaldehyde-- 89

ln[A-Ainf.] versus time, [HSO3-]=1.69e-4 M, for
p-nitrocinnamaldehyde-- 89

ln[A-Ainf.] versus time, [HSO3-]=5.58e-4 M, for
o-nitrocinnamaldehyde-- 90

ln[A-Ainf.] versus time, [HSO3-]=8.34e-4 M, for
o-nitrocinnamaldehyde-- 90

ln[A-Ainf.] versus time, [HSO3-]=6.97e-4 M, for
o-nitrocinnamaldehyde-- 90

k' versus [HSO3-] for o-nitrocinnamaldehyde------------------------------------ 91

ln[A-Ainf.] versus time, [HSO3-]=2.77e-4 M, for
m-nitrocinnamaldehyde-- 92

ln[A-Ainf.] versus time, [HSO3-]=4.15e-4 M, for
m-nitrocinnamaldehyde-- 92

ln[A-Ainf.] versus time, [HSO3-]=5.54e-4 M, for
m-nitrocinnamaldehyde-- 92

ln[A-Ainf.] versus time, [HSO3-]=8.30e-4 M, for
m-nitrocinnamaldehyde-- 93

k' versus [HSO3-] for m-nitrocinnamaldehyde------------------------------------93

ln[A-Ainf.] versus time, [HSO3-]=2.60e-4 M, for
m-bromocinnamaldehyde---94

ln[A-Ainf.] versus time, [HSO3-]=1.30e-4 M, for
m-bromocinnamaldehyde---94

ln[A-Ainf.] versus time, [HSO3-]=3.90e-4 M, for
m-bromocinnamaldehyde---94

k' versus [HSO3-] for m-bromocinnamaldehyde----------------------------------95 ln[A-Ainf.] versus time, [HSO3-]=1.11e-3 M, for o-methoxycinnamaldehyde------96

ln[A-Ainf.] versus time, [HSO3-]=8.31e-4 M, for o-methoxycinnamaldehyde------96

ln[A-Ainf.] versus time, [HSO3-]=5.54e-4 M, for o-methoxycinnamaldehyde------96

k' versus [HSO3-] for o-methoxycinnamaldehyde------97

ln[A-Ainf.] versus time, [HSO3-]=2.81e-4 M, for p-bromocinnamaldehyde------98

ln[A-Ainf.] versus time, [HSO3-]=5.62e-4 M, for p-bromocinnamaldehyde------98

ln[A-Ainf.] versus time, [HSO3-]=8.43e-4 M, for p-bromocinnamaldehyde------98

k' versus [HSO3-] for p-bromocinnamaldehyde------99

ln[A-Ainf.] versus time, [HSO3-]=5.38e-4 M, for p-chlorocinnamaldehyde------100

ln[A-Ainf.] versus time, [HSO3-]=2.69e-4 M, for p-chlorocinnamaldehyde------100

ln[A-Ainf.] versus time, [HSO3-]=1.35e-4 M, for p-chlorocinnamaldehyde------100

k' versus [HSO3-] for p-chlorocinnamaldehyde------101

ln[A-Ainf.] versus time, [HSO3-]=1.61e-3 M, for p-methylcinnamaldehyde------102

ln[A-Ainf.] versus time, [HSO3-]=1.01e-3 M, for p-methylcinnamaldehyde------102

ln[A-Ainf.] versus time, [HSO3-]=2.01e-3 M, for p-methylcinnamaldehyde------102

k' versus [HSO3-] for p-methylcinnamaldehyde------103

ln[A-Ainf.] versus time, [HSO3-]=8.43e-4 M, for *trans*-cinnamaldehyde------104

ln[A-Ainf.] versus time, [HSO3-]=5.62e-4 M, for *trans*-cinnamaldehyde------104 ln[A-Ainf.] versus time, [HSO3-]=1.12e-3 M, for *trans* -cinnamaldehyde---------- 104

k' versus [HSO3-] for *trans* -cinnamaldehyde---------- 105

TABLE OF SPECTRA

1H NMR of p-methoxycinnamaldehyde---31
1H NMR of m-nitrocinnamaldehyde---33
1H NMR of o-methoxycinnamaldehyde---35
1H NMR of p-dimethylaminocinnamaldehyde--------------------------------------- 107
1H NMR of p-methylcinnamaldehyde--- 108
1H NMR of trans-cinnamaldehyde--- 109
1H NMR of o-nitrocinnamaldehyde--- 110
1H NMR of p-nitrocinnamaldehyde--- 111
1H NMR of p-chlorocinnamaldehyde--- 112
1H NMR of m-bromocinnamaldehyde---113
1H NMR of p-bromocinnamaldehyde---114
^{13}C NMR of p-dimethylaminocinnamaldehyde---------------------------------------115
^{13}C NMR of p-methoxycinnamaldehyde--- 116
^{13}C NMR of p-methyxcinnamaldehyde---117
^{13}C NMR of trans-cinnamaldehyde---118
^{13}C NMR of o-nitrocinnamaldehyde---119
^{13}C NMR of p-nitrocinnamaldehyde---120
^{13}C NMR of p-chlorocinnamaldehyde--- 121
^{13}C NMR of o-methoxycinnamaldehyde--- 122
^{13}C NMR of m-bromocinnamaldehyde--- 123
^{13}C NMR of m-nitrocinnamaldehyde---124

^{13}C NMR of p-bromocinnamaldehyde-- 125

APT of m-bromocinnamaldehyde-- 126

HETCOR of p-dimethylaminocinnamaldehyde--------------------------------------127

HETCOR of p-methoxycinnamaldehyde--- 128

HETCOR of o-nitrocinnamaldehyde-- 129

HETCOR of p-methylcinnamaldehyde-- 130

HETCOR of p-nitrocinnamaldehyde--131

HETCOR of m-bromocinnamaldehyde--132

HETCOR of o-methoxycinnamaldehyde-- 133

HETCOR of m-nitrocinnamaldehyde-- 134

HETCOR of p-bromocinnamaldehyde--135

UV-VIS spectra of o-nitrocinnamaldehyde-------------------------------------- 137

UV-VIS spectra of o-methoxycinnamaldehyde-------------------------------138

UV-VIS spectra of p-bromocinnamaldehyde--------------------------------- 139

UV-VIS spectra of m-nitrocinnamaldehyde---------------------------------- 140

UV-VIS spectra of p-nitrocinnamaldehyde-------------------------------------141

UV-VIS spectra of p-methoxycinnamaldehyde-------------------------------142

UV-VIS spectra of m-bromocinnamaldehyde-------------------------------143

UV-VIS spectra of p-methylcinnamaldehyde-------------------------------- 144

UV-VIS spectra of p-chlorocinnamaldehyde--------------------------------145

INTRODUCTION

The Bisulfite-Addition Reaction:

Since the 1960s, there has been growing concern over the problem of increasing acidity of precipitation on the environment. It is believed that this acidity arises from the oxidation of SO_2 and various oxides of nitrogen (NOx) produced by coal and oil burning plants and from motor vehicle exhaust (1). These oxides are then oxidized to sulfuric and nitric acids which precipitate to do damage to the natural environment. Understanding the complex atmospheric processes is important in the efforts to alleviate this growing problem.

We are primarily concerned with the reactions of aqueous sulfur dioxide in this work. As sulfur dioxide is dissolved into the aqueous phase, it equilibrates between three species as follows:

$$SO_2 \text{ ---->} SO_2 \cdot H_2O + HSO_3^- + SO_3^{2-} \quad \text{(Rxn 1)}$$

However, between pH 2-6, the predominant species present is bisulfite (2).

The sulfur dioxide oxidation can be represented as a chemical reaction as follows: S(IV) --> S(VI), where the numbers represent the oxidation state of the sulfur. This oxidation can take place in several phases: gas, liquid, and through reaction on the surface of solid particles in the atmosphere (1). While most scientists agree that the gaseous and liquid phases are the more important of the three phases, there is some question as to which phase most of the oxidation of the S(IV) species takes place. However, Finlason-Pitts and Pitts have postulated that 90% of the oxidation takes place in the aqueous phase (2). In the aqueous phase there are three possible oxidants: oxygen catalyzed by trace metals in the atmosphere, ozone, and hydrogen peroxide. Finlason-Pitts and Pitts believe that hydrogen peroxide is the most important of these oxidants in the aqueous phase. Their evidence for this conclusion is the higher solubility of H_2O_2 and the relatively faster production of S(VI) by this pathway. If we assume that S(IV) oxidation takes place in the aqueous phase and through the action of hydrogen peroxide, than the total process of dissolution and oxidation can be represented as follows:

$$SO_2(g) \text{ ----> } HSO_3\text{-}(aq) + H^+(aq) \quad \text{(Rxn. 2)}$$

$$S(IV)(aq) + H_2O_2(aq) \text{ ----> } S(VI)(aq) + H_2O(l) \quad \text{(Rxn 3)}$$

These reactions, however, are not the grand total of all processes taking place in the atmosphere. Also present in the atmosphere are various carbonyl species. These carbonyl species can form an adduct with bisulfite through nucleophilic attack of the negatively charged bisulfite ion on the carbonyl carbon forming a chiral center. The reaction is represented below:

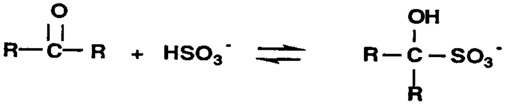

$$R-\overset{\overset{O}{||}}{C}-R + HSO_3^- \rightleftharpoons R-\underset{R}{\overset{OH}{C}}-SO_3^-$$

(Rxn. 4)

where R=alkyl group or H (2). The effect of removing bisulfite through adduct formation can be examined through a simple LeChatlier approach. If we examine equation 2 above, we see that removing bisulfite will cause the reaction to shift towards further dissolution of the S(IV) within the aqueous phase (3). Indeed, Munger found concentrations of S(IV) in cloud and fog water in California to be far in excess of that expected from the gaseous concentrations of S(IV) in the atmosphere (3).

Several scientist have confirmed the presence of carbonyls in the atmosphere. Schulam, Newbold and Hull measured aldehyde levels for the Schenectady, New York and found significant levels of formaldehyde and acetaldehyde (4). Amounts of formaldehyde in urban Schenectady ranged from 0.7 to 30.5 ppb while amounts of acetaldehyde were much lower. The group also measured aldehyde levels on Whiteface Mtn. in Wilmington, NY and found the formaldehyde levels ranged from 0.6 to only 2.6 ppb. This lower range for rural Whiteface Mtn. is expected from the lower amounts of pollution sources in Wilmington versus Schenectady. The group found that peaks in the daily concentrations of formaldehyde correlated well with traffic patterns with a peak in early morning and one in late evening.

Grosjean found that S(IV) levels measured in Los Angeles cloud water were higher than expected even taking into account the formaldehyde levels (5). He thus concluded that higher aldehydes and ketones must also be present. He found the presence of formaldehyde (up to 48ppb), acetaldehyde (≤35 ppb), propanal (≤14 ppb), butanal (≤7 ppb), 2-butanone (≤14 ppb) and benzaldehyde (≤1 ppb). He also found that the total carbonyl level in Claremont reached a maxima when LA smog fronts hit Claremont, confirming pollution as a source of carbonyls in the atmosphere. Munger postulated that the two largest sources of carbonyls in the atmosphere are combustion and photochemical oxidation of hydrocarbons present in the atmosphere.

What effect can the formation of these bisulfite-adducts have on the oxidation of S(IV)? We have already pointed out that the formation of these adducts leads to a heightened level of S(IV) within the cloud. However the rate of oxidation of S(IV) to S(VI) is much faster than the rate of adduct formation. Richards found that the lifetime of S(IV) in the presence of >40μM H_2O_2 is less than one second. Jacob and Hoffmann, on the other hand, found that Keq for the formation of the bisulfite addition product of formaldehyde (HMSA) is 75,000 M-1 at 298 K. Thus reaction 4 cannot compete kinetically with the irreversible reaction 3. However, the bisulfite adducts formed via reaction 4 are stable to oxidation by hydrogen peroxide (2). Thus, the oxidation of S(IV) is inhibited since the reverse of reaction 4 is very slow (k^{-1} for HMSA= 4x 10^{-5} s^{-1}) (6). Richards found further evidence for the inhibition of reaction 3 by bisulfite-adduct formation. He found that H_2O_2 and S(IV) to be coexistant for over an hour in the presence of carbonyls (7).

Clearly, the kinetics and equilibrium of reaction 4 are important in determining how important a particular carbonyl will be in inhibiting the oxidation of S(IV). We will be primarily concerned with the equilibrium and kinetics of a series of substituted trans-cinnamaldehydes.

The equilibrium constant and the foward rate constant were determined by UV-visible spectroscopy by the method used by LeTarte (8). The method used was similar to one used to determine Keq for the addition of bisulfite to benzaldehyde developed by Kokesh and Hall (9). The method takes advantage of the fact that the aldehydes absorb at a longer wavelength than their bisulfite-addition products. Using their method, the decrease in absorbance of the aldehyde in buffer solution is followed at its wavelength maxima for several bisulfite additions. This method assumes that there is no absorbance of buffer or bisulfite at the wavelengths of interest. It also assumes that bisulfite is in excess at all times in which they are coexistant in solution.

Adherence to Beer's Law is necessary for use of this method. Plots of absorbance versus concentration of aldehyde were made for several of the aldehydes and were found to be linear.

L. LeTarte derived equations for the determination of Keq, the equilibrium constant and k1, the foward rate constant (8). Keq was determined from a plot of the following equation (as developed by Kokesh and Hall):

$$1/A = K_{eq}\ [B] / \varepsilon\ [A] + 1 / \varepsilon\ [A]$$

where A is the absorbance at equilibrium, Keq is the equilibrium constant, [B] is the bisulfite concentration, [A] is the aldehyde concentration and ε is the extinction constant of the aldehyde. 1/A for a series of bisulfite additions is plotted against the concentration of bisulfite at time of injection to yield a linear graph. Keq is determined by dividing the slope by the intercept.

The foward rate constant, k_1, was determined by following the decrease in absorbance of the aldehyde with respect to time after an injection of excess bisulfite. A value for the pseudo first-order rate constant, k', can be determined from the following equation:

$$k' = -\mathrm{slope}(A_o - A_{inf.}) / A_o$$

where A_o is the intial absorbance of aldehyde before addtion of bisulfite, $A_{inf.}$ is the absorbance at equilibrium, and the slope is the slope of a plot of $\ln[A - A_{inf.}]$ versus time in seconds. The second-order rate constant, k_1, can be determined from the pseudo first-order rate equation:

$$\mathrm{rate} = k'[A], \quad \text{where } k' = k_1\ [B]$$

Thus k1 is determined from a plot of k' versus concentration of bisulfite. The reverse rate constant, k-1, is determined from the following equation:

$$k_{-1} = k_1 / Keq$$

Substituent Effects:

Scientists have long been concerned with the ability of substituents to sterically and electronically effect the equilibrium and kinetics of a particular reaction. In 1937, L. P. Hammett examined the effect of substituents on the equilibrium and kinetics on a series of substituted benzoic acids (10). He derived the following equation (now called the Hammett equation) from free-energy equations to express the effect of substituents on a reaction site in the molecule:

$$\log K/Ko = \sigma \rho$$

where K is the equilibrium or rate constant of a substituted molecule, Ko is the equilibrium or rate constant of the unsubstituted species, σ is a measure of the electronic effect of the substituent, and ρ is a measure of the sensitivity of the reaction to these substituents. Hammett defined his sigma values to be based on the dissociation of benzoic acids, thus involving both inductive and resonance effects. Sigma values are negative for electron-donating substitutents and positive for electron-withdrawing substituents. Hydrogen has a sigma value of zero. Since the equilibrium or rate constant of a reaction should correlate with the substitutent effect, a plot of log K/Ko versus σ (Hammett's plot) should be linear with a slope of ρ. ρ was defined by Hammett to be 1.000 for the dissociation of benzoic acids.

We will be mostly concerned with the inductive and resonance effects of various substituents on the addition of bisulfite to trans-cinnamaldehyde. Trans-cinnamaldehyde was chosen for several reasons. Due to its extensive conjugation, trans-cinnamaldehyde and its substituted forms absorb at convenient wavelengths (291 nm for trans-cinnamaldehyde) where absorbance of the buffer or bisulfite cannot interfere. Its high extinction coeffient, 25,400, enables the equilibrium and kinetic data to be determined from a small (10^{-5}M) concentration of the aldehyde. Finally, the reaction site in t-cinnamaldehyde is separated by a large distance from the aromatic ring. Thus, steric effects should not be operating at the para, meta, or, perhaps, the ortho positions. At the same time, the extensive conjugation of the molecule should transmit the electronic effect to a measurable extent.

Table 1: Rate and Equilibrium Constants for the Reaction of Bisulfite with Substituted Acetophenones

Substituent	Keq/M-1	k1/M-1 s-1
p-OCH3	1	23
p-CH3	3	46
H	5.5	77
p-Cl	8	192
p-Br	9	228
m-Br	16	384
p-NO2	44	1900

A similar study to this one was done by Young and Jencks on the addition of bisulfite to substituted acetophenones. Table 1 shows the results of this study (12). Clearly, Keq increases for more electron-withdrawing substituents. The carbonyl carbon of acetophenone is partially positive and would be stabilized by electron-donating substituents, while electron-withdrawing substituents would destabilize acetophenone and cause it to become more reactive.

Similar results were obtained by L. LeTarte and L. Nicosia for the addition of bisulfite to p-dimethylamino, p-nitro, and trans-cinnamaldehyde. Their results are shown in Table 2:

Table 2: Summary of the results of LeTarte and Nicosia

Substituent	Keq/M-1	k1/M-1 s-1
p-N(Me)2	299	4.0
H	1030	25
p-NO2	1340	42

L. Nicosia justified the trend toward increasing Keq for more electron-withdrawing substituents from a slightly different viewpoint. She postulated that, since the attacking species is negatively charged, the electron-withdrawing substituents could stabilize the transition state, causing the higher Keq and k1(11). Both arguments can be equally justified.

There are several different ways in which a substituent can influence the kinetics or equilibrium of a reaction. The first is by direct conjugative interactions. These are resonance effects arising from a delocalization of electron density between the substituent and the reactant site. Conjugative effects are found only for molecules in which there are direct resonance interactions with the reaction site. The second way in which a substituent can influence a reaction is by polar effects. Polar effects have two contributions, one from resonance and one from inductance. The polar effects arising from resonance contributions do not directly involve the reaction site but instead involve only part of the aromatic system. The inductive contribution has to do with the electronegative or electropositive character of the atom of the substituent which is directly attached to the aromatic system. Ortho substituents can effect the reaction in additional ways due to their close proximity to the reaction site. These additional effects are collectively known as proximity effects and include such interactions such as steric retardation of reactant attack, nonplanar effects, and enhanced electrostatic interactions (13). Many different values of σ have been derived by chemists to obtain the optimum correlation for their particular reaction series and thus, to obtain the most accurate value for ρ. It has already been mentioned that σ values were derived from the dissociation of benzoic acids. σ^o values, derived by Taft, were derived from a select set of m-derivatives in which at least one methylene group insulated the reaction site from the rest of the molecule (13). These σ^o values are free of conjugative effects and reflect polar effects. σ^n values are virtually the same as σ^o values. $\sigma+$ values were derived by Brown and Okamoto from the solvolysis of para-substituted t-cumyl chlorides in 90% aqueous acetone (10). The product of this reaction has a formal +1 charge on the cumyl carbon which can be resonance stabilized by electron-donating substituents to a large extent. Thus $\sigma+$ values are used in reactions where a charge is developed and can be stabilized by conjugative interactions.

Young and Jencks obtained the best correlation of their data by using a modified Yukawa-Tsuno equation, using σ^n and $\sigma+$ values (12). This method allowed them to use sigma values between σ^n and $\sigma+$. In other words, this method allowed them to vary the sensitivity of the reaction to polar effects, σ^n values, and conjugative effects, $\sigma+$ values.

Many researchers have also attempted to correlate NMR chemical shifts with substituent constants in an attempt to evaluate resonance and inductive effects. Taft and coworkers concentrated on the correlation of m- and p-substituted fluorobenzenes with

σ_R and σ_I values (14,15). Since the effect of substituents on ^{19}F nuclear magnetic shielding is very large, the ^{19}F chemical shifts can be quite accurately measured. The chemical shifts of the substituted fluorobenzenes were referenced to the chemical shift of unsubstituted fluorobenzene by simply substracting the chemical shifts. Taft found that the chemical shifts of m-substituted fluorobenzenes correlated very well with his σ_I substituent constants (14). In an attempt to separate inductive and resonance effects, Taft and Lewis proposed the following equations from experimental equilibrium and kinetics data on aliphatic systems, $\sigma_m = \sigma_I + \alpha\ \sigma_R$ and $\sigma_p = \sigma_I + \sigma_R$, where σ_I represents the inductive effect of a substituent, σ_R accounts for the resonance effect of a substituent, and α accounts for the lower amount of resonance effects involved in m-substituted substrates. He thus concluded that meta substituents contribute to reactivity mostly by inductance.

In a later study, Taft studied the ^{19}F chemical shifts of p-substituted benzenes (15). He found that the best correlation was obtained from a plot of the difference between para and meta ^{19}F chemical shifts versus σ_R. He concluded that the amount of inductive effect in p-substituted fluorobenzenes is nearly the same for that in m-substituted fluorobenzenes. Thus by substracting the chemical shifts, Taft, in effect, canceled out the inductive effect of the p-substituents to yield mostly resonance effects; hence, the good correlation with σ_R values.

Maciel and Natterstad examined the ^{13}C chemical shifts of ring carbons in monosubstituted benzenes (16). Among the ring carbons studied were the carbon at which the substituent was attached and the ortho, meta and para ring carbons. They found that the substituted carbon atom experienced the largest chemical shift (more than 70 ppm). They attributed this to the large polar and conjugative effects of the attached substituent, as well as the "neighbor anisotropy" effect (or magnetic effects due to the substituents). The usefulness of this carbon shift is limited due to the difficulty in separating the electronic effects from the magnetic effects. They also concluded that all these effects are important at the ortho carbon (chemical shifts in the range of 26 ppm), thereby compromising its usefulness. The range of chemical shifts for the meta ring carbons were on the order of 4.0 ppm, while those for the para ring carbons were about 20 ppm. Maciel and Natterstad concluded that the meta and para carbons both were probably free from magnetic effects. They postulated that the meta carbon chemical shifts could probably be interpreted in terms of polar effects and that, due to their distance from the substitution position, the para carbon chemical shifs could be interpreted as conjugative effects. In a comparison of plots of δp versus σ_R and δp-δm (where the chemical shift of the para ring carbon is corrected by the meta carbon chemical shift) versus σ_R, significantly better correlations were obtained from the δp-δm plot, although both plots yielded linear correlations. This indicates that some of the electronic effect effect of the substituent is felt through polar effects by the para carbon.

In our work, we wish to examine the correlation of ^{13}C chemical shifs of various carbons in cinnamaldehyde versus different substituent constants and versus log K/K_o and log k/k_o as obtained from the equilibrium and kinetics determinations from the bisulfite-addition reaction. The carbons that will be examined are shown in the diagram below:

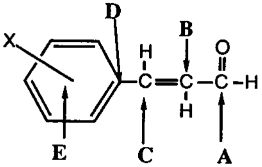

The E carbon we would expect to experience the largest chemical shifts; however, as was concluded by Maciel and Natterstad, the usefulness of this carbon is limited by potential magnetic effects. By writing resonance structures for a substituted t-cinnamaldehyde, we can gauge the distribution of influence due to conjugative effects. The pertinent resonance forms of p-nitrocinnamadehyde are seen below:

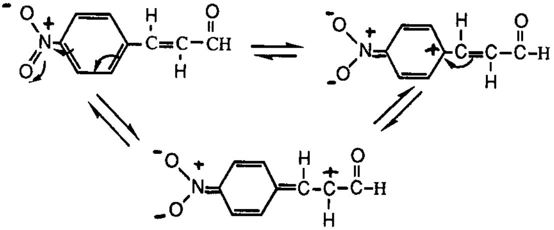

As can be seen, the positive charge is delocalized onto the B and D carbons. Thus these ^{13}C shifts should be due mostly to conjugative effects, although the B carbon is so far distanced from the substituent site that the ^{13}C shifts will be smaller with more room for error. The C carbon never has the positive charge delocalized onto it; therefore, the corresponding chemical shifts should be influenced mostly by polar substituent effects. ^{13}C chemical shift of the A carbon should also be influenced by polar effects but to a much smaller extent than those from the C carbon due to the relatively larger distance of the A carbon from the substituent. In conclusion, correlations will be made between these ^{13}C chemical shifts and the equilibrium and kinetic experimental data, as well as various substituent constants. In this way, we hope to gain a complete picture of the influence of substituents on not only the bisulfite-cinnamaldehyde reaction, but on ^{13}C NMR chemical shifts.

Synthesis of substituted t-cinnamaldehydes:

o-Nitrocinnamaldeyde, p-nitrocinnamaldehyde, and t-cinnamaldehyde were obtained from the Aldrich Chemical Co. The remainder of the aldehydes were synthesized by a crossed aldol condensation reaction between acetaldehyde and the corresponding substituted benzaldehyde:

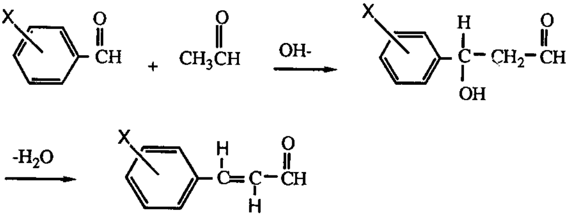

where X is the substituent. The alpha hydrogen of the acetaldehyde is pulled off by the sodium hydroxide. The anion produced by this step then attacks the carbonyl carbon of the benzaldehyde to form the hydroxyl intermediate. The final step is the loss of a molecule of water to form the double bond. This last step usually proceeds without any help due to the highly stable conjugated system which is formed.

Physical data for all para, meta, and ortho substituted cinnamaldehydes by the aldol condensation reaction was found in Beilstein. The first cinnamaldehyde synthesized was p-methylcinnamaldehyde. The original synthesis was done in 1884. This synthesis was modified and used for the synthesis of p-methyl, p-chloro, p-bromo, and p-methoxycinnamaldehyde (18).

m-Nitrocinnamaldehyde was obtained from a scaled down version of the procedure of Markovac (19). This procedure was scaled down by a factor of 250 and used virtually unchanged.

EXPERIMENTAL

SOLUTIONS

Buffer:

A 1.0 M, 1:1 acetic acid: sodium acetate buffer of pH=4.63 was used to maintain a constant pH and an ionic strength of 1.0 during the equilibrium and kinetics measurements. 82 g of sodium acetate was weighed directly into a 1 L volumetric flask and one mole of acetic acid was pipetted into the flask. The flask was then diluted almost to the mark with deionized water. The pH was then adjusted from the 4.80 intial reading to 4.63 by the addition of concentrated HCl. The flask was then diluted to the mark and the pH checked again. The buffer solution was stored in a 1 L bottle. The sodium acetate/acetic acid buffer was chosen because it does not absorb strongly at the wavelengths of interest in this project.

Sodium bisulfite:

A stock solution of approximately 0.8 M $NaHSO_3$ was made by weighing 41.625g of $NaHSO_3$ directly into a 500 ml volumetric flask and diluting to the mark with deionized water. This solution was titrated with a 0.100 M iodine solution to determine its exact molarity. To prevent the oxidation of the S(IV) species to S(VI), the stock bisulfite solution was stored under nitrogen and tightly sealed with paraffin. Under these conditions, the concentration of the solution changed very little. The solution was retitrated approximately every month. For the equilibrium and kinetic determinations, solutions on the order of 8×10^{-2}M were needed. Since these dilute solutions are easily oxidized, they were prepared daily by pipetting 1 ml of stock sodium bisulfite into a 10 ml volumetric flask and diluting to the mark with deionized water. These solutions were stored in brown glass vials under nitrogen at -4°C.

Standard Iodine Solution:

To dissolve iodine in water, a 10:1 I^-: I_2 solution was made. 183g of potassium iodide was weighed directly into a 1 L volumetric flask and then, 500 ml of deionized water was added. 25.38 g of I_2 was then weighed into the the KI solution. The flask was then diluted to the mark with deionized water. A stirring bar was added to the flask and the solution was stirred vigorously to ensure dissolvation of all the iodine. The solution was tightly sealed with paraffin.

Titration of the Bisulfite Stock:

5.00 ml of the stock sodium bisulfite solution was pipetted into a 50 ml volumetric flask. A stirring bar and 2-3 drops of starch indicator were added and the flask was sealed with paraffin film. The solution was then acidified to pH 2 by the addition of several drops of sulfuric acid through the paraffin cover. The solution was then titrated with the 0.100 M iodine standard with vigorous stirring until the violet starch endpoint was reached. Three titrations were usually carried out and then an average was taken. If this procedure was not followed, inaccurate and inprecise results were obtained.

Aldehyde Solutions:

Solutions of the t-cinnamaldehydes on the order of 10^{-2} M were needed for the UV-VIS spectroscopic determinations. These solutions were made by weighing the aldehyde directly into a 10 ml volumetric flask and then diluting with ethanol. However, since o-nitrocinnamaldehyde was not soluble in ethanol, it was dissolved in dioxane by the same procedure. t-Cinnamaldehyde, p-nitrocinnamaldehye, o-nitrocinnamaldehyde, and o-methoxycinnamaldehyde were available from the Aldrich Chemical Co. The purity of these compounds was checked by NMR analysis. The other aldehydes used were synthesized. The purity of the end product was checked by NMR and by melting point determinations. The aldehyde solutions were stored in small, brown glass bottles under nitrogen at -4°C.

INSTRUMENTATION

All absorbances and absorbance spectra were taken on a Perkin-Elmer Lambda 3B absorption spectrophotometer interfaced with a Perkin-Elmer 3600 microcomputer. Silica absorption cells (1.000 cm) were used throughout the absorbance experiments. The temperature within the cell compartment in the spectrophotometer was controlled by a Neslab Endcol RT-9 refrigerated circulating bath. The actual temperature of the solution within the cells was taken using an Orion 871 thermometer. Absorption scans taken of the aldehyde during the equilibrium determinations were taken using a Perkin-Elmer program called IFL3. The program used to collect data for the foward rate constant determination was called KINS. The timer used to determine the time of injection of bisulfite solution during the kinetics determinations was a GCA/Precision Scientific timer.

All HPLC separations were done on a Varian Model 5000 HPLC with self-contained 256 nm UV absorption detector. The HPLC, in addition, was attached to a Tracor 970A variable wavelength detector.

The pH determination for the buffer solution was done on a Orion 701A Digital Ionalyzer.

All ^1H and ^{13}C NMR spectra were obtained on a Varian Gemini 200 MHz NMR. All NMR spectra were plotted on a Hewlett-Packard 7574A plotter.

SYNTHESIS OF ALDEHYDES

The acetaldehyde and each of the benzaldehydes were analyzed for purity by NMR spectroscopy. The benzaldehydes were obtained from the Aldrich Chemical Co. A solution of 10% NaOH was made by weighing 10 g of NaOH into a 100 ml volumetric and diluting with deionized water. Table 1 summarizes the amount of acetaldehyde used in the synthesis of each cinnamaldehyde:

Table 3: Acetaldehyde used in Synthesis of Cinnamaldehydes

Substituent	Acetaldehyde/g
p-Methyl	0.367
p-Chloro	0.313
p-Bromo	0.250
p-Methoxy	0.323
m-Nitro	1.053
m-Bromo	0.520

*The benzaldehyde and acetaldehyde were present in a 1:1 mole ratio so the amount of acetaldehyde varied from synthesis to synthesis.

p-Chlorocinnamaldehyde:

The reaction gave the best yields when a 1:1 mole ratio of benzaldehyde to acetaldehyde was used.

The reaction was carried out in a 250-ml three-necked flask, with a condenser off the left neck, a thermometer off the right neck and a separatory funnel in the center. 1.00 g of p-chlorocinnamaldehyde was dissolved in 8.0 g of ethanol. To this was added 0.700 g of the 10% NaOH solution. This solution was then placed directly in the three-necked flask along with a stirring bar. The acetaldehyde (see Table 3 for amount) was weighed directly into the 40 g of water and quickly stoppered to prevent evaporation of the volatile acetaldehyde. This mixture was then added to the separatory funnel and stoppered with a glass stopper. The temperature of the experiment was kept constant at 40-45°C by a heated water bath. The acetaldehyde-water solution was added every half-hour in equal portions over four hours with vigorous stirring. At the end this time, an additional hour was allowed for the further reaction of the benzaldehyde. After five hours, the stirring and heating were discontinued and the reaction mixture was saturated with NaCl. The mixture was then added to a separatory funnel and washed three times with 25 ml of diethylether. The bright yellow ether solution was then allowed to dry over magnesium sulfate for a half-hour. The solution was filtered into a 250-ml round-bottom flask to remove any magnesium sulfate. To strip off the ether, a rotary evaporation was used.

Due to the high ratio of cinnamaldehyde to benzaldehyde obtained from the synthesis, p-chlorocinnamaldehyde crystallized from the crude aldehyde mixture immediately following the removal of the ether by rotary evaporation. The solid p-chlorocinnamaldehyde was dissolved in about five mililiters of ethanol and deionized water was added dropwise until a cloudy solution was obtained. The beaker was then inserted in an ice bath. Scratching of the bottom of the beaker with a glass stirring rod induced rapid crystallization. The crystals were filtered by Buchner funnel and allowed to dry. Approximately half of these crystals were then recrystallized from about 2.5 ml ethanol-water. The crystals were filtered by Hirsch funnel and allowed to dry overnight in a dessicator. The purity of these crystals was confirmed by melting point and NMR.

p-Bromocinnamaldehyde:

For the synthesis of p-bromocinnamaldehyde, the procedure for the synthesis of p-chlorocinnamaldehyde was followed except that 15.0 g of ethanol was used to dissolve the aldehyde due to its lower solubility. p-Bromocinnamaldehyde was isolated and purified by much the same method as that used for p-chlorocinnamaldehyde. The first crystallization was done from an ethanol-water couple while, for the second recrystallization, a hexane-ethyl acetate couple was used.

p-Methylcinnamaldehyde:

Using the same procedure outlined for p-chlorocinnamaldehyde, p-methylcinnamaldehyde was synthesized. However, p-methylcinnamaldehyde did not crystallize from either a ethanol-water couple or a hexane-ethyl acetate couple. The p-methylcinnamaldehyde was instead isolated by chromatography. A column chromatography experiment was set up using a silica-gel column. To make the column, a slurry of silica-gel and hexane was made and poured into the column. In this way, extensive channeling in the column was avoided. Approximately 0.5 g of the crude p-methylcinnamaldehyde (PMC) mixture was pipetted into the column and 50 ml of hexane was passed through the column. The mobile phase was then increased from 25% ether-hexane to 100% ether. Once the yellow band reached the bottom of the column, eleven 10 ml fractions were taken. ^{1}H NMR spectra taken of the fractions showed that fractions 4-6 contained the highest ratio of PMC to p-methylbenzaldehyde, approximately 6:1.

Fractions 4-6 were combined and 1 ml of a 0.1 M solution of PMC in acetonitrile was made by weighing the column chromatography mixture directly into a glass vial and pipetting one milliliter of acetonitrile into the vial. This solution was used for an HPLC isolation. The HPLC was programmed to run from 55% to 65% acetonitrile-water over a 10 minute period with a flow rate of 1.5 ml/min. The absorption detectors were set at 256 nm and 300 nm. An absorption at 256 nm with a retention time of 5.1 minutes was attributed to the p-tolylaldehyde while a very strong absorption at 300 nm with a retention time of 6.3 minutes was attributed to PMC. The fractions collected at 6.3 minutes in the HPLC run (~1 ml) were used for the UV-Vis determinations.

To determine the melting point of PMC and to obtain an NMR, crystals were needed. Another column chromatography experiment was set-up. This time, a alumina-gel column was used with a hexane-ether mobile phase. 0.5 ml of the crude PMC mixture was used and the mobile phase was alternated from 100% hexane to 25% ether-hexane. From the NMR analysis, fractions 4 and 5 were found to contain nearly 100% PMC. They were rotovaced to remove the $CDCl_3$ and placed in a vial in the freezer to crystallize. The crystals obtained were allowed to dry overnight in the dessicator. These crystals were used for ^{13}C shift determinations and melting point determination.

A 0.01 M solution of the PMC crystals was made in acetonitrile and an injection of 10 μL was made for an HPLC run. The program used to obtain fractions for the UV-Vis determinations was utilized. The retention time of the PMC of 6.3

minutes confirmed the identity of the fractions used for the UV-Vis determinations.

p-Methoxycinnamaldehyde:

Once again, the procedure used for the synthesis of p-chlorocinnamaldehyde was used for the synthesis of p-methoxycinnamaldehyde. Chromatography was used to isolate p-methoxycinnamaldehyde (PMEOC) since the ratio of p-methoxybenzaldehyde to PMEOC was very unfavorable, 1.4: 1. An alumina-gel column with a hexane-ether mobile phase was used. 1 g of PMEOC was injected. The mobile phase was alternated from 100% hexane to 30% ether-hexane. Despite the overloading of the column and channeling, fraction 5 provided an extremely pure and clean NMR spectra. The d-chloroform used in the NMR experiment was then removed from this fraction by rotary evaporation and the resulting liquid allowed to crystallize under nitrogen in a vial in the freezer. The crystals obtained were used for all melting point and UV-Vis determinations.

m-Nitrocinnamaldehyde:

The synthesis of Markovac (18) was scaled down by a factor of 250. 0.238 g of NaOH were dissolved in 120 ml of deionized water. This solution was placed in a 500-ml roundbottom flask. 3.000 g of m-nitrobenzaldehyde was dissolved in 60 ml of ethanol and was then added to the NaOH-water solution. The solution was heated to about 45°C in a water bath. A solution of 1.053 g acetaldehyde in 1 ml of ethanol was added to the roundbottom flask in two additions over 5 minutes (the flask was kept stoppered during the heating). After the addition of the acetaldehyde was complete, a yellow-white solid was observed in the bottom of the flask. The reaction mixture was heated for 1 hour. At the end of the hour, the heating was discontinued. The solid in the flask was collected by vacuum filtration and were washed with 50 ml of cold deionized water.

The crystals were purified by recrystallization. The crystals were dissolved in 10 ml hot chloroform and 4 ml hot methanol was added. Crystals were obtained by scratching the bottom of the test tube in an ice-bath. After 3 recrystallizations, pure m-nitrocinnamaldehyde crystals were obtained. These crystals were washed with hexane and allowed to dry in a dessicator. The purity of the crystals was confirmed by NMR and melting point determination.

m-Bromocinnamaldehyde:

The procedure used for the synthesis of p-chlorocinnamaldehyde was followed with a few exceptions: 2.000 g of m-bromobenzaldehyde in 5 g of ethanol and 0.520 g of acetaldehyde. The crude mixture was mixed with 50 ml of carbon tetrachloride and rotary evaporated in order to strip off the excess ethanol. The liquid m-bromobenzaldehyde could not be purified either through crystallization in a liquid nitrogen-hexane low temperature bath or through various chromatographic methods (including column chromatography, dry column chromatography, and HPLC). Finally, a crude mixture of m-bromocinnamaldehyde was used for the equilibrium, kinetics, and NMR determinations. The mixture was 7:1 cinnamaldehyde to benzaldehyde and 7:1 cinnamaldehyde to trimer.

METHOD

Determination of Keq:

During these measurements, the absorbance of the aldehyde was measured initially and after a series of bisulfite injections. Initially, three ml of buffer was pipetted into the reference and sample cells. For p-methylcinnamaldehyde (PMC), the HPLC fraction, ~1 ml, was pipetted into the sample cell and then approximately 2 ml of buffer were added. The initial concentration of PMC is unknown but the initial absorbance at 297.4 nm was 0.963. A scan from 500 to 190 nm was made to determine the wavelength maxima. The wavelength maxima in buffer was 304.7 nm; however the wavelength maxima in ethanol of 297.4 nm was used. A 10 µL injection of 0.08048 M bisulfite was made using a 10µL syringe into both the reference and sample cells. 6-10µL injections of the bisulfite solution were made, corresponding to a concentration of 0 to 1.61×10^{-3}M bisulfite in the cells. After each injection the cell was shaken and allowed to equilibrate in the water bath for 10 minutes. The absorbance at 297.4 nm was then recorded. After 60 µL of bisulfite had been injected, another scan from 500 to 190 nm was taken and saved on disk. The volume of the cell was measured by graduated cylinder since it was uncertain initially.

The procedure for p-chlorocinnamaldehyde (PCLC) was essentially that described above, except that initially 3 ml of buffer were pipetted into the cells and then 11µL of a 0.0099 M solution of PCLC was injected into the cell for a intial concentration of 3.63×10^{-5} M. The concentration of bisulfite in the cell ranged from 0 to 8.07×10^{-4} M. The absorbance measurements were made at 297.6 nm.

The wavelength maxima, the concentration of cinnamaldehyde in the cell and the range of bisulfite concentrations used for the remaining cinnamaldehydes are summarized in Table 4.

Table 4: λ_{max}, [Cinnamaldehyde], [HSO3-] for Keq Determinations

X	λ_{max}	[Cinnamaldehyde]	[HSO3-]
p-Bromo	300	3.42×10^{-5}	0 to 8.43×10^{-4}
p-Methoxy	323	4.45×10^{-5}	0 to 1.69×10^{-4}
p-Nitro	308	3.99×10^{-5}	0 to 4.99×10^{-4}
o-Nitro	315	4.52×10^{-5}	0 to 4.99×10^{-4}
m-Nitro	294	4.14×10^{-5}	0 to 4.15×10^{-4}
o-Methoxy	323	5.33×10^{-5}	0 to 1.38×10^{-3}
m-Bromo	285.3	4.60×10^{-5}	0 to 6.24×10^{-4}

Determination of ε of the bisulfite-addition product:

p-Nitrocinnamaldehyde (ε):

An excess of bisulfite corresponding to a concentration of 8.43×10^{-3}M in the cell was injected to the sample cell containing an initial concentration of PNC of 3.99×10^{-5}M. The cell was allowed to equilibrate for an hour in the water bath at 25°C and the absorbance was recorded. Using the intial absorbance of the PNC alone and the absorbance after the excess of bisulfite was added, an average value for ε for the bisulfite addition product was obtained after two determinations.

o-Nitrocinnamaldehyde (ε):

An excess of bisulfite corresponding to a concentration of 8.43×10^{-3}M in the cell was injected to the sample cell containing an initial concentration of o-nitrocinnamaldehyde (ONC) of 4.52×10^{-5}M. The cell was allowed to equilibrate for an hour in the water bath at 25°C and the absorbance was recorded. Three runs were done and a Beer's Law plot was made to determine the extinction coefficient for the ONC-bisulfite addition product. It was also necessary to make a Beer's Law plot of A versus [ONC] to determine the extinction coefficient of ONC itself.

Determination of Rate Constants:

In these determinations, a known quantity of bisulfite is injected into a cell containing the aldehyde, whose initial absorbance is known, and the absorbance is then measured with respect to time until equilibrium is reached. 3.00 ml of buffer are pipetted into a reference and sample cell, and then several µL of aldehyde stock solution are injected by a 10µL syringe into the sample cell. The resulting concentrations of aldehyde in the cell are the same as the intial concentrations of aldehyde in the Keq determinations. t-Cinnamaldehyde's kinetics were redetermined and the initial concentration of t-cinnamaldehyde in the cell was 3.60×10^{-5} M. The cells are placed in the cell compartment and allowed to reach 25°C. The temperature initially is then recorded and the time drive program is started. A stop watch is started once the first point appears on the computer graph of absorbance versus time. Once the computer display shows a steady intial absorbance at the wavelength of interest, the reference cell is removed and an injection of bisulfite is made using a 50µL or 100µL syringe. Table 5 shows the concentrations of bisulfite used for each of the cinnamaldehydes.

The reference cell is replaced and an equal amount of bisulfite is injected into the sample cell. The sample cell is then upended quickly and returned to the cell compartment. The timer is stopped as the bisulfite is injected so that the exact value of t_0 or the initial time of bisulfite addition can be determined. This can be done by taking the time recorded by the TDRV program and subtracting the time recorded by

Table 5: Concentrations of Bisulfite for Kinetics Runs

Aldehyde	Bisulfite Concentrations/x10^4 M
p-methylcinnamaldehyde	10.2, 16.1, 20.1
p-chlorocinnamaldehyde	1.35, 2.69, 5.38
p-bromcinnamaldehyde	2.81, 5.62, 8.43
p-nitrocinnamaldehyde	0.843, 1.69, 2.81
o-nitrocinnamaldehyde	5.58, 6.97, 8.34
p-methoxycinnamaldehyde	8.15, 9.50, 10.9, 12.2, 13.6, 21.7
m-nitrocinnamaldehyde	2.77, 4.15, 5.54, 8.30
o-methoxycinnamaldehyde	5.54, 8.31, 11.1
m-bromocinnamaldehyde	1.30, 2.60, 3.90
t-cinnamaldehyde	5.60, 8.43, 11.2

the stopwatch. The absorbance of the solution is recorded by the TDRV program every 0.5 seconds for a time period between 10 to 12 minutes. The solution in cell comes to equilibrium well before five minutes so the absorbance at infinity or equilibrium is taken as the absorbance at the end of the kinetics run. A printout of the absorbance versus time during the decrease is obtained using the KINS program on the IFL3 disk.

^{1}H and ^{13}C NMR:

Samples for NMR were generally on the order of 30 mg in 1 ml of deuterochloroform.

RESULTS

Synthesis:

p-Nitro-, o-nitro-, o-methoxy-, and t-cinnamaldehyde were obtained from Aldrich. The remainder of the aldehydes were synthesized via the crossed-aldol condensation reaction between acetaldehyde and the corresponding benzaldehyde, as described in the "Introduction" and "Experimental" sections. Table 6 shows the ratio of cinnamldehyde to benzaldehyde in the crude reaction mixture. This ratio was obtained from a ratio of the integrations of the aldehyde proton peaks.

Table 6: Ratio of Cinnamaldehyde to Benzaldehyde in Synthesis

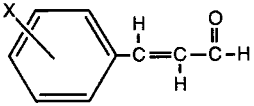

X	Cinnamaldehyde/Benzaldehyde Ratio
p-MeO	0.7 / 1
p-Me	1.7 / 1
p-Cl	5.1 / 1
p-Br	5 / 1
m-Br	7 / 1
m-NO_2	17 / 1
H	Aldrich
p-NMe_2	Aldrich
p-NO_2	Aldrich
o-NO_2	Aldrich
o-MeO	Aldrich

The purity of each of the aldehydes was confirmed by ^1H NMR and by melting point. Table 7 shows a comparison of the actual and literature melting points for each of the aldehydes synthesized. The literature values were obtained from Beilstein.

Table 7: Physical Data for Synthesized Cinnamaldehydes

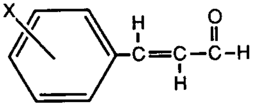

X	m.p./°C	Lit. (Beilstein)
p-Cl	60-60.5	61-62
p-Br	76-77	81
p-MeO	53-54	58
m-NO2	114-115	116
p-Me	37	41.5
p-NO2	Aldrich	
p-NMe2	Aldrich	
o-NO2	Aldrich	
H	Aldrich	
o-MeO	Aldrich	
m-Br	Liquid crude*	

* Note: m-Bromocinnamaldehyde was not purified and its identity was confirmed by ^{1}H NMR.

NMR:

Proton assignments:

Para-substituted cinnamaldehydes:

Although ^{1}H NMR were not used for statistical correlations, they had great importance in vertifying the identity of the aldehydes from synthesis and for assignment of ^{13}C absorptions (through HETCOR). Proton NMR for cinnamaldehydes generally have distinctive splitting patterns. The molecule can be represented as below with the hydrogens labeled **a** through **e**.

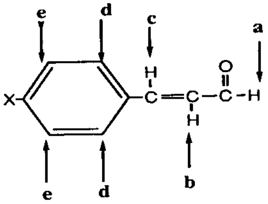

Using p-methoxycinnamaldehyde as an example (Spectra 1), we see a doublet at 9.62 ppm due to the **a** proton. It is split by the neighboring **b** proton. The **b** proton shows up as a doublet of doublets at 6.58 ppm. It is split into a doublet by the **a** proton and then is split again by the *trans* **c** proton. The J or coupling constant of the **b** proton was large, 16 Hz. Since the coupling constant for *trans* -substituted hydrogens is usually between 11-18 ppm compared to the 8-14 ppm for *cis* protons, the **c** and **b** protons are indeed *trans* to each other. The **c** proton absorbs as a doublet at 7.4 ppm and is readily separated from the aromatic proton absorption by its large *trans* coupling constant. The splitting patterns observed for the **a**, **b**, and **c** protons of p-methoxycinnamaldehyde are the same for all para, meta, and ortho cinnamaldehydes. The aromatic carbons, however, show large differences from para to meta to ortho substituted cinnamaldehydes. For p-methoxycinnamaldehyde, we see two doublets, one at 6.92 ppm and one at 7.5 ppm, due to the equilvalent **d** and **e** protons. Their coupling constant, J, is about 7.8 Hz. This is far smaller than the trans coupling constant for the **c** doublet; thus the **c** doublet can be readily separated from the aromatic doublets.

CHART XL SERIES PART NO 997259 GRAPHIC CONTROLS CORPORATION BUFFALO NEW YORK PRINTED IN U.S.A.

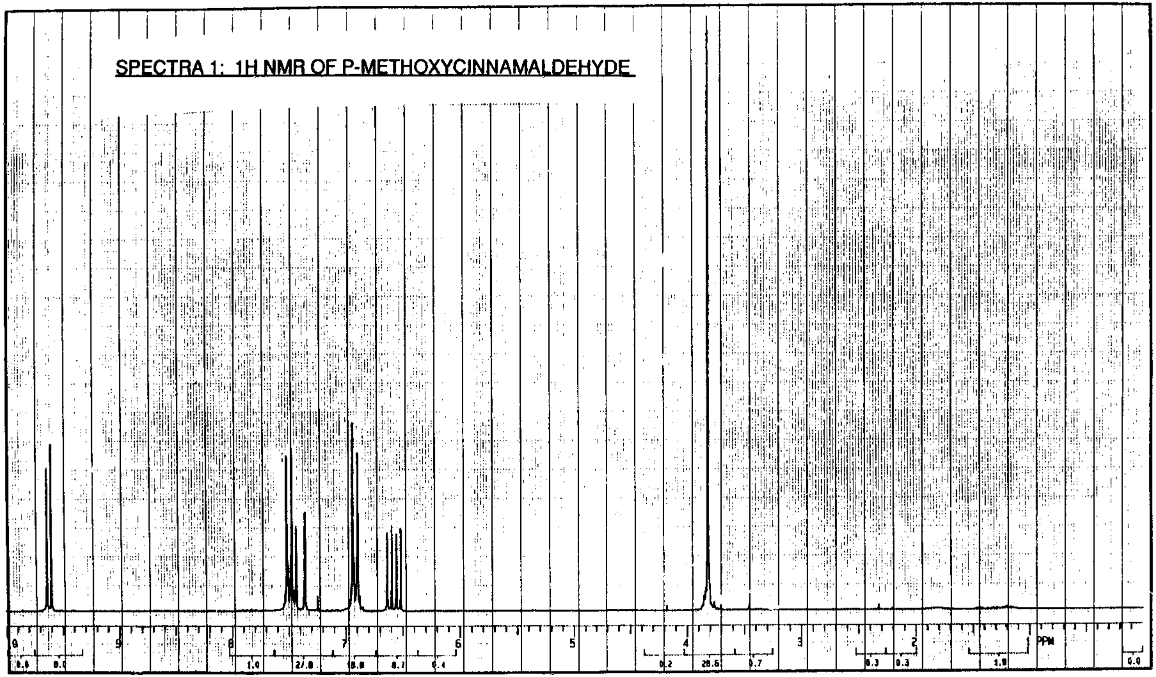

SPECTRA 1: 1H NMR OF P-METHOXYCINNAMALDEHYDE

OBSERVE

Nucleus 1.000 Freq 200 MHz
Spec Width 3000.3 Hz Offset 0 Hz
Acq Time 2.000 sec Delay 0 sec
Pulse Width 14.2 μsec Transients 16

DECOUPLE

Nucleus 1.000 Offset -300.0 Hz
Mode NNN Power 20.0 db
Modulation Mode C Freq 200 Hz
Pulse Width μsec Power Mode 1.0

PLOT/PROCESSING

FN 16 K RE sec CD sec
LB Hz AJ sec CCD
Width 2000.0 Hz/ppm Start 0 Hz ppm
Reference

EXPERIMENT

Pulse Sequence S2PUL
Tube OD mm
Temp °C
Solvent CDCl3

SAMPLE

P-METHOXYCINN.
FRACTION 5

Number
File HPMEC2
Date 11-09-88
12:04:11
XL GEM 200

Meta-substituted cinnamaldehdydes:

Using m-nitrocinnamaldehyde as an example (Spectra 2), we can assign the proton splittings. The hydrogens for a meta-substituted cinnamaldehyde are labeled below:

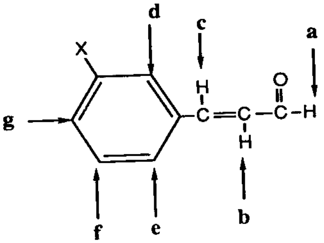

The **a**, **b**, and **c** protons, as has already been mentioned, show the same splitting patterns. The **d** proton for m-nitrocinnamaldehyde appears as a singlet at 8.45 ppm. It is a singlet because it has no actual neighboring protons (though it shows some fine splitting due to the conjugated pi system). There is a doublet at 8.3 ppm and a doublet at 7.9 ppm. The doublet at 8.3 ppm is probably due to the **g** proton, which is right next to the deshielding nitro group. The other doublet at 7.4 ppm is then due to the **e** proton. Both are split by the one neighboring proton, the **f** proton. The **f** proton appears as a triplet at 7.58 ppm. It is split into a triplet by its two neighboring protons, **e** and **g**.

As was noted in the "Experimental" section, m-bromocinnamaldehyde was difficult to purify and a crude sample containing cinnamaldehyde, benzaldehyde, and trimer was used. This complicated the interpretation of the NMR considerably; however, due to the very small amounts of benzaldehyde and trimer present relative to m-bromobenzaldehyde (MBC), it was still possible to identify the proton

SPECTRA 2: 1H NMR OF M-NITROCINNAMALDEHYDE

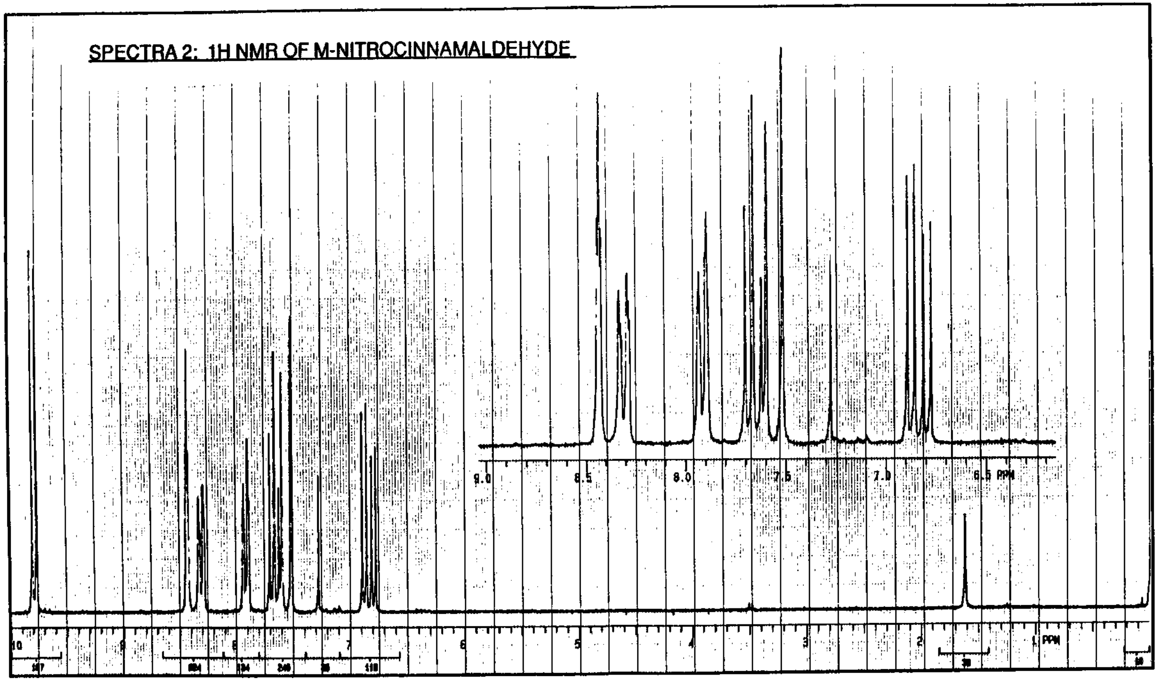

OBSERVE
Nucleus 1.000
Spec Width 3000.3 Hz
Acq Time 2.000 sec
Pulse Width 14.2 μsec
Freq 200 MHz
Offset 0 Hz
Delay 0 sec
Transients 16

DECOUPLE
Nucleus 1.000
Mode 1001
Modulation Mode C
Pulse Width μsec
Offset 300.0 Hz
Power 20.0 db
Freq 200 Hz
Power Mode 1.0

PLOT/PROCESSING
FN 16 K
RE sec
CD sec
LB Hz
AF sec
CLD
Width 2000.0 Hz ppm
Start 0 Hz/ppm
Reference

EXPERIMENT
Pulse Sequence S2PUL
Tube OD mm
Temp °C
Solvent CDCL3

SAMPLE

M-NITROCINNAMALDEHYDE
RECRYST. SYNTHESIS #2
2/10/89 IN CDCL3
2nd recrystallization

Number
File N
Date 02-08-89
13:14:19
XL GEM 200

chemical shifts of MBC. The chemical shifts of m-bromobenzaldehyde were identified and substracted out. Remaining large peaks were a singlet at 7.68 ppm, a doublet at 7.55ppm, a doublet at 7.48 ppm, a doublet at 7.37ppm, and a triplet at 7.28 ppm. The doublet at 7.28 ppm was identified by its coupling constant to be the **c** proton. The other proton absorptions are due to the characteristic meta aromatic protons. The **a** and **b** protons were once again readily identify due to the unique chemical shifts.

Ortho-substituted cinnmaldehydes:

The proton splittings for ortho substituted cinnamaldehydes are even more complicated than the meta substituted splittings. The hydrogens are labeled below:

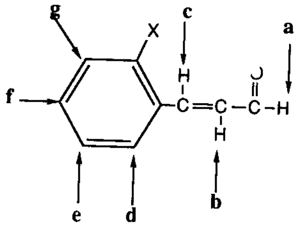

Using o-methoxycinnamaldehyde as an example (Spectra 3), we see that the **a** and **b** protons appear at their characteristic chemical shifts. The **c** carbon is once again in the aromatic region, at 7.81 ppm (J=16 Hz.). There is a doublet at 7.51 ppm, a triplet at 7.4 ppm and what appears to be a doublet superimposed on a triplet between 6.9 and 7.0 ppm. The two doublets would be due to the **d** and **g** protons; however it is impossible to assign them. The **d** and **g** protons each are split into a doublet by the neighboring proton, **e** and **f** respectively. The

SPECTRA 3: 1H NMR OF O-METHOXYCINNAMALDEHYDE

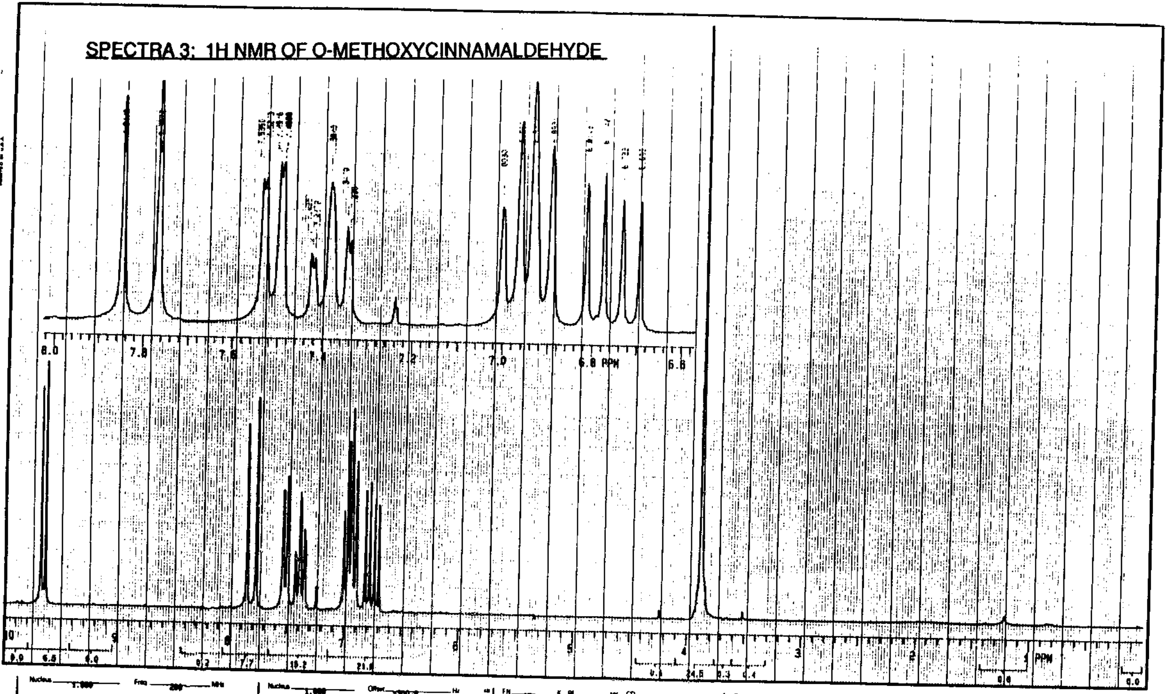

OBSERVE
Nucleus 1.000
Spec Width 3000.3 Hz
Acq Time 2.000 sec
Pulse Width 19.3 μsec
Freq 200 MHz
Offset 0 Hz
Delay 0 sec
Transients 16

DECOUPLE
Nucleus 1.000
Mode NNN
Modulation Mode C
Pulse Width μsec
Offset 300.0 Hz
Power 20.0 db
Freq 200 Hz
Power Mult 1.0

PLOT/PROCESSING
FN 16 K
RE sec
CD sec
LB Hz
AT sec
CCD
Width 2000.0 Hz ppm
Start 0 Hz ppm
Reference

EXPERIMENT
Pulse Sequence S2PUL
Tube O.D. mm
Temp °C
Solvent CDCL3

SAMPLE
~~[illegible]~~
O-methoxycinnamaldehyde

Number
File N
Date 04-28-88
12:40:16
XL 200

two triplets are due to the **e** and **f** protons. They are split by two neighboring protons.

Carbon and HETCOR:

The ^{13}C NMR chemical shifts needed to be referenced for their use in the statistical correlations. The middle peak of $CDCl_3$ was referenced to TMS and its chemical shift was found to be 77.23 ppm. Every ^{13}C spectrum was thereafter referenced to this value for the midpeak of $CDCl_3$.

Once again, we can label the important carbons as A through E. Table 8 shows the ^{13}C chemical shifts for each of the aldehydes.

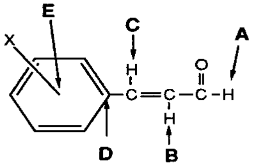

Table 8: C-13 NMR chemical shifts, ∂

X	∂A/ppm	∂B/ppm	∂C/ppm	∂D/ppm	∂E/ppm
p-NO2	193.42	132.04	149.32	140.29	149.24
m-NO2	193.36	131.24	149.45	136.07	149.18
o-NO2	193.73	132.95	147.78	130.35	148.36
p-Cl	194.00	129.30	151.55	132.84	137.68
p-Br	193.94	129.31	151.55	133.21	126.00
H	194.33	131.31	153.28	134.32	128.91
p-Me	194.39	128.05	153.41	131.67	142.41
p-MeO	194.24	126.79	153.15	127.06	162.60
p-NMe2	194.24	124.11	154.41	122.05	152.80
o-MeO	195.13	129.34	148.65	123.21	158.68
m-Br	193.81	129.95	151.09	136.37	123.53

* See Appendix B for All 1H, 13C, and HETCOR Spectra.

Assignment of the para substituted cinnamaldehyde carbons was simplified by the equivalency of the two aromatic carbons ortho to the E carbon and the equivalency of the two aromatic carbons ortho to the D carbon. Due to the Nuclear Overhauser Effect, these ^{13}C peaks are nearly twice the size of the B and C carbon peaks, which each have only one proton attached. The quaternary carbons D and E are the smallest. To assign these carbons, Heteronuclear Chemical Shift Correlation Experiments, HETCOR, were run on all cinnamaldehydes except t-cinnamaldehyde and p-chlorocinnamaldehyde. Assignments of the carbons of t-cinnamaldehyde and p-chlorocinnamaldehyde were found in the Aldrich Directory of NMR spectra. Since the **a** proton doublet and the **b** proton doublet of doublets are easily identified due to their unique splitting patterns and chemical shifts, these carbons were readily assigned. The C carbon peak was assigned by its correlation with the doublet in the ^{1}H spectrum with J>14 Hz. and by its size relative to the aromatic carbon peaks. The D and E carbons both show no correlation with the ^{1}H spectrum since they have no attached protons. They were identified by examining ^{13}C chemical shift data for monosubstituted benzenes and by examining the corresponding chemical shifts of the quaternary carbons of their starting benzaldehydes.

The ^{13}C peak of the E carbon of o-nitrocinnamaldehyde was not seen under normal conditions. The carbon peak was not seen since the carbon did not have time to relax under normal conditions. It is thought this is due to the attached highly electron-withdrawing nitro group. Another ^{13}C NMR experiment was run using a longer acquision time (AT=1.000 second). The quaternary carbon then showed up around 148.5 ppm.

The ^{13}C shifts of the ortho and meta substitued cinnamaldehydes were harder to identify since none of the aromatic carbons are equivalent. Therefore, since all the aromatic carbons now have one equivalent attached hydrogen, these ^{13}C peaks are the same size as the B and C carbons. Identification of these carbons are complicated by both this and the complexity of the ^{1}H spectra. HETCOR experiments were also run to assign these carbons.

As was already noted, m-bromocinnamaldehyde's NMR were difficult to interpret due to the impurity of the sample. The carbons with one attached proton were readily identified by their relatively large size. A HETCOR was run to identify the A, B, and C carbons. The D and E quaternary carbons were harder to identify due to their smaller size. There were many aromatic peaks of comparable size from benzaldehyde and the trimer and from noise. A new carbon was run using 1735 transients to improve the signal-to-noise ratio. An APT (Appendix B, Spectra B20), attached proton test, was run to separate the quaternary carbons from the carbons with one attached protons (due to the benzaldehyde and trimer). Only two carbon peaks were up in the APT. They were assumed to be the D and E carbons and were assigned by the chemical shifts for mono-substituted bromobenzenes.

Equilibrium:

p-Methoxycinnamaldehyde:

Since a literature value for the extinction coefficient of p-methoxycinnamaldehyde (PMEOC) was not found, it was assumed to be approximately 25,400, the extinction coefficient of *trans*-cinnamaldehyde. Using Beer's Law ($A=\varepsilon bc$, where b=pathlength of the cell or 1.000 cm), a concentration of PMEOC was calculated which would produce an intial absorbance of approximately one. 3 μL of a 0.0445 M solution of PMEOC was injected into the cell containing 3 ml buffer to produce an initial concentration of 4.45×10^{-5} M. A scan from 500 to 190 nm was taken and the wavelength maxima, 323 nm, determined (see Appendix C for absorption spectra of all cinnamaldehydes). Several aliquots of 0.08430 M bisulfite were added for a concentration range of 0 to 1.629×10^{-3} M bisulfite. The first injection of bisulfite made the [HSO3-] in excess of the aldehyde. The decrease in absorption at 323 nm at equilibrium was followed for each injection of bisulfite. The temperature was always kept at 25°C.

1/A was plotted against [HSO3-] in Figure 1. As described in the "Introduction", Keq was determined by dividing the slope by the intercept to give a value of 422 M-1.

p-methylcinnamaldehyde:

The same procedure used to calculate Keq for p-methoxycinnamaldehyde was followed for p-methylcinnamaldehyde except that, as described in the "Experimental" section, HPLC fractions were used instead of injections of a stock solution of the aldehyde. See Appendix A, Figure A1, for the plot of 1/A versus [HSO3-]. Keq was determined to be 549 M-1.

p-nitrocinnamaldehyde:

For p-nitrocinnamaldehyde we observed curvature in the 1/A versus concentration of bisulfite plot. Using p-nitrostyrene as a model structure for the bisulfite addition product, the ε at 308 nm was found to be 20,000 which is nearly the same as ε at 308 nm for p-

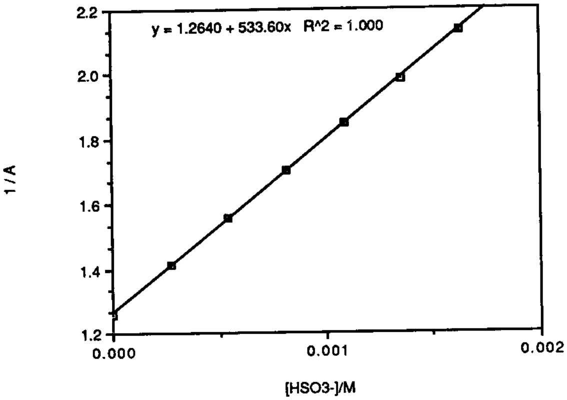
Figure 1: 1/A versus [HSO3-] for p-methoxycinnamaldehyde

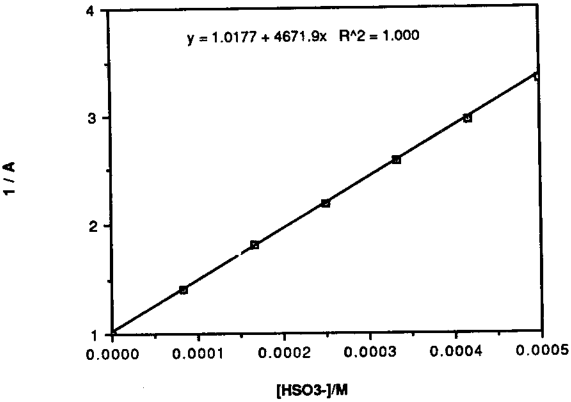
Figure 2: 1/A versus [HSO3-] for p-nitrocinnamaldehyde

nitrocinnamaldehyde (ε of p-nitrocinnamaldehyde =23,190 from L. Nicosia's thesis). This was a good indication that the bisulfite addition product absorbs strongly at the wavelength of interest. To correct for this, ε for the bisulfite addition product had to be determined. An excess of bisulfite corresponding to a concentration of 8.43×10^{-3}M in the cell was injected to the sample cell containing an initial concentration of PNC of 3.99×10^{-5}M. The cell was allowed to equilibrate for an hour in the water bath at 25°C and the absorbance was recorded. This was done twice.

From the initial absorbance, A_o=0.851 for both runs, and ε for PNC, the initial concentration of PNC, c_o, was determined from Beer's Law; $c_o=3.67\times10^{-5}$ M for both runs. If we assume that the aldehyde reacts fully with the excess bisulfite, then the concentration of the product equals the initial concentration of the aldehyde since, at any time, $c_1+c_2=c_o$, where c_1=[aldehyde] and c_2=[bisulfite additon product]. ε_2, the extinction coefficient of the product, can be determined from c_2 and the absorbance at the end of the bisulfite addition, A_2. Table 9 shows A_2, c_2, and ε_2.

Table 9: Determination of Extinction Coefficient of PNC-Bisulfite Addition Product

Run #	A_2	c_2/M	ε_2
1	0.544	3.67×10^{-5}	13,500
2	0.502	3.67×10^{-5}	13,600
		Average:	13,600

If we assume that at any time, $A=c_1\varepsilon_1 + c_2\varepsilon_2$, where 1=PNC and 2=bisulfite addition product of PNC, and $c_1+c_2=c_0$, then we can derive an expression for the true concentration of PNC:

$$c_1 = A - c_0\varepsilon_2 / \varepsilon_1 - \varepsilon_2$$

and Beer's Law says that $A_1=c_1 * \varepsilon_1$. We can then convert the absorbances for each injection of bisulfite to A_1 values. The new plot of $1/A_1$ versus [HSO3-] for PNC is shown in Figure 2. This graph is linear (Figure 2) and Keq for p-nitrocinnamaldehyde is 4590 M-1.

o-Nitrocinnamaldehyde:

As for p-nitrocinnamaldehyde, we observe curving in the 1/A versus [HSO3-] plot. First a value for the extinction coefficient of o-nitrocinnamaldehyde (ONC), ε_1, had to be determined. The absorbance at 315 nm was followed for a series of injections of ONC. The absorbance was plotted against [ONC] (Figure 3) and the slope was taken to be ε_1 or 6940.

Following the same procedure used for PNC, we made three injections of excess bisulfite to determine ε_2. Table 10 summarizes the results of this procedure.

Table 10: Determination of Extinction Coefficient of the ONC-Bisulfite Addition Product

Run #	C_2/M	A_2
1	4.45x10-5	0.143
2	2.75x10-5	0.094
3	1.97x10-5	0.067

Instead of taking an average of calculated ε_2's, A_2 was plotted versus c_2 (Figure 4) in a Beer's Law type plot. The slope was determined to be ε_2

Figure 3: A versus [ONC] for o-nitrocinnamaldehyde

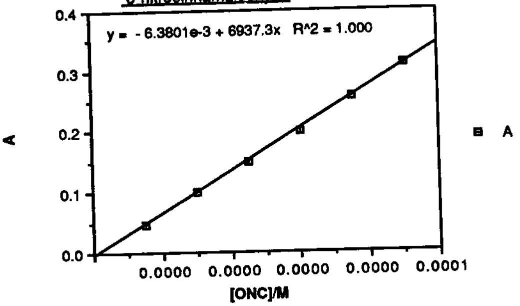

Figure 4: A2 versus C2 for Bisulfite Adduct of o-Nitrocinnamaldehyde

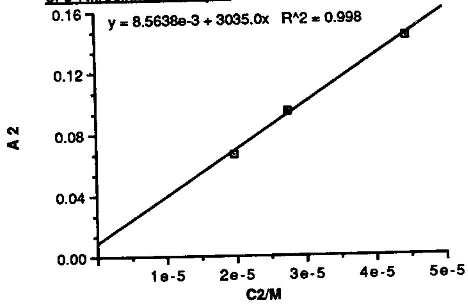

Figure 5: 1/A1 versus [HSO3-] for o-nitrocinnamaldehyde

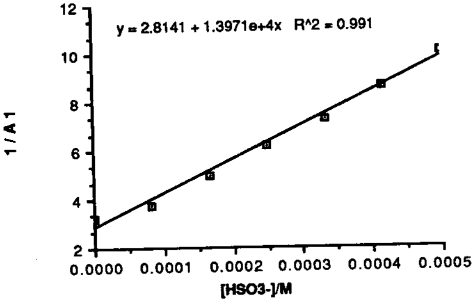

and was found to be equal to 3035. As for p-nitrocinnamaldehyde, the data was transformed and a new plot of 1/A versus [HSO3-] was made (Figure 5). This plot still curves somewhat but in the opposite direction. We may have overcorrected for the absorbance of the product. Keq for o-nitrocinnamaldehyde was determined to be 4960 M-1.

m-Nitrocinnamaldehyde:

Since the other nitrocinnamaldehydes had showed absorbance of the product at the wavelength maxima, we expected this to be the case for m-nitrocinnamaldehyde. However, though the product did absorb at the wavelength maxima, 279 nm, it did not absorb at the higher wavelength of 294 nm. Thus all absorbance measurements were made at 294 nm and a straight plot of 1/A versus [HSO3-] was obtained (Appendix A, Figure A2). Keq was determined from the slope and the intercept to be 2720 M-1.

Other cinnamaldehydes:

The same procedure for calculating Keq for p-methoxycinnamaldehyde was followed for p-bromo-, p-chloro-, m-bromo-, and o-methoxycinnamaldehyde. See Appendix A, Figures A3-A6, for the plots of 1/A versus [HSO3-]. The initial concentrations of the aldehydes, the range of concentrations of bisulfite, and the wavelengths used are summarized in the "Experimental" section.

The values obtained for Keq for all cinnamaldehydes are summarized in Table 11.

Table 11: Summary of Equilibrium Constants, Keq

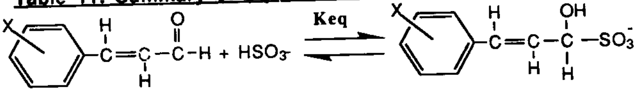

X	Keq/M-1	
o-NO_2	4960	±200
p-NO_2	4590	±190
m-NO_2	2720	±110
p-Cl	1747	±70
p-Br	1330	±50
m-Br	1320	±50
H	1030	±40
o-MeO	810	±30
p-Me	549	±20
p-MeO	422	±20
p-NMe_2	299	±10

Kinetics

p-methoxycinnamaldehyde:

The foward and reverse rate constants were determined for p-methoxycinnamaldehyde (PMEOC). The intial concentration of PMEOC in the cell was 4.45x10-5M. The decrease in absorbance with respect to time was followed for several different concentrations of bisulfite as outlined by the procedure in the "Experimental" section. Figures 6-11 show plots of ln[A-Ainf.] versus time for several different concentrations of bisulfite. k' was calculated from the slope of this plot, as described in the "Introduction". Table 12 summarizes the intial concentration of the aldehyde, the concentrations of bisulfite used for each run, and k' for each aldehyde.

Table 12: [Cinnamaldehyde], [HSO3-], and k' for Kinetics Determination

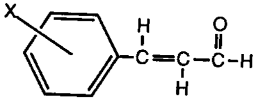

X	[Cinnamaldehyde]/10^5	[HSO3-]/10^4	k'/s-1
p-MeO	4.45	8.15	6.37
	-	9.50	7.45
	-	10.9	8.38
	-	12.2	9.17
	-	13.6	9.63
	-	21.7	16.3
p-Me	HPLC fraction	10.2	9.99
	-	16.1	14.5
	-	20.1	17.5
p-Cl	3.63	1.35	3.26
	-	2.69	7.71
	-	5.38	16.8
p-Br	3.42	2.81	7.61
	-	5.62	14.3
	-	8.43	21.2
o-NO2	4.52	5.58	45.7
	-	6.97	66.4
	-	8.34	58.1
p-NO2	3.99	0.843	8.39
	-	1.69	15.9
	-	2.81	27.4
m-NO2	4.14	2.77	19.4
	-	4.15	29.2
	-	5.54	39.1
	-	8.30	63.7
o-MeO	5.33	5.54	7.67
	-	8.31	11.2
	-	11.1	14.2
m-Br	4.60	1.30	3.35
	-	2.60	7.34
	-	3.90	11.3
H	3.60	5.62	13.3
	-	8.43	19.6
	-	11.2	26.2

Figure 6: ln[A-Ainf.] versus time, [HSO3-]=1.36e-3 M, for p-methoxycinnamaldehyde

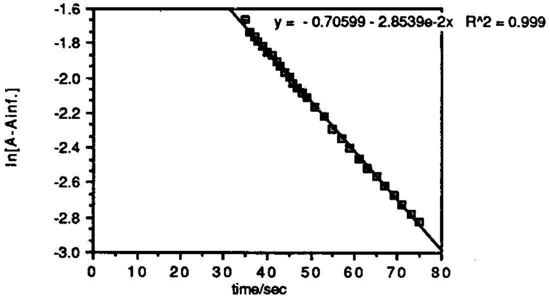

Figure 7: ln[A-Ainf.] versus time, [HSO3-]=1.09e-3 M, for p-methoxycinnamaldehyde

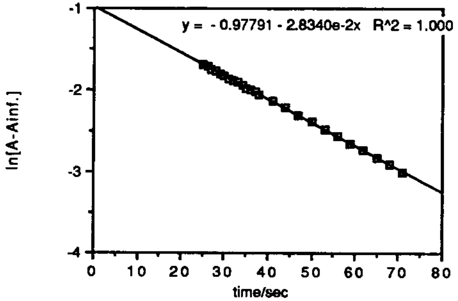

Figure 8: ln[A-Ainf.] versus time, [HSO3]=8.15e-4 M, for p-methoxycinnamaldehyde

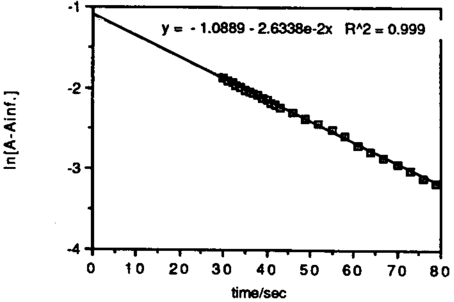

Figure 9: ln[A-Ainf.] versus time, [HSO3-]=1.22e-3 M, for p-methoxycinnamaldehyde

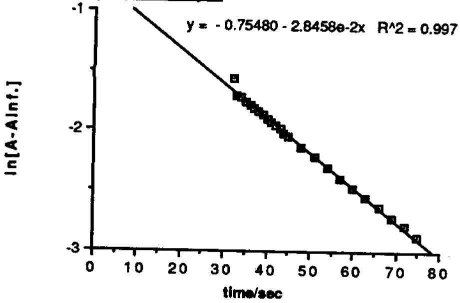

Figure 10: ln[A-Ainf.] versus time, [HSO3-]=9.50e-4M, for p-methoxycinnamaldehyde

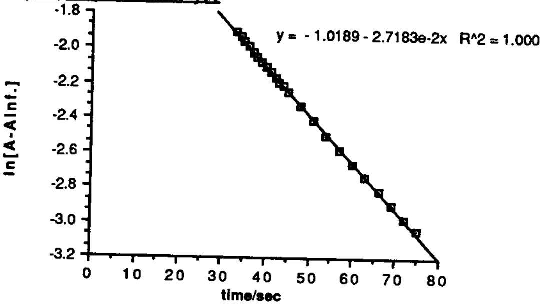

Figure 11: ln[A-Ainf.] versus time, [HSO3-]=2.17e-3 M, for p-methoxycinnamaldehyde

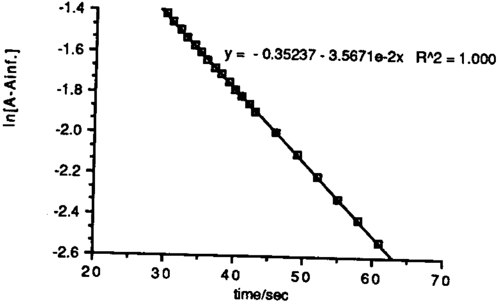

Figure 12: k' versus [HSO3-] for p-methoxycinnamaldehyde

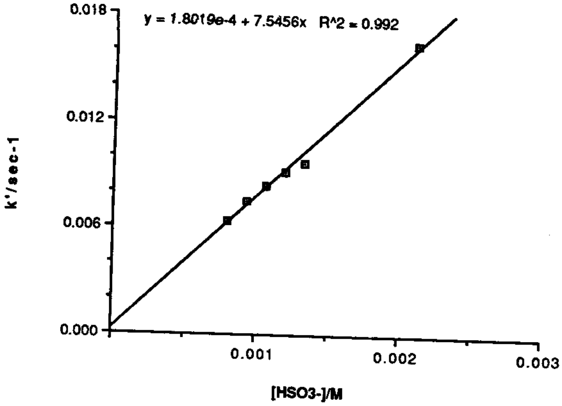

Figure 13: k' versus [HSO3-] for p-nitrocinnamaldehyde

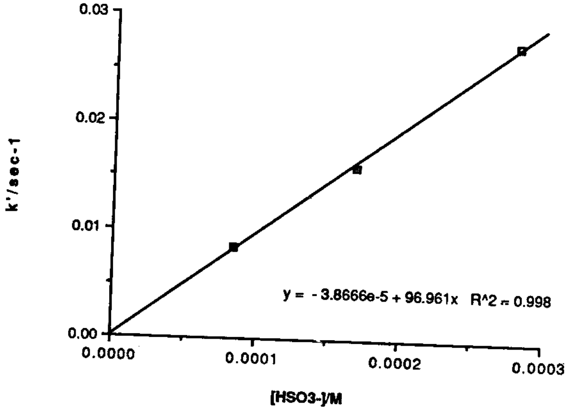

k' was then plotted against [HSO3-] in Figure 12. The slope of this plot is equal to the forward rate constant, k1, since k'=k1[HSO3-]. k1 was found to be 7.25 M-1s-1. k-1, the reverse rate constant, was calculated by dividing k1 by Keq. k-1 was calculated to be 0.0172 s-1.

p-nitrocinnamaldehyde:

The same procedure as that followed for p-methoxycinnamaldehyde was used to determine k_1 and k_{-1}. However, as was already mentioned, the product absorbs at the wavelength of interest. The plots of ln[A-$A_{inf.}$] versus time, (Appendix A, Figures A7-A9), did not have to be corrected since A and $A_{inf.}$ are effected to the same extent and the slope is the same corrected or uncorrected. k', however, is calculated from the slope of this plot, A_o, and $A_{inf.}$ $A_{inf.}$ had to be corrected for the absorbance of the product by using the following equations:

$$c_1 = A_{inf.} - c_0\varepsilon_2 / \varepsilon_1 - \varepsilon_2 \qquad \text{and} \qquad A_{inf.}\,(\text{true}) = \varepsilon_1 * c_1$$

Note that these are the same equations used to correct the absorbance points for the equilibrium determinations for p-nitro- and o-nitrocinnamaldehyde. From the corrected value of $A_{inf.}$, corrected values for k' were calculated (Table 12) and k' was plotted against [HSO3-] to determine k_1 (Figure 13). k1 was found to be 96 $M^{-1}s^{-1}$ and k^{-1} was calculated to be 0.0210 s^{-1}.

o-nitrocinnamaldehyde:

The same procedure used to determine k1 and k-1 for p-nitrocinnamaldehyde was used for o-nitrocinnamaldehyde. k1 was determined to be 75 M-1s-1 while k-1 was found to be 0.0151 s-1. See Appendix A for plots of ln[A-Ainf.] versus time, (Figures A10-A12), and k' versus [HSO3-], (Figure A15).

m-nitrocinnamaldehyde:

The same procedure used to determine k1 and k-1 for p-methoxycinnamaldehyde was used for m-nitrocinnamaldehyde with one exception. After the intial decrease in absorbance of the aldehyde due to the bisulfite addition, the absorbance increased over time for the rest of the kinetics run. It was thought that this was due to the low solubility of m-nitrocinnamaldehyde in the buffer solution. As the ionic bisulfite addition product was formed, the solubility of the aldehyde would increase causing the absorbance to rise. To minimize this increase, lower concentrations of the aldehyde were used. Ainf. was taken as the absorbance right after the decrease due to the bisulfite addition and before the increase in absorbance later in the run.

k1 was determined to be 80.3 M-1s-1 and k-1 was calculated to be 0.0295 s-1. See Appendix A for plots of ln[A-Ainf.] versus time, (Figures A14-A17), and k' versus [HSO3-], (Figure A18).

Other cinnamaldehydes:

The foward and reverse rate constants of p-methyl-, p-bromo-, p-chloro-, m-bromo-, o-methoxy, and *trans* -cinnamaldehyde were determined by method used for p-methoxycinnamaldehyde. The data for k' is summarized in Table 12 and k1 and k-1 are summarized in Table 13. For plots of ln[A-Ainf.] versus time and k' versus [HSO3-], see Appendix A.

Table 13: Summary of Rate Constants, k1 and k-1

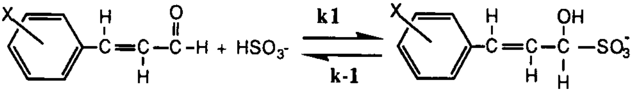

X	k1/M-1s-1		k-1/s-1
p-NO2	96.	±0.9	0.0210
m-NO2	80.3	±0.7	0.0295
o-NO2	75.	±0.7	0.0151
p-Cl	33.6	±0.3	0.0192
m-Br	30.6	±0.3	0.0232
p-Br	24.2	±0.2	0.0180
H	23.	±0.2	0.0240
o-MeO	12.6	±0.1	0.0156
p-Me	7.59	±0.1	0.0138
p-MeO	7.25	±0.1	0.0172
p-NMe2	4.0	±0.04	0.013

Table 14 summarizes the equilibrim, kinetics, and NMR data for the 11 substituted cinnamaldehydes. Table 14 also contains a summary of σ values for the various substituents.

Table 14: Summary of Equilibrium, Kinetics, NMR, and σ Data*

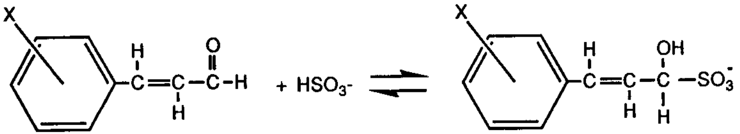

X	Keq/ M-1	k1/ M-1s-1	k-1 s-1	∂A/ ppm	∂B/ ppm	∂C/ ppm	∂D/ ppm	σ^o	σ	σ+
p-NMe$_2$	299	4.0	0.013	194.33	124.11	154.41	122.05	-0.44	-0.83	-1.7
p-MeO	422	7.25	0.0172	194.24	126.79	153.15	127.06	-0.12	-0.27	-0.7
p-Me	549	7.59	0.0138	194.39	128.05	153.41	131.67	-0.15	-0.17	-0.31
H	1030	23.	0.024	194.33	131.64	153.28	134.32	0.00	0.00	0.00
p-Br	1330	24.2	0.018	193.94	129.31	151.55	133.21	0.26	0.23	0.15
p-Cl	1747	33.6	0.0192	194.00	129.30	151.55	132.84	0.27	0.23	0.11
p-NO$_2$	4590	96.	0.021	193.42	132.04	149.32	140.29	0.82	0.78	0.79
m-NO$_2$	2720	80.3	0.0295	193.36	131.24	149.45	136.07	0.70	0.71	0.67
o-NO$_2$	4960	75.	0.0151	193.73	132.95	147.78	130.35	------	------	------
o-MeO	810	12.6	0.0156	195.13	129.34	148.65	123.21	------	------	------
m-Br	1320	30.6	0.232	193.81	129.95	151.09	136.37	0.38	0.39	0.40

* Note: σ^o, σ, and σ+ given in reference (21).

DISCUSSION

Synthesis:

It is evident from Table 6, that the ratio of cinnamaldehyde to benzaldehyde is highest for the synthesis of cinnamaldehydes with electron-withdrawing substituents. Remember from the "Introduction" that the first step of the aldol condensation reaction involves the abstraction of an alpha hydrogen on acetaldehyde to form a negatively charged anion. In the second step, this anion acts a nucleophile and attacks the benzaldehyde carbonyl carbon. An electron-withdrawing substituent would cause the benzaldehyde to be more labile by two means. One, the electron-withdrawing substiuent would destabilize the reaction site by withdrawing electron density from the already electron deficient carbonyl carbon. Two, an electron-withdrawing substituent would stabilize a transition state involving the attack of a negatively charged species. Thus, the ratio of cinnamaldehyde to benzaldehyde is higher for electron-withdrawing substituents versus electron-donating substituents.

Absorption Spectra:

Appendix C contains UV-visible absorbance spectra for each cinnamaldehyde before any bisulfite addition. These scans were taken from 500 to 190 nm.

The absorption spectra of meta and para substiuted cinnamaldehyes show one distinct peak between 400 to 250 nm with no structural features. However the absorption spectra of the ortho substituted cinnamaldehydes showed multiple peaks See Appendix C, Spectra C1 and C2). o-nitrocinnamaldehyde showed a large peak at 260 nm with shoulders at ~280 and 320 nm. o-methoxycinnamaldehyde showed a peak at 288 nm and a less intense peak at 323nm. Benzene itself has two main bands caused by $\pi \rightarrow \pi^*$

transitions, one at 203 nm, the ^1L_a band, and one at 256 nm, the ^1L_b band (19). In benzene, these transitions are forbidden and thus are low in intensity (ε~100). However as substituents are added, the symmetry is perturbed and the bands become much more intense. In nitrobenzene, only one band is observed, occuring at 268.5 nm (19). Since the nitro group is a highly conjugative substituent, the ^1L_a bands experiences a bathochromic shift which causes it to swamp the less intense ^1L_b band. This evidently explains why, in our highly conjugated meta and para substituted cinnamaldehyde sytems, there is only one band observable.

When Labhart examined the spectrum of nitrobenzene is in a strong field, he found that there are actually three bands visible, an intense band at 250 nm, a very weak band at 330, and a shoulder at 280 nm (20). Labhart assigned the band at 330 to the $n\text{->}\pi^*$ transition and the band at 280 nm to the $\pi\text{->}\pi^*$ transition corresponding to the ^1L_a band of benzene. The band at 250 nm he called a CT band or intramolecular charge transfer band, in which the aromatic ring itself is the electron-donator and the nitro group is the electron-acceptor.

In the ortho case, the system becomes much more sterically crowded and rotation of the aldehyde chain may occur to alleviate the steric strain. The effect of rotation about this essentially single bond is to lower the amount of conjugation in the system. This would cause hypsochromic shifts of the $\pi\text{->}\pi^*$ transitions while the CT band should not be effected. Thus the separation of the CT and ^1L_a band should increase and more resolution should be obtained for greater steric crowding. Thus, in o-methoxycinnamaldehyde, two peaks are observed where the band at 323 nm is due to the CT band (charge transfer from the o-MeO group to the electron deficient carbonyl) and the band at 288 nm is probably due to the ^1L_a transiton of benzene. In, o-nitrocinnamaldehyde the bands at 260 and 280 are probably due to the ^1L_a and CT bands while the small shoulder at 320 nm is probably either the forbidden n->π* transition or the ^1L_b benzene band or some combination of these two. Even if the band transitions cannot be assigned exactly, it is clear that the side chains in the ortho substituted cinnamaldehydes are not coplanar and that, thus, there is some reduction of conjugative effects.

Equilibrium:

The standard error in the slope and intercept in the 1/A versus [HSO_3-] plot for p-methylcinnamaldehyde and p-chlorocinnamaldehyde was estimated using the JMP statistical program. An average of the standard errors for the slope and intercept of both of these plots was taken. The errors were found to be 2.8% in the slope and 1.5% in the intercept. The error in Keq was then taken as the sum of these percent errors since Keq=slope/intercept. Therefore the error in Keq was estimated to be 4.1%.

The error in the value of Keq for m-nitrocinnamaldehyde is probably higher than that reported in Table 11. As was noted in the "Results" section, the absorbance versus time plot for the kinetics showed an increase in absorbance as time went to infinity. This increase could be corrected for in the kinetics measurements by assuming that Ainf. was the absorbance immediately following the decrease in absorbance from the bisulfite addition. However, since absorbance measurements for Keq determination were taken at equilibrium, the value of Keq was uncorrected. This increase in absorbance should become more important for later aliquots of bisulfite since the overall aldehyde absorption is much smaller. Since Keq is determined from a plot of 1/A versus [HSO_3-], Keq may be lower than the value in Table 11.

Kinetics:

The error in k1 was estimated in much the same way as it was for Keq. Remember that k1 is simply the slope of the plot of k' versus [HSO_3-]. The average error in the slope and thus in k1 was found to be approximately 0.9%. The calculated error for each value of k1 is summarized in Table 13.

If the plots of k' versus [HSO_3-] are examined for the wide range of substituted cinnamaldehydes, it is found that the straight line often does not go through 0,0. At first since the plots for p-methyl-, o-methoxy-, p-bromo- and o-nitro- and trans-cinnamaldehyde have positive y-intercepts, it was thought that this was evidence of some fast reaction. L. Nicosia, who observed a positive intercept for the k' versus [HSO_3-] plot for p-dimethylaminocinnamaldehyde, hypothesized the involvement of the sulfite ion in some fast reaction. However, since we also observe negative intercepts for m-bromo-, m-nitro-, and p-chlorocinnamaldehyde, the presence of some fast reaction in the mechanism is not supported. There is also no obvious correlation between electronic substiuent effects and the magnitude of the intercept. It is more likely that the non zero intercept is due to error in the plot. Errors can arise when only three points are used to obtain a straight line. The intercept for k' versus [HSO_3-] for p-methoxycinnamaldehyde, which used six points, is nearly zero.

Substituent Effects:

Table 15 shows a correlations matrix for single parameter linear regressions for the meta and para substituted cinnamaldehydes only. The table contains the R values for each of these correlations. The R values in bold type face indicate the best correlations obtained.

Figure 14 shows a plot of log K/KH versus log k/kH, where K is the equilibrium constant for a substituted cinnamaldehyde, KH is the equilibrium constant for the cinnamaldehyde where H is the substituent, k is the rate

UN82 HOFF. S.M. LINEAR FREE ENERGY CORRELATIONS OF THE EFFECT OF SUBSTITUENTS. etc
H6981/1990 CHEMISTRY HRS. 6/90 2 of 3

Table 15: Correlations Matrix for meta and para Substituents (R values for linear correlations between variables)

Variable	∂ A ppm	∂ B ppm	∂ C ppm	∂ D ppm	log Keq	log k1	sig°	sig	sig+	∂E/ppm
∂ A ppm	1.0000	-0.6331	0.9728	-0.7188	-0.8746	-0.8848	-0.9468	-0.8787	-0.7687	-0.0022
∂ B ppm	-0.6331	1.0000	-0.7458	0.9512	0.8727	0.8969	0.8218	0.8885	0.9375	-0.4342
∂ C ppm	0.9728	-0.7458	1.0000	-0.8328	**-0.9403**	**-0.9425**	**-0.9912**	-0.9588	-0.8825	0.1113
∂ D ppm	-0.7188	0.9512	-0.8328	1.0000	0.9103	0.9090	0.8907	0.9436	**0.9767**	-0.4355
log Keq	-0.8746	0.8727	**-0.9403**	0.9103	1.0000	0.9882	**0.9692**	0.9594	0.9260	-0.2615
log k1	-0.8848	0.8969	**-0.9425**	0.9090	0.9882	1.0000	**0.9720**	0.9686	0.9364	-0.2753
sig°	-0.9468	0.8218	**-0.9912**	0.8907	**0.9692**	**0.9720**	1.0000	0.9812	0.9237	-0.1728
sig	-0.8787	0.8885	-0.9588	0.9436	0.9594	0.9686	0.9812	1.0000	0.9786	-0.2793
sig+	-0.7687	0.9375	-0.8825	**0.9767**	0.9260	0.9364	0.9237	0.9786	1.0000	-0.4186
∂E/ppm	-0.0022	-0.4342	0.1113	-0.4355	-0.2615	-0.2753	-0.1728	-0.2793	-0.4186	1.0000

constant for a substituted cinnamaldehyde, and kH is the rate constant for the cinnamaldehyde where H is the substituent. This plot gave the best correlation of all with an R^2 value of 0.960 and a slope of 1.129. The ortho substituents were included in this plot and the log k/kH values correlate well with the log K/KH values. This was expected since the substrate and reactant (cinnamaldehyde and bisulfite) were the same for the two reaction systems. If we define σ=log K/KH, then log k/kH=$\rho\sigma$ and ρ=1.13 for this reaction system.

Note from Table 15, that the best correlation of log Keq or log k1 versus σ values was that versus σ°. The R^2 value for the plot of log K/KH (Figure 15) was 0.939 while the R^2 value for the plot of log k/kH versus σ° (Figure 16) was 0.945. Table 16 summarizes the sources of σ, σ+, and σ°. As is said in Table 15, σ° values were obtained from meta substituted benzene derivatives in which the reaction site was isolated from the substituent by a least one methylene group. In this way, resonance interactions between the reaction site and the substiutuent were eliminated. σ° is therefore a polar substituent parameter. The excellent correlation obtained between the equilibrium and kinetics data of the cinnamaldehyde-bisulfite reaction and σ° suggests that the substituents effect the rate and equilibrium mostly by polar effects, not by conjugative

Table 16: Sources of Various σ-Values

σ-value	Source
σ	benzoic acid dissociation
σ°	correlations of several series of m-substituted aromatics having a methylene-isolated reaction site
σ+	solvolysis of t-cumyl chlorides

Figure 14: log k/kH versus log K/KH

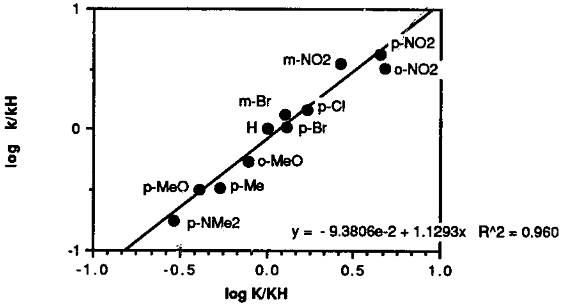

Figure 15: log K/KH versus sigma°

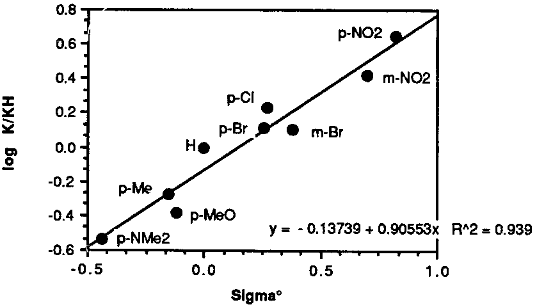

Figure 16: log k/kH versus sigma°

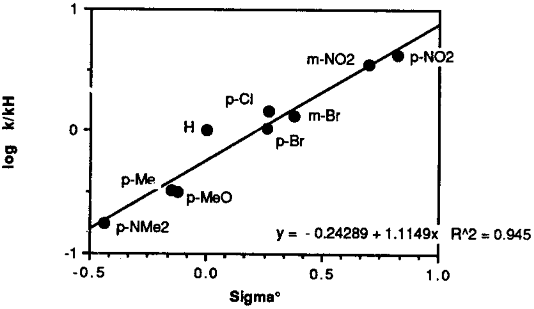

effects. This leads us to two conclusions. First, stabilization of the starting aldehyde as suggested by Young and Jencks must be of less importance than stabilization of an intermediate since it can be stabilized by direct conjugative interactions with electron-donating substituents (See Figure 17).

Figure 17: Resonance Structures for Cinnamaldehyde Stabilization by An Electron-Donating Group (p-MeO)

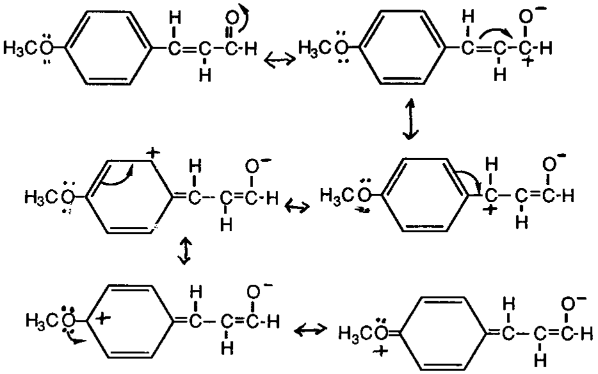

It also suggests that the transition state in the reaction is one that cannot be stabilized by direct conjugative effects. As will be mentioned, this mechanism involves a two step process with an intermediate (See Figure 19); therefore, there are actually two transition states. Since the first step will prove to be the rate-determining step, we will, for the most part, concern ourselves only with this first transition state. A proposed transition state would be one in which the double bond of the carbonyl group is eliminated to preclude any conjugative interactions (Figure 18):

Figure 18: Proposed First Transition State for the Nucleophilic Attack of Bisulfite on Cinnamaldehyde

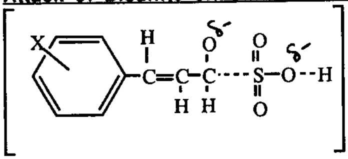

Note however that the correlation for log k/kH versus σ° (Figure 15) is better than that for log K/KH versus σ° (Figure 16). This could be due to two reasons: One, that there is less error in the rate measurements or two, that there is more of a conjugative effect for the equilibrium constants than for the kinetics constants. There is some support for the first conclusion; the ρ for Figure 15 is 0.9055 versus 1.115 for Figure 16. This indicates that the rate is more sensitive to substituent effects than is the equilibrium. This was evident qualitatively from Table 14: note that Keq only increases by a factor of 15.3 from p-dimethylaminocinnamaldehyde to p-nitrocinnamaldehyde while k1 increases by a factor of 24. Therefore a small error in the kinetics measurements is less important than it is in the equilibrium measurements.

There is, however, some evidence that the conjugative effect is more important in the equilibrium measurements than in the kinetics measurements. A case in point is p-methoxycinnamaldehyde. We see that its equilibrium constant, 422 M^{-1}, is 1.3 times as small as the equilibrium constant for p-methylcinnamaldehyde, while its rate constant, 7.25 $M^{-1}s^{-1}$, is nearly the same as the rate constant for p-methylcinnamaldehyde. The p-methoxy group is inductively electron-withdrawing due to the electronegativity of the oxygen atom, while it is electron-donating by resonance due to the lone pair of electrons in the p orbital parallel to the delocalized pi system of the aromatic ring. Since in our reaction system, electron-donating substituents tend to decrease Keq and k1, Keq of p-methoxycinnamaldehyde is much more effected by resonance than is k1. However, since we do not see a pronounced effect like the one for p-methoxycinnamaldehyde for any of the other substituents (particularly p-dimethylaminocinnamaldehyde), this may not be extremely important.

From Figures 15 and 16, we see that ρ is positive. This indicates that the slow step in the mechanism involves attack of the negative bisulfite molecule rather than protonation of the carbonyl oxygen. Protonation of the carbonyl oxygen would tend to increase the rate for more electron-donating substituents, resulting in a negative value for ρ. A consistent mechanism is seen in Figure 19, in which the slow step is the attack of the negative bisulfite ion on the carbonyl carbon and the fast step involves the protonation of the O- atom to form the hydroxy group:

Figure 19: Mechanism of the Cinnamaldehyde-Bisulfite Reaction

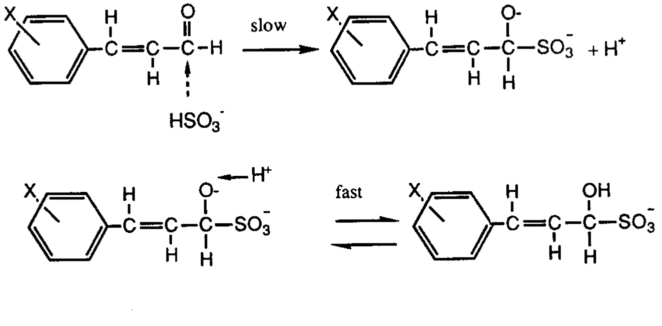

The correlations of the 13C NMR chemical shifts of the various cinnamaldehyde carbons with the experimental equilibrium and rate data can be examined for possible trends. The pertinent carbons are again labeled below:

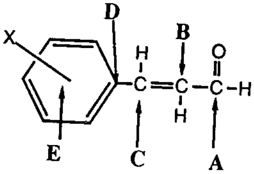

When we look at the correlations of the chemical shifts of the various cinnamaldehyde carbons with log Keq or log k1 (Table 15), we see that the best correlations of the experimental data are those with the C carbon. Figure 20 shows the correlation of log K/KH with ∂C-∂CH and Figure 21 shows the correlation of log k/kH with ∂C-∂CH (R^2=0.884 for Figure 20 and R^2=0.888 for Figure 21). To realize the significance of this correlation, we must first understand how the substituent may electronically effect the chemical shift of the C carbon. First of all, from Table 14, we see that the best correlation of ∂C with the various σ values is the one between ∂C and σ° (see Figure 22). We have already discussed that σ° may be used as a polar substituent constant. Therefore the excellent correlation shown in Figure 22 indicates that substituents effect ∂C by polar effects not by conjugative interactions. The reason for this fact become evident when we examine the resonance structures for a substituted cinnamaldehyde such as p-nitrocinnamaldehyde (Figure 23).

Figure 20: log K/KH versus ∂C-∂CH

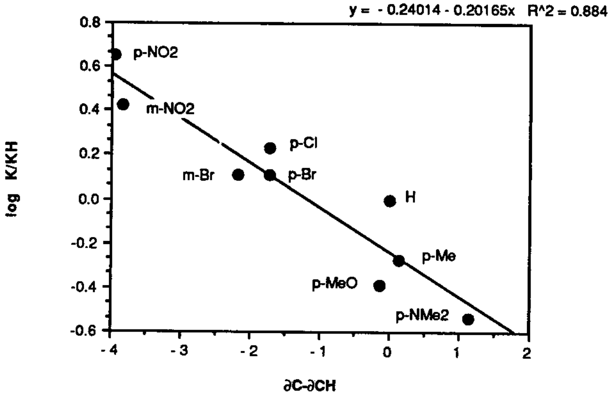

Figure 21: log k/kH versus ∂C-∂CH

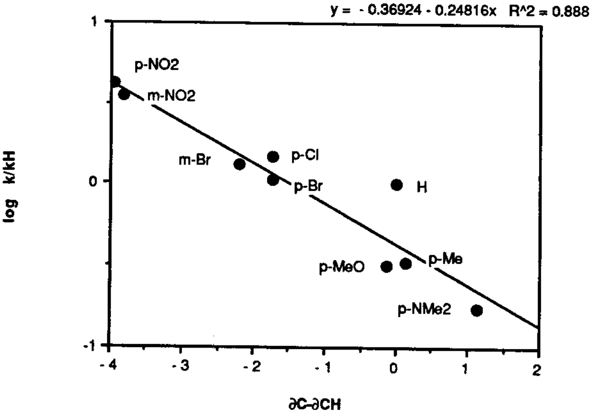

Figure 23: Resonance Structures of p-Nitrocinnamaldehyde

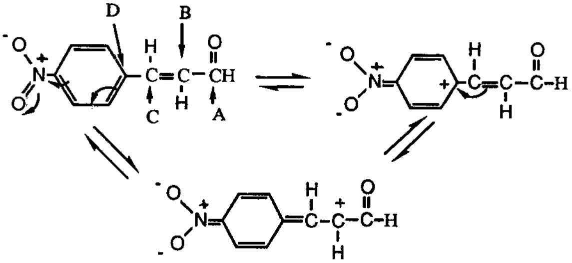

The charge is never delocalized onto the C carbon. Thus, the substituent influences the chemical shift of C carbon by polar effects not by direct conjugative interactions. We can therefore think of ∂C as a polar substituent parameter. The good correlation of log K/KH and log k/kH with ∂C provides further evidence for the proposed transition state of Figure 18.

We can now consider the importance of the other carbon chemical shifts as possible substituent parameters. The D carbon, for example, gives an excellent correlation with σ+ (Figure 24). σ+, according to Table 15, is derived from the solvolysis of t-cumyl chlorides. During this reaction a positive charge is formed at the reaction site which can have direct conjugative interactions with the substituent. Therefore σ+ is primarily a conjugative parameter. The correlation of ∂D with σ+ indicates that substituents may effect the chemical shift of the D carbon primarily by conjugative interactions. This conclusion is supported by the resonance structures of Figure 25 for p-nitrocinnamaldehyde. The positive charge is delocalized directly onto the D carbon; therefore, the chemical shift of the D carbon is influenced to a great extent by direct conjugative interactions with the substituent.

Figure 22: ∂C versus sigma°

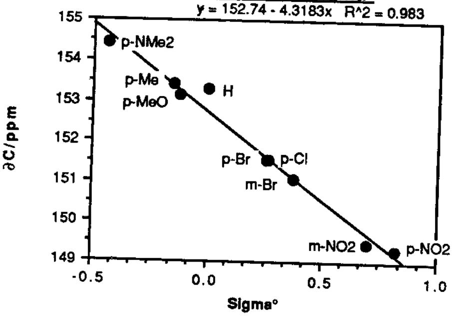

Figure 24: ∂D versus Sigma+

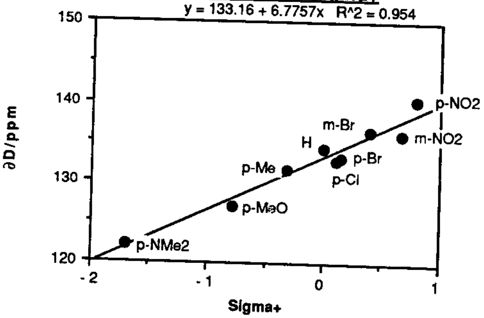

Figure 25: ∂D-∂C versus sigma+

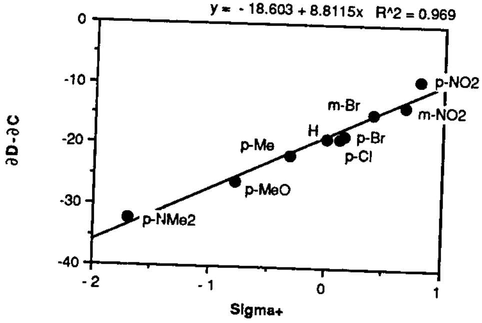

Although ∂D may be thought of as primarily a conjugative substituent parameter, it may still be influenced to a much smaller extent by the polar contribution of the substituent. In fact, as is shown by Figure 23, σ+ correlates better with ∂D-∂C than with ∂D alone (R^2=0.954 for ∂D vs. σ+ and R^2=0.969 for ∂D-∂C vs. σ+). By substracting ∂C from ∂D, we are substracting the polar effect from the chemical shift of the D carbon. Keep in mind, however, that the polar effect at the C carbon is probably smaller than that at the D carbon due to the relative distances of these carbons from the substituent position.

The chemical shift of the E carbon, ∂E, does not appear to correlate with any of the other variables in Table 14. As was mentioned in the Introduction, the carbon at which the substituent is attached is subject to many other factors unrelated to the electronic effect of the substituent such as purely magnetic effects. Therefore ∂E has little use as a electronic substituent parameter.

∂A's best correlation seems to be with σ° (Table 15, R=0.948) and with ∂C (Table 15, R=0.9728). From the resonance diagrams of Figure 23, we see that the positive charge is never delocalized onto the A carbon. Therefore, it is expected that ∂A would be influenced by polar effects; thus, the good correlation with σ° and ∂C.

∂B's best correlation seems to be with σ+ (Table 15, R=0.9375) and with ∂D (Table 15, R=0.9512). From the resonance diagrams of Figure 23, we see that the positive charge is delocalized directly onto the B carbon. Therefore, ∂B would experience the electronic effect of a substituent mostly by conjugative interactions; thus, the good correlation with σ+ and ∂D.

Although ∂A and ∂B may be thought of as inductive and resonance substituent constants respectively, the A and B carbons are physically much further from the substituent site than are the C and D carbons. Thus the change in chemical shift for the A and B carbons is much smaller than for the C and D carbons and there is much more room for error. The chemical shift for the A carbon changes by only 1.77 ppm while the chemical shift for the C carbon changes by 5.76 ppm. By the same token, the chemical shift for the B carbon changes by only 8.84 ppm while the chemical shift for the D carbon changes by a hefty 18.24 ppm. Since ∂C and ∂D are much more accurate due to their larger range, ∂A and ∂B are of little use in obtaining optimum correlations and will be ignored in the correlations involving the ortho substituents.

Table 17 shows the matrix for correlations of variables involving para, meta, and ortho substituents. Note that the correlation of log Keq and log k1 versus ∂C is much lower than the correlation obtained from the exclusion of the ortho substituents in Table 15. Clearly log K/KH and log k/kH for the ortho substiuents do not correlate with ∂C. However, one important fact was obtained from the correlations of Table 17: although ∂C and ∂D show some correlation with log Keq and log k1, the correlation between ∂C and ∂D is very poor (R=-0.2575). This indicates that ∂C and ∂D measure completely independent effects. As has been said earlier, ∂C can be used as an polar substituent constant, while ∂D can be used as a conjugative substituent constant.

To correlate the ortho substituents with the meta and para substituents by Hammett's equation, new σ constants were calculated from the equilibrium data and ∂C and ∂D. In his correlation of benzoic acid dissociations, Hammett defined a linear relationship, log K/KH=ρσ, where ρ=1.000 and σ=0 for H. We defined a relationship where:

$$\log K/KH=[c^*(\partial C-\partial CH) + d^*(\partial D-\partial DH)]\,\rho,$$

where: ∂C-∂CH=the polar substituent effect
∂D-∂DH=the conjugative substituent effect
c= the sensitivity of the cinnamaldehyde-bisulfite reaction to polar effects
d=the sensitivity of the cinnamaldehyde-bisulfite reaction to conjugative effects

Table 17: Correlation Matrix for All Substituents Including Ortho (R values for linear correlations between variables)

Variable	∂ A ppm	∂ B ppm	∂ C ppm	∂ D ppm	∂E/ppm	log Keq	log k1
∂ A ppm	1.0000	-0.4755	0.2990	-0.7595	0.2439	-0.7028	-0.7466
∂ B ppm	-0.4755	1.0000	-0.7281	0.6875	-0.2911	0.8921	0.8976
∂ C ppm	0.2990	-0.7281	1.0000	-0.2575	-0.1653	-0.8022	-0.7549
∂ D ppm	-0.7595	0.6875	-0.2575	1.0000	-0.5497	0.6895	0.7650
∂E/ppm	0.2439	-0.2911	-0.1653	-0.5497	1.0000	-0.1861	-0.2445
log Keq	-0.7028	0.8921	-0.8022	0.6895	-0.1861	1.0000	0.9799
log k1	-0.7466	0.8976	-0.7549	0.7650	-0.2445	0.9799	1.0000

The individual parameters ∂C, ∂CH, ∂D, and ∂DH are defined below:

∂C=chemical shift of the C carbon in the substituted molecule
∂CH=chemical shift of the C carbon in the unsubstituted molecule
∂D=chemical shift of the D carbon in the substituted molecule
∂DH=chemical shift of the D carbon in the unsubstituted molecule

Both the equiliibrim and NMR data is referenced to H, as Hammet did for the benzoic acid dissociation. We then defined $\rho=1.000$ for the cinnamaldehyde-bisulfite reaction as Hammet did for the benzoic acid dissociation. The system then simplified to a system of two unknowns, c and d, and 10 equations for each substituent (H is eliminated since log 1=0, ∂CH-∂CH=0, and ∂DH-∂DH=0). The program, SEQS 2.02, Simultaneous Equation Solver, was used to obtain the values of c and d which minimized the errors for the equation matrix.

The following values were obtained from SEQS: c, -0.107, and d, +0.0407. Note that the signs of c and d are opposite. This was expected since the correlation of ∂C with log Keq and log k1 was negative while the correlation of ∂D with log Keq and log k1 was positive. c is also over twice the size of d in magnitude, indicating that the transference of the substituent effects occurs to a larger extent by polar effects than by direct conjugative interactions, as was expected from the good correlation seen in Figures 15, 16, 20 and 21.

We can now calculate new values of σ called σ_{SH}. Remember that we defined a relationship:

$$\log K/KH = [c^*(\partial C-\partial CH) + d^*(\partial D-\partial DH)]\ \rho$$

This is virtually the same as Hammet's equation:

$$\log K/KH = \sigma\ \rho \qquad \text{where } \sigma = \sigma_{SH} = [c^*(\partial C-\partial CH) + d^*(\partial D-\partial DH)]$$

From ∂C, ∂D, c, and d, a set of σ_{SH} values were defined for all 11 substituents. Table 18 shows the values of σ_{SH} obtained from these calculations.

The order of the values of the σ_{SH} constants is consistent with their overall polar character. Polar effects have two components: resonance effects and inductance effects. p-NMe$_2$ is the most electron-donating substituent due to the donation of electrons through resonance and thus has the most negative σ_{SH} value. The σ_{SH} value of p-MeO falls between the σ_{SH} values of p-NMe$_2$ and p-Me. This is due to the electron-donating character of the p-MeO group through the resonance interactions discussed earlier. The para substituted halogens fall on the electron-withdrawing side of the σ_{SH} scale. p-Cl and p-Br both have some electron-donating character by resonance since the lone pairs can be donated by resonance. However this electron-donating character is far outweighed by the extreme inductive electronegative character of the halogen atoms. m-Br which shows much less electron-donating character because of its lack of resonance interactions with the reaction side chain, shows, as expected, a more positive σ_{SH} value than p-Br. The nitro substituents show similar sorts of effects. The p-NO$_2$ group can withdraw electron density both by inductance and by resonance, while the m-NO$_2$ group can withdraw electron density only by inductive means. Therefore, p-NO$_2$ has a more positive σ_{SH} value than m-NO$_2$.

The ortho σ_{SH} values, o-MeO and o-NO$_2$, are also consistent with experimental observations. In examining the absorbance spectra of o-methoxycinnamaldehyde and o-nitrocinnamaldehyde, we hypothesized that, due to the proximity of the ortho substituent to the side chain, there was some rotation of the side chain to alleviate the steric strain involved in the coplanar form. In the coplanar form, where there is no rotation of the side chain, the polar effect is delocalized all the way to the B carbon or the carbon α to the reaction site. As the value of the rotation angle increases there is less and less pi

Table 18: σ_{SH} Values

Substituent	σ_{SH}
p-NMe_2	-0.6209
p-MeO	-0.2819
p-Me	-0.1219
H	0.0000
o-MeO	0.0432
p-Cl	0.1250
p-Br	0.1401
m-Br	0.3181
o-NO_2	0.4273
m-NO_2	0.4815
p-NO_2	0.6673

overlap and the delocalized polar effect at the B carbon is reduced. Therefore, we should expect the σ_{SH} values of o-NO_2 to be less positive (electron-withdrawing) than the σ_{SH} value of p-NO_2, which it is. o-MeO should show a reduced resonance polar effect (MeO is electron-donating by resonance and electron-widthdrawing by inductance) and its σ_{SH} value should become more positive, which it does.

Figure 26 shows the plot of log K/KH versus σ_{SH}. The correlation constant, R^2, for this line is 0.887. This correlation, while not excellent, is significantly higher than the correlation of log K/KH versus ∂C-∂CH for which R^2=0.644. The o-NO2 and o-MeO points appear to be well correlated by the σ_{SH} values. The only outstanding deviation from the line is the point for m-NO_2. Remember that the values were more inaccurate for Keq for m-nitrocinnamaldehyde than for k1. It appears that this error is significant from Figure 26.

Figure 27 shows the plot of log k/kH versus σ_{SH}. R^2 for this plot equals 0.918, which is significantly better than the correlation of log K/KH versus σ_{SH}.

Figure 26: log K/KH vs. sigma SH

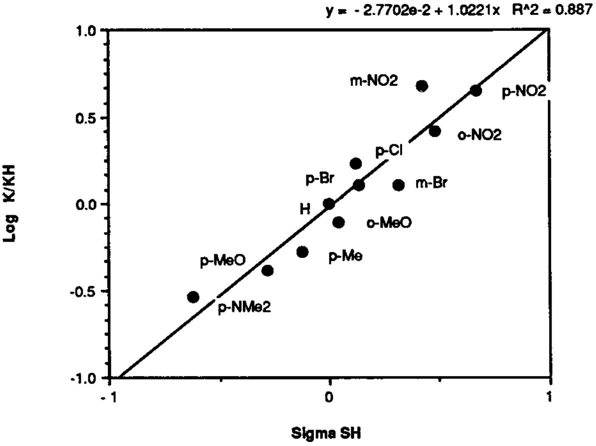

Figure 27: log k/kH versus SigmaSH

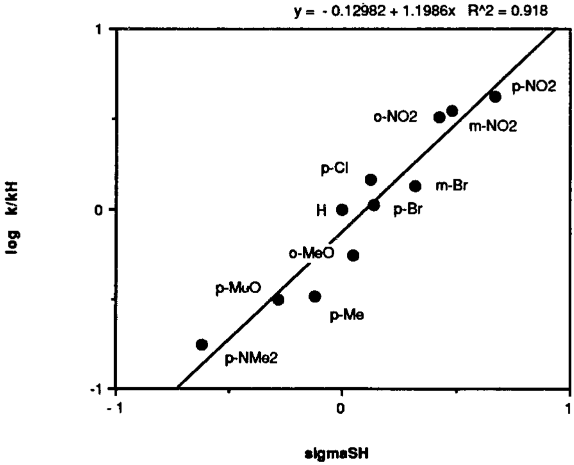

One other difference besides the better correlation is noted for Figure 27 versus Figure 26; from Table 17, we see that ρ for log k/kH versus σ_{SH} is 1.199, compared to ρ=1.022 for log K/KH versus sSH. This means that k1 is more sensitive to substituent effects than is Keq for the cinnamaldehyde-bisulfite reaction.

The importance of any σ value is limited by its range of applicability. If our σ_{SH} values apply only to the equilibrium and kinetics of the cinnamaldehyde-bisulfite adduct formation reaction, they will have little use. Therefore, correlations involving other reaction series with σ_{SH} values were attempted. Figure 28 shows the attempted correlation of σ_{SH} with log K/KH for the dissociation of benzoic acids (23). It is evident that o-NO2 and o-MeO do not correlate with the σ_{SH} values although there is limited correlation of the meta and para substiutents. However, the benzoic acid dissociation series is one in which conjugative effects are important due to the direct attachment of the carboxyl group to the aromatic ring. Since we have already stated that the σ_{SH} are much more dependent on polar effects over conjugative effects, we would not expect the benzoic acid dissociation series to correlate.

A reaction series which we would expect to correlate with the σ_{SH} values is the dissociation of trans-cinnamic acids (23) due to the obvious similarity of the cinnamic side chains. Figure 29 shows the plot of log K/KH versus σ_{SH} for trans-cinnamic acid dissociation. This correlation which included o-nitrocinnamic acid is quite good, R^2=0.951. In fact it is much better than the correlation of the cinnamaldehyde-bisulfite reaction with σ_{SH}! Some caution should be exercised over this correlation, however, since only seven substituents are used and a K value for o-methoxycinnamic acid could not be

Figure 28: log K/KH versus SigmaSH for Ionization of Benzoic Acids

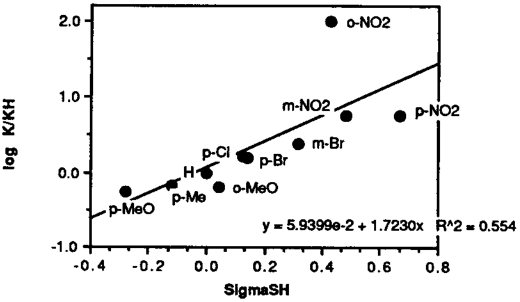

Figure 29: log K/KH versus SigmaSH for the Ionization of trans-cinnamaic acids

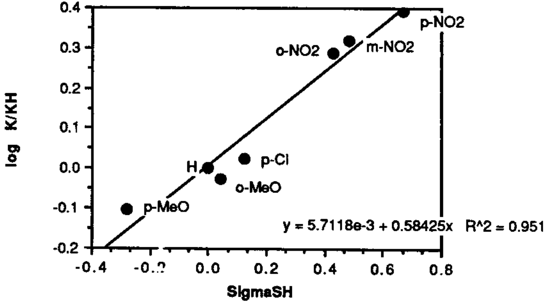

Figure 30: log K/KH versus SigmaSH for the Ionization of Phenylacetic acids

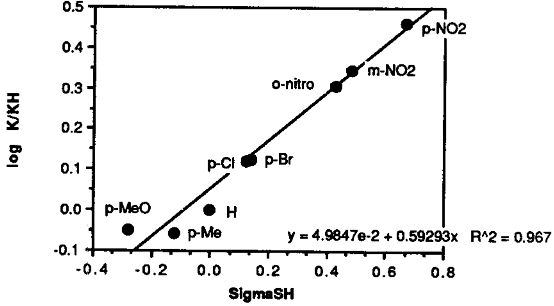

found.

Another reaction series for which we would expect good correlation with σ_{SH} values was the dissociation of phenylacetic acids (23). We expect a good correlation because of phenylacetic acid's similarity to cinnamaldehyde in two respects. First of all, the side chain is longer than benzoic acid by one carbon so that less steric interference with reaction site in the ortho substituted acids should be expected. Second, the methylene group insulates the carboxyl group from direct conjugative effects. Figure 30 shows the plot of log K/KH versus σ_{SH} for phenylacetic acid dissociation. The correlation is excellent, R^2=0.967.

We expected good correlation for phenoxyacetic acid dissociation due to the similarity of this acid to phenylacetic acid. Figure 31 shows the plot of log K/KH versus σ_{SH}. However the correlation was not good at all (R^2=0.818) particularly for the ortho substituents. One hypothesis for this inconsistency is that the oxygen atom in the phenoxy group causes additional proximity effects in the ortho substituted phenoxyacetic acids such as repulsive interactions with the o-MeO group and enhanced resonance interactions with the o-NO_2 group.

Table 19 summarizes the values of ρ and R^2 for all correlations involving σ_{SH}. From Table 19, we see that the ρ's for both cinnamaic acid dissociation and for phenylacetic acid dissociation are much smaller than the ρ for the cinnamaldehyde-bisulfite reaction though still positive in sign. This can be explained by refering to potential energy diagrams for each of these reaction series. For the cinnamaldehyde-bisulfite reaction we would expect that there would be two peaks in the potential energy diagram since the mechanism involves an intermediate. Each of the peaks represents a transition state. Figure 33 shows a proposed potential energy diagram for the cinnamaldehyde-

Figure 31: log K/KH vs. SigmaSH for the Ionization of Phenoxyacetic Acids

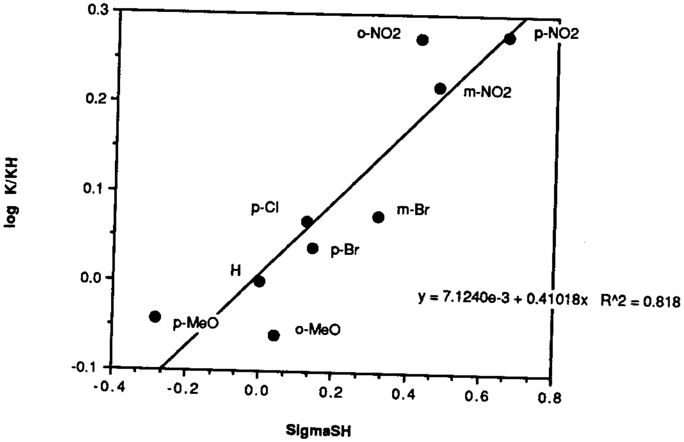

Figure 32: log k/kH versus sigmaSH for the Hydrolysis of Phenyl Acetates

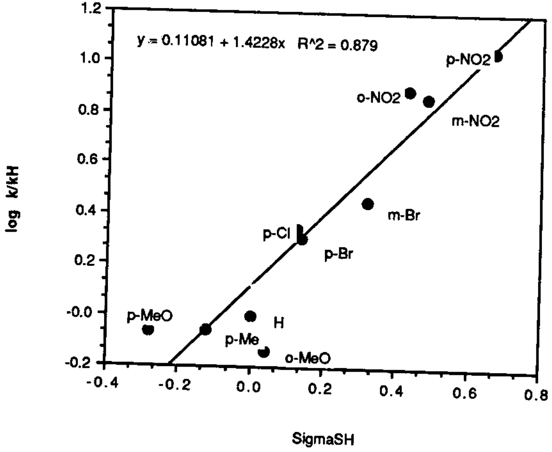

Table 19: ρ and R^2 Values for Correlations Involving σ_{SH} Values

Reaction series	ordinate	ρ	R^2
X-C6H4-CH=CH-CHO + HSO3-	log K/KH	1.022	0.887
X-C6H4-CH=CH-CHO + HSO3-	log k/kH	1.199	0.918
X-C6H4-CH=CH-COOH ionization	log K/KH	0.584	0.951
X-C6H4-CH2-COOH ionization	log K/KH	0.593	0.967
X-C6H4-COOH ionization	log K/KH	*	0.554
X-C6H4-O-CH2-COOH ionization	log K/KH	*	0.818
X-C4H6-CH2-COOC2H5 hydrolysis	log k/kH	*	0.879

* Note: Correlation was poor so an accurate value for ρ was notobtained.

bisulfite reaction.

Note from the reaction mechanism in Figure 19, that the intermediate involves a formal negative charge on the oxygen attached to a tetrahedral sp^3 hybridized carbon. Since the carbon does not have any available p orbitals, the negative charge cannot be stabilized by resonance. Therefore the intermediate should be very unstable and high in energy as seen in Figure 33. By Hammond's postulate the transition states should resemble the intermediate more closely than the starting aldehyde since they are closer in energy to the intermediate than the starting aldehyde. Since the transition states are high in energy, substituents should have a greater effect on the activation energy than for a reaction having a low energy transition state.

Figure 33: Potential Energy Diagram for the Cinnamaldehyde-Bisulfite Reaction

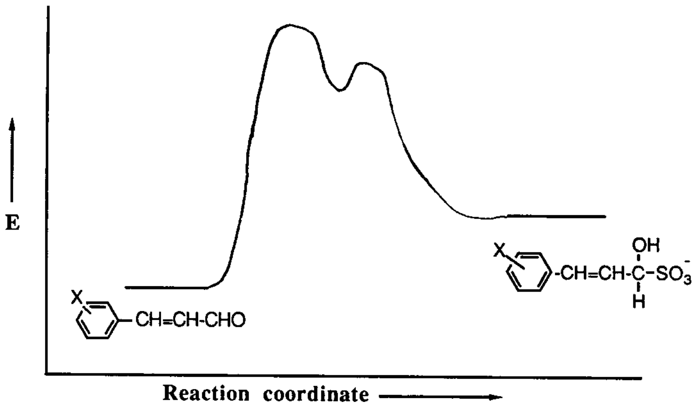

Acid dissociations are one step processes which can be represented by the mechanism below:

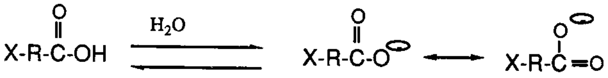

$$\text{X-R-}\overset{\overset{O}{\|}}{C}\text{-OH} \xrightleftharpoons{H_2O} \text{X-R-}\overset{\overset{O}{\|}}{C}\text{-O}^{\ominus} \longleftrightarrow \text{X-R-}\overset{\overset{O^{\ominus}}{|}}{C}\text{=O}$$

A possible potential energy diagram for an acid dissociation is seen in Figure 34.

There is only one peak since there is only one transition state involved in an acid dissociation. Since acid dissociations are usually endothermic, by Hammond's postulate, the transition state should resemble the product more than the starting acid since the product is closer in energy to the transition state. The product has a formal -1 charge on one oxygen atom which can be stabilized by resonance with the carbonyl group. Therefore, the transition state

Figure 34: Potential Energy Diagram for Acid Dissociation

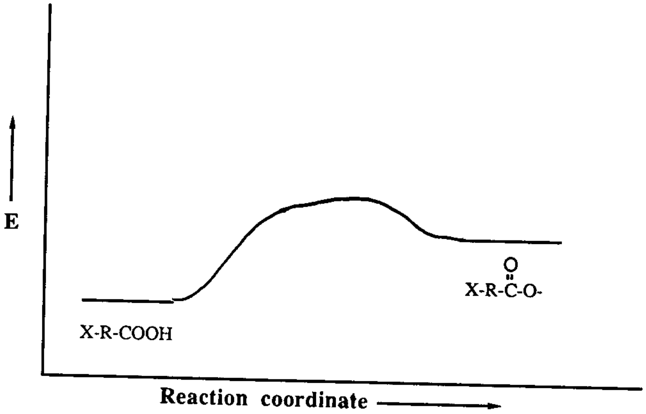

(which resembles the product) is lower in energy, and the reaction has a low energy of activation. Substituents should therefore have a much lower effect in stabilizing or destabilizing the transition state. Thus the values of ρ for the acid dissociations are much lower than the ρ value for the cinnamaldehyde-bisulfite reaction.

All the reaction series discussed so far, except the cinnamaldehyde-bisulfite reaction, have been acid ionizations. Does σ_{SH} correlate with reaction rates? To answer this question, the correlation of the rates of phenyl acetate hydrolysis (22) with σ_{SH} were examined; o-nitrophenyl acetate and o-methoxyphenyl acetate were included in this correlation.

This system was chosen for its similarity to the cinnamaldehyde-bisulfite reaction system in the lack of conjugative interactions with the reaction site. Figure 32 shows the correlation of log k/kH versus

σ_{SH} for phenyl acetate hydrolysis. The correlation for this system is not impressive (R^2=0.879). However, the R^2 value for Figure 32 is comparable to the R^2 value from the correlation of log K/KH versus σ_{SH} for the cinnamaldehyde-bisulfite reaction (R^2=0.887).

The largest deviations from the line in Figure 32 are p-MeO and o-MeO. Remember that p-MeO showed the largest deviation from the line for the correlation of log K/KH versus σ_{SH} for the dissociation of phenylacetic acids. This deviation for p-MeO is in the positive log K/KH direction. Therefore, K is higher than expected from that predicted by σ_{SH}. Since p-MeO is electron-donating by resonance and electron-donation would slow either acid dissociation or ester hydrolysis, the high value of K indicates that conjugative effects are less important for the phenylacetic/phenylacetate systems than they are in the cinnamaldehyde-bisulfite reaction system. This effect is due to the insulation of the reaction site by methylene group in phenylacetate. On the other hand, conjugative effects do play a small role in effecting the equilibrium and kinetics of the cinnamaldehyde-bisulfite. For example, an electron-donating group can stabilize the cinnamaldehyde by conjugative effects and thereby slow the reaction. The conjugative effect is less important than the polar effect, though, since conjugative interactions only effect the ground-state energy of the reactants in Figure 33 while polar interactions can make great changes in the energy of the transition state.

It is uncertain why the rate for the hydrolysis of o-methoxyphenylacetate is lower than that predicted by σ_{SH}. Based on what was said for p-MeO, we would expect the rate for o-MeO to be higher. In any case, it appears that the differences in conjugative interactions between the phenylacetic and cinnamic reaction systems is too great for extremely precise correlations.

Based on the limited correlations of other reaction series, the use of

σ_{SH} values in linear free energy correlations seems to have potential for correlations of reaction series including ortho substiuents. They are limited, however, in their application due to the relative importance of polar versus conjugative effects. In order to correctly assess the viability of σ_{SH} values to correlate reaction series involving ortho substituents, a wider range of σ_{SH} values is needed, particularly for ortho substituents. Further work should concentrate in expanding the present range of meta and ortho σ_{SH} values so that a more thorough examination of substituent effects can be exacted.

REFERENCES

1. V.A. Mohnen, Scientific American, *30* , 259 (1988).

2. B.J. Finlayson-Pitts and J.N. Pitts, Jr., Atmospheric Chemistry, (New York: John Wiley & Sons, Inc., 1986).

3. W. Munger, D.J. Jacob, M.R. Hoffmann, J. Atmos. Chem., *1*, 335 (1984).

4. P. Schlulam, R. Newbold and L.A. Hull, Atmos. Environ., *13*, 123 (1979).

5. D. Grosjean, Environ. Sci. Technol., *16*, 254 (1982).

6. M.R. Hoffmann, D.J. Jacob, J. Geophys. Res., *88*, 6611 (1983).

7. L.W. Richards, J.A. Anderson, D.L. Blumenthal, J.A. McDonald, Atmos. Environ. *17*, 911 (1983).

8. L.A. LeTarte, Senior Thesis, Union College, (1987).

9. F.C. Kokesh and R.E. Hall, J. Org. Chem., *40*, 1632 (1975).

10. T.H. Lowry, K.S. Richardson, Mechanism and Theory in Organic Chemistry (New York: Harper & Row, 1976).

11. L. Nicosia, Senior Thesis, Union College, (1989).

12. P.R. Young, W.D. Jencks, J. Am. Chem. Soc., *101*, 3288 (1979).

13. P.R. Wells, Linear Free Energy Relationships, (London: Academic Press Inc. (London) Ltd., 1968).

14. R.W. Taft, E. Price, I.R. Fox, I.C. Lewis, K.K. Andersen, G.T. Davis, J. Am. Chem. Soc., *85*, 709, (1963).

15. R.W. Taft, E. Price, I.R. Fox, I.C. Lewis, K.K. Andersen, G.T. Davis, J. Am. Chem. Soc., *88*, 3146 (1963).

16. G.E. Maciel, J.J. Natterstad, J. Chem Phys., *2*, 2427 (1965).

17. Ber., 853 (1884).

18. A. Markovac, A.R. Patel, M.P. LaMontagne, A.B. Ash, J. Heterocyclic Chem., *14*, 147 (1977).

19. Jaffe, H.H., Orchin, M., Theory and Applications of Ultraviolet Spectroscopy, (New York: John Wiley & Sons, Inc., 1962).

20. Suzuki, H., Electronic Absorption Spectra and Geometry of Organic Molecules, (New York: Academic Press, Inc., 1967).

21. Ritchie, C.D., Sager, W.F., Progress in Physical Organic Chemistry, *2*, 323 (1964).

22. Nishioka, T., Fujita, T., Kitamura, K., Nakajima, M., J. Org. Chem., *40*, 2520, (1975).

23. Kortum, G., Vogel, W., Andrussow, K., Dissociation Constants of Organic Acids in Aqueous Solution, (London: Butterworth & Co., Ltd., 1961).

Appendix A

Equilibrium and Kinetics Plots

Figure A1: 1/A versus [HSO3-] for p-methylcinnamaldehyde

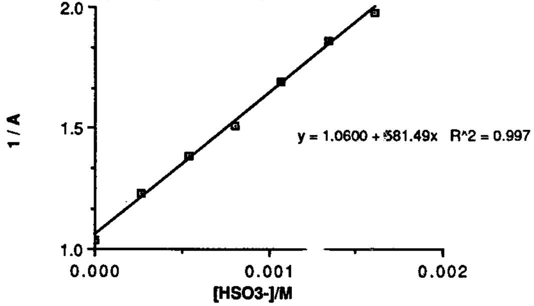

Figure A2: 1/A versus [HSO3-] for m-nitrocinnamaldehyde

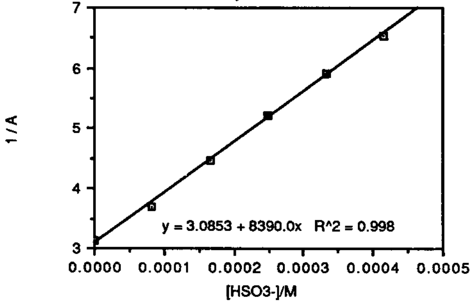

Figure A3: 1/A versus [[illegible]SO3-] for p-bromocinnamaldehyde

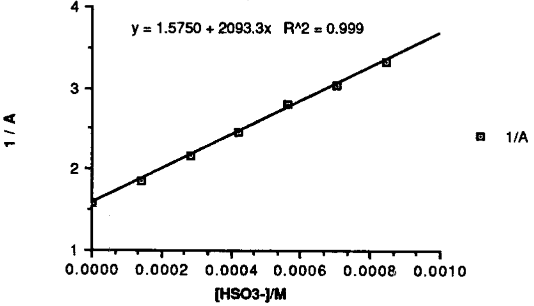

Figure A4: 1/A versus [HSO3-] for p-chlorocinnamaldehyde

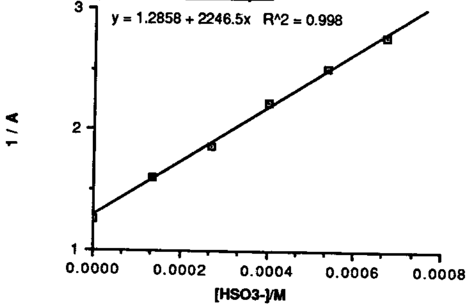

Figure A5: 1/A versus [HSO3-] for m-bromocinnamaldehyde

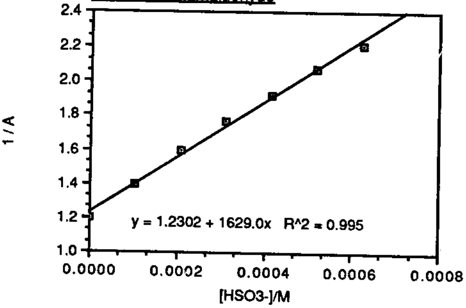

Figure A6: 1/A vs. [HSO3] for o-methoxycinnamaldehyde

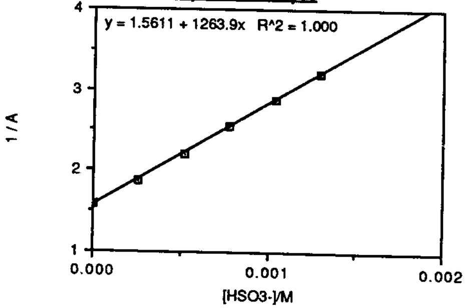

Figure A7: ln[A-Ainf.] versus time. [HSO3-]=8.43e-5 M. for p-nitrocinnamaldehyde

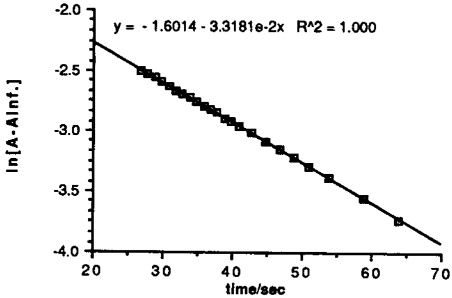

Figure A8: ln[A-Ainf.] versus time. [HSO3-]=2.81e-4 M. for p-nitrocinnamaldehyde

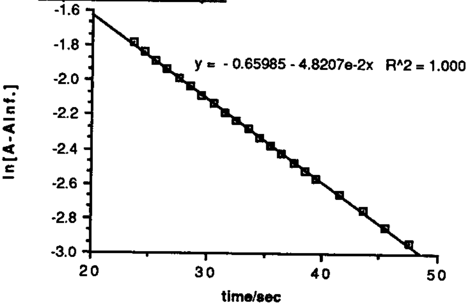

Figure A9: ln[A-Ainf.] versus time. [HSO3]=1.69e-4 M. for p-nitrocinnamaldehyde

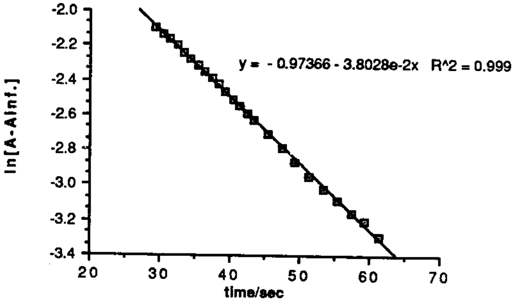

Figure A10: ln[A-Ainf.] versus time. [HSO3-]=5.58e-4 M. for o-nitrocinnamaldehyde

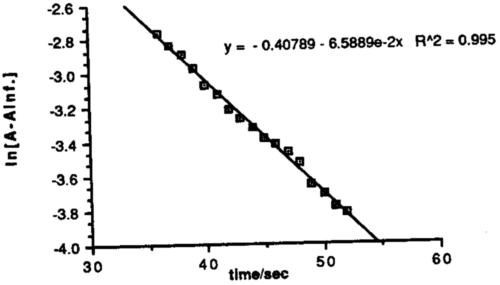

Figure A11: ln[A-Ainf.] versus time. [HSO3-]=8.34e-4 M. for o-nitrocinnamaldehyde

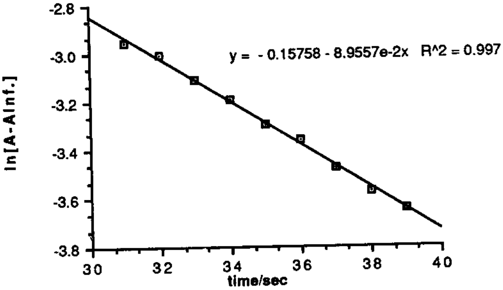

Figure A12: ln[A-Ainf.] versus time. [HSO3-]=6.97e-4 M. for o-nitrocinnamaldehyde

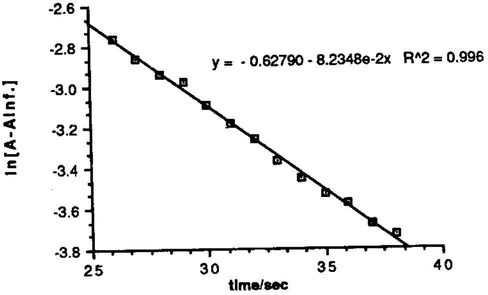

Figure A13: k' versus [HSO3-] for o-nitrocinnamaldehyde

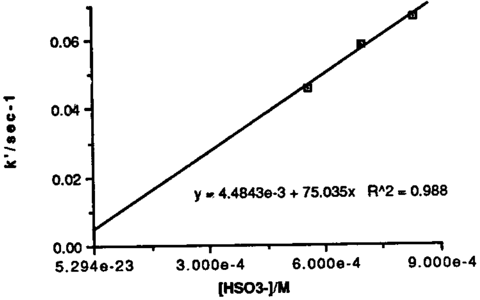

Figure A14: ln[A-Ainf.] versus time, [HSO3-]=2.77e-4 M, for m-nitrocinnamaldehyde

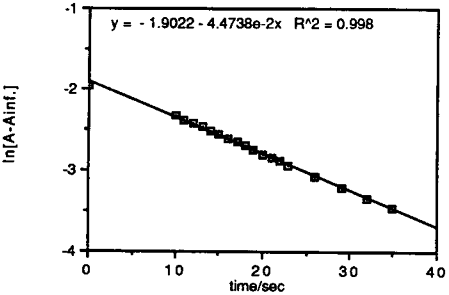

Figure A15: ln[A-Ainf.] versus time, [HSO3-]=4.15e-4 M, for m-nitrocinnamaldehyde

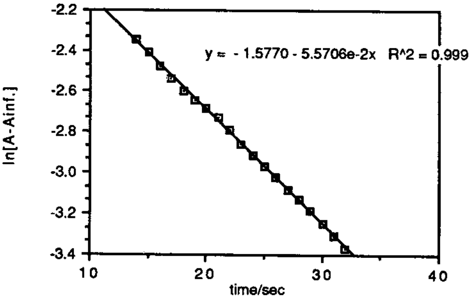

Figure A16: ln[A-Ainf.] versus time, [HSO3-]=5.54e-4 M, for m-nitrocinnamaldehyde

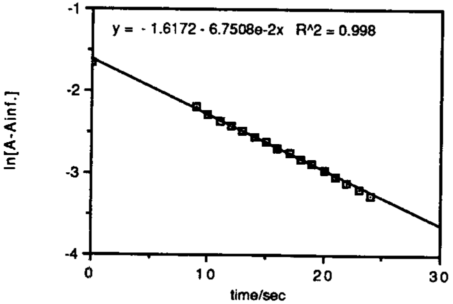

Figure A17: ln[A-Ainf.] versus time, [HSO3-]=8.30e-4 M, for m-Nitrocinnamaldehyde

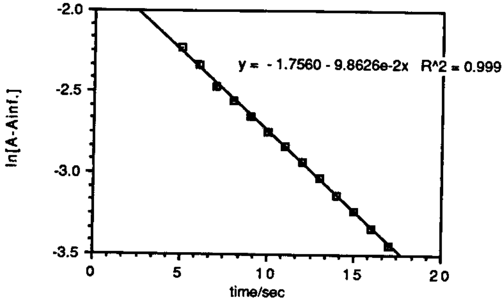

Figure A18: k' versus [HSO3-] for m-Nitrocinnamaldehyde

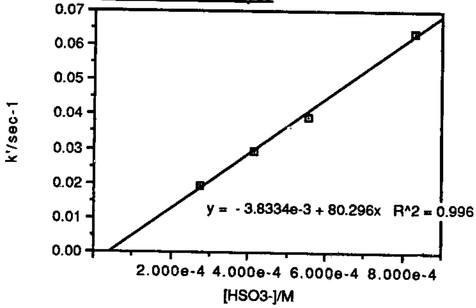

Figure A19: ln[A-Ainf.] vs. time, [HSO3-]=2.60e-4 M, for m-bromocinnamaldehyde

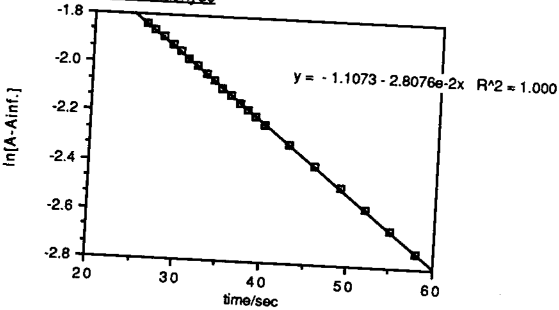

Figure A20: ln[A-Ainf.] versus time, [HSO3-]=1.30e-4 M, for m-bromocinnamaldehyde

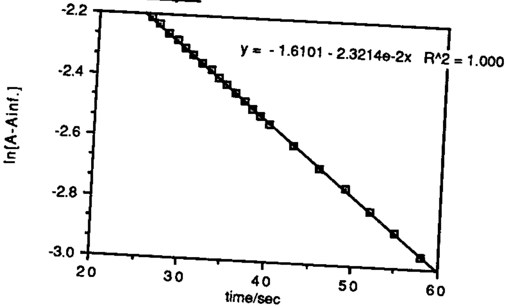

Figure A21: ln[A-Ainf.] versus time, [HSO3-]=3.90e-4 M, for m-bromocinnamaldehyde

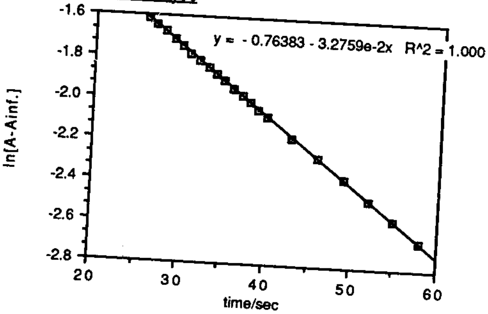

Figure A22: k' versus [HSO3-] for m-bromocinnamaldehyde

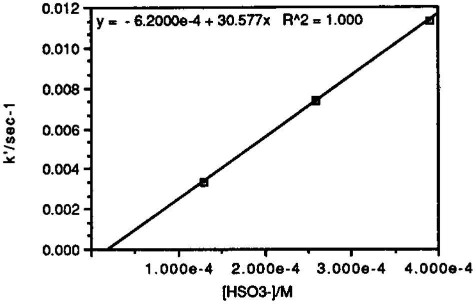

Figure A23: ln[A-Ainf.] versus time, [HSO3-]=1.11e-3 M, for o-methoxycinnamaldehyde

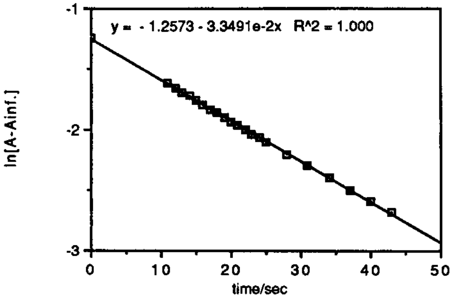

Figure A24: ln[A-Ainf.] versus time, [HSO3-]=8.31e-4 M, for o-methoxycinnamaldehyde

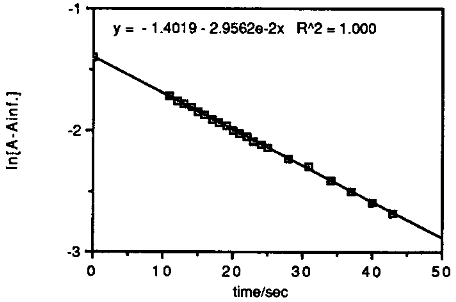

Figure A25: ln[A-Ainf.] versus time, [HSO3-]=5.54e-4 M, for o-methoxycinnamaldehyde

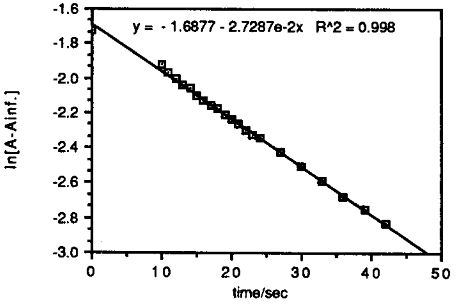

Figure A26: k' versus [HSO3-] for o-methoxycinnamaldehyde

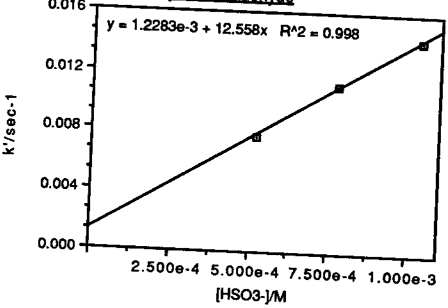

Figure A27: ln[A-Ainf.] versus time, [HSO3-]=2.81e-4 M, for p-bromocinnamaldehyde

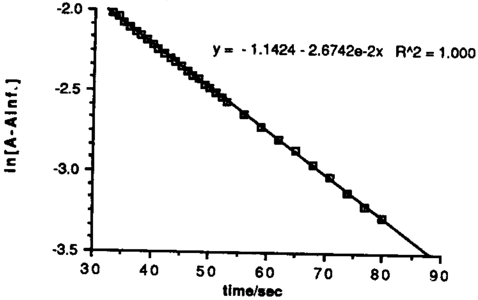

Figure A28: ln[A-Ainf.] versus time, [HSO3-]=5.62e-4 M, for p-bromocinnamaldehyde

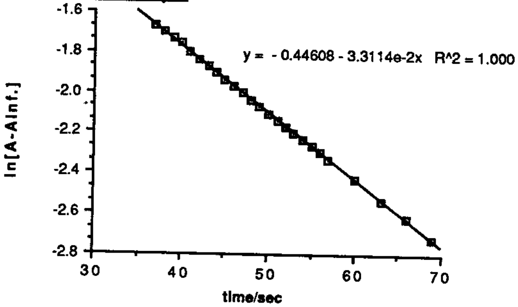

Figure A29: ln[A-Ainf.] versus time, [HSO3-]=8.43e-4 M, for p-bromocinnamaldehyde

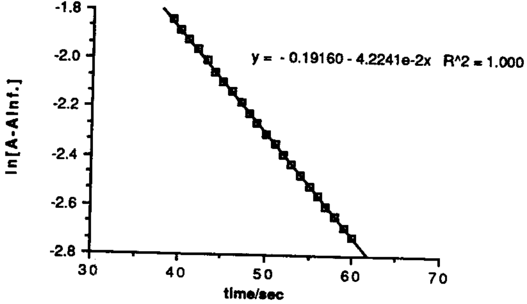

Figure A30: k' versus [HSO3-] for p-bromocinnamaldehyde

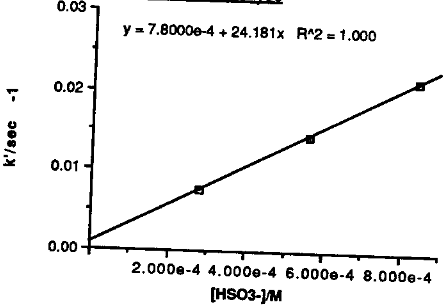

Figure A31: ln[A-Ainf.] versus time, [HSO3-]=5.38e-4 M, for p-chlorocinnamaldehyde

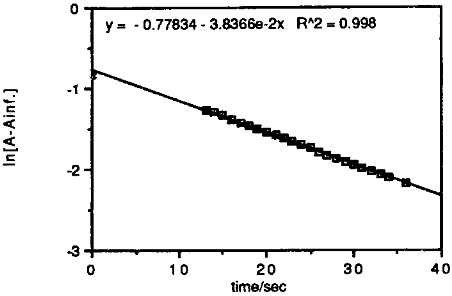

Figure A32: ln[A-Ainf.] versus time, [HSO3-]=2.69e-4 M, for p-chlorocinnamaldehyde

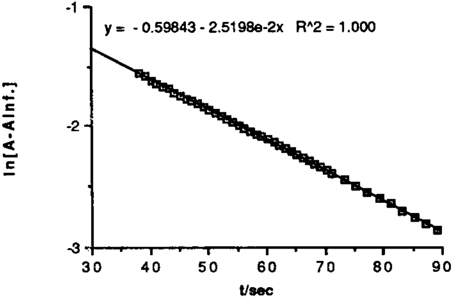

Figure A33: ln[A-Ainf.] versus time, [HSO3-]=1.35e-4 M, for p-chlorocinnamaldehyde

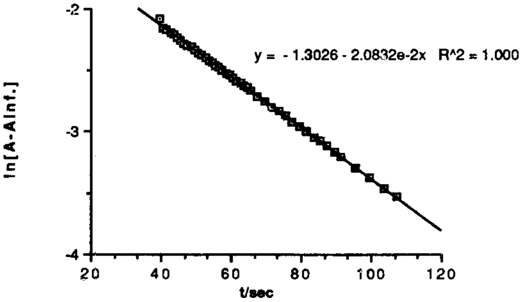

Figure A34: k' versus [HSO3-] for p-chlorocinnamaldehyde

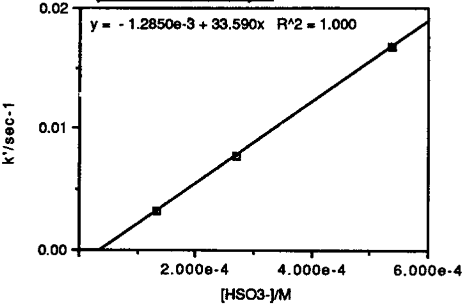

Figure A35: ln[A-Ainf.] versus time, [HSO3-]=1.61e-3 M, for p-methylcinnamaldehyde

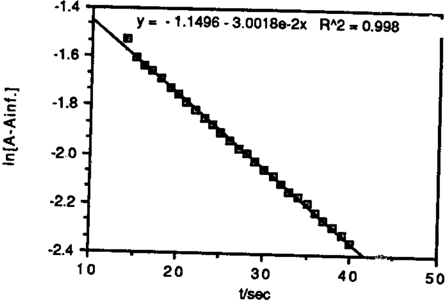

Figure A36: ln[A-Ainf.] versus time, [HSO3-]= 1.01e-3 M, for p-methylcinnamaldehyde

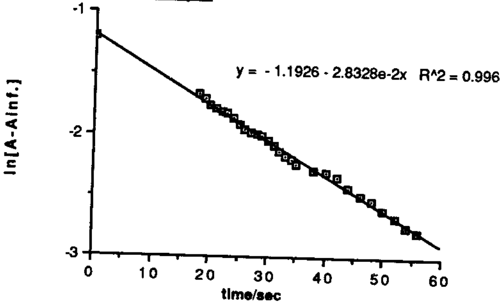

Figure A 37: ln[A-Ainf.] versus time, [HSO3-]=2.01e-3 M, for p-methylcinnamaldehyde

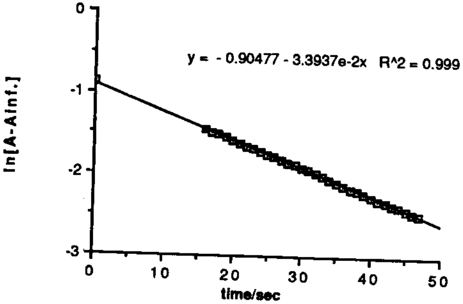

Figure A38: k' versus [HSO3-] for p-methylcinnamaldehyde

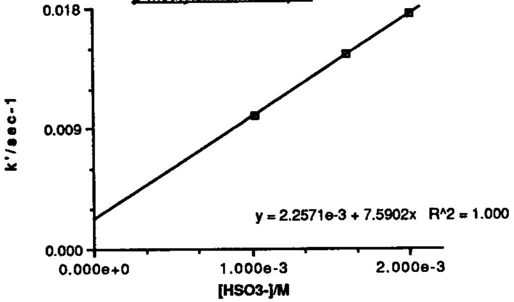

Figure A39: ln[A-Ainf.] versus time, [HSO3-]=8.43e-4 M, for t-cinnamaldehyde

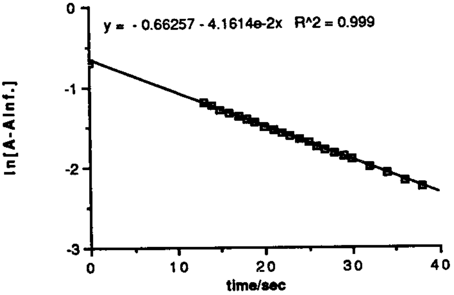

Figure A40: ln[A-Ainf.] versus time, [HSO3-]=5.62e-4 M, for t-cinnamaldehyde

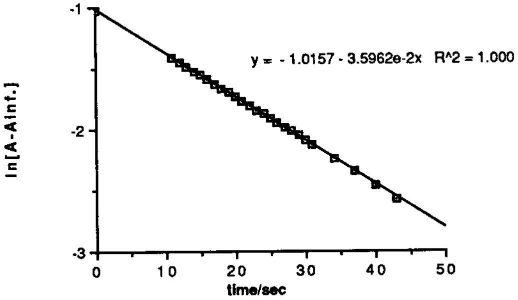

Figure A41: ln[A-Ainf.] versus time, [HSO3-]=1.12e-3 M, for t-cinnamaldehyde

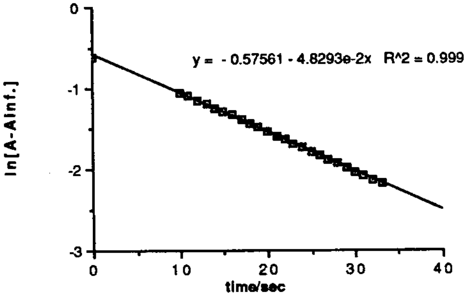

Figure A42: k' versus [HSO3-] for t-cinnamaldehyde

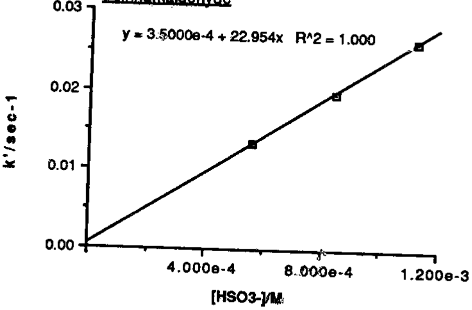

Appendix B

1H, 13C, APT, and HETCOR

SPECTRA B1: 1H NMR OF P-DIMETHYLAMINOCINNAMALDEHYDE

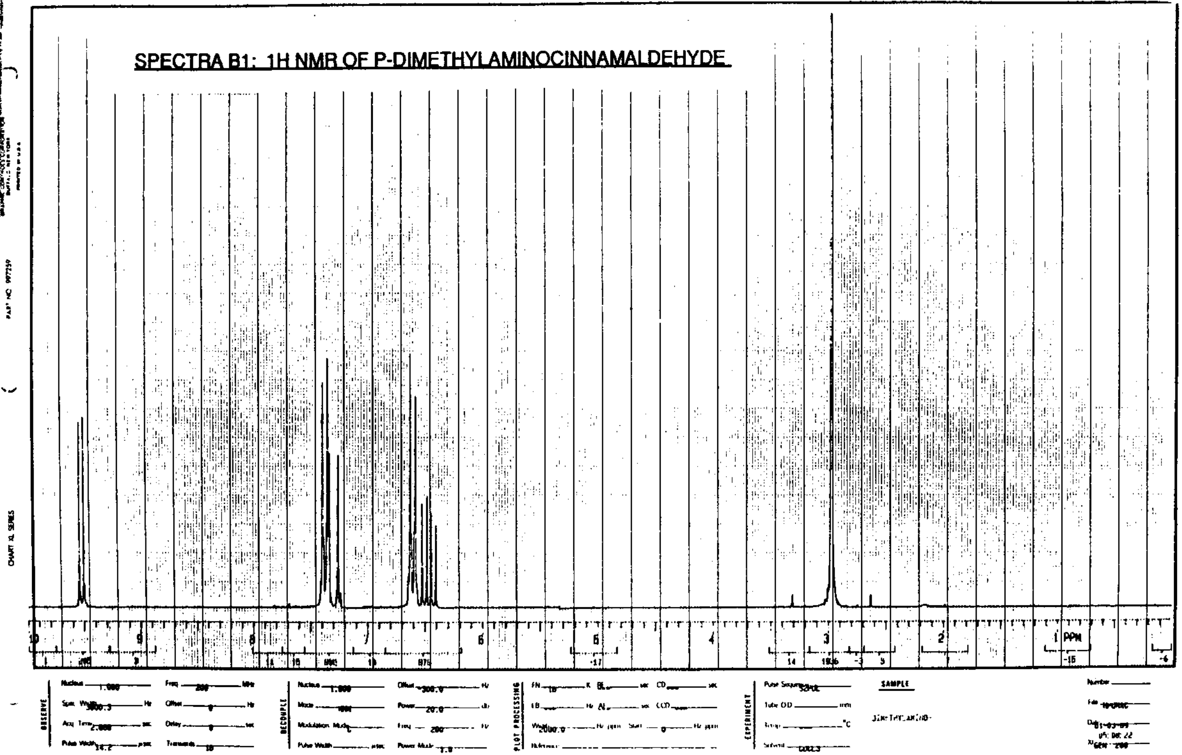

OBSERVE
Nucleus 1.000
Spec. Width 3000.3 Hz
Acq. Time 2.000 sec
Pulse Width 14.2 μsec
Freq 200 MHz
Offset 0 Hz
Delay 0 sec
Transients 10

DECOUPLE
Nucleus 1.000
Mode 1000
Modulation Mode
Pulse Width μsec
Offset -300.0 Hz
Power 20.0 db
Freq 200 Hz
Power Mode 1.0

PLOT PROCESSING
FN 18 K
LB Hz
Width 2000.0 Hz/ppm
Reference
BL sec
AL sec
Start 0 Hz/ppm
CD sec
CCD

EXPERIMENT
Pulse Sequence S2PUL
Tube OD mm
Temp °C
Solvent CDCl3

SAMPLE
DIMETHYLAMINO-

Number
File
Date 01-03-89
XL GEN 200

SPECTRA B2: 1H NMR OF P-METHYLCINNAMALDEHYDE

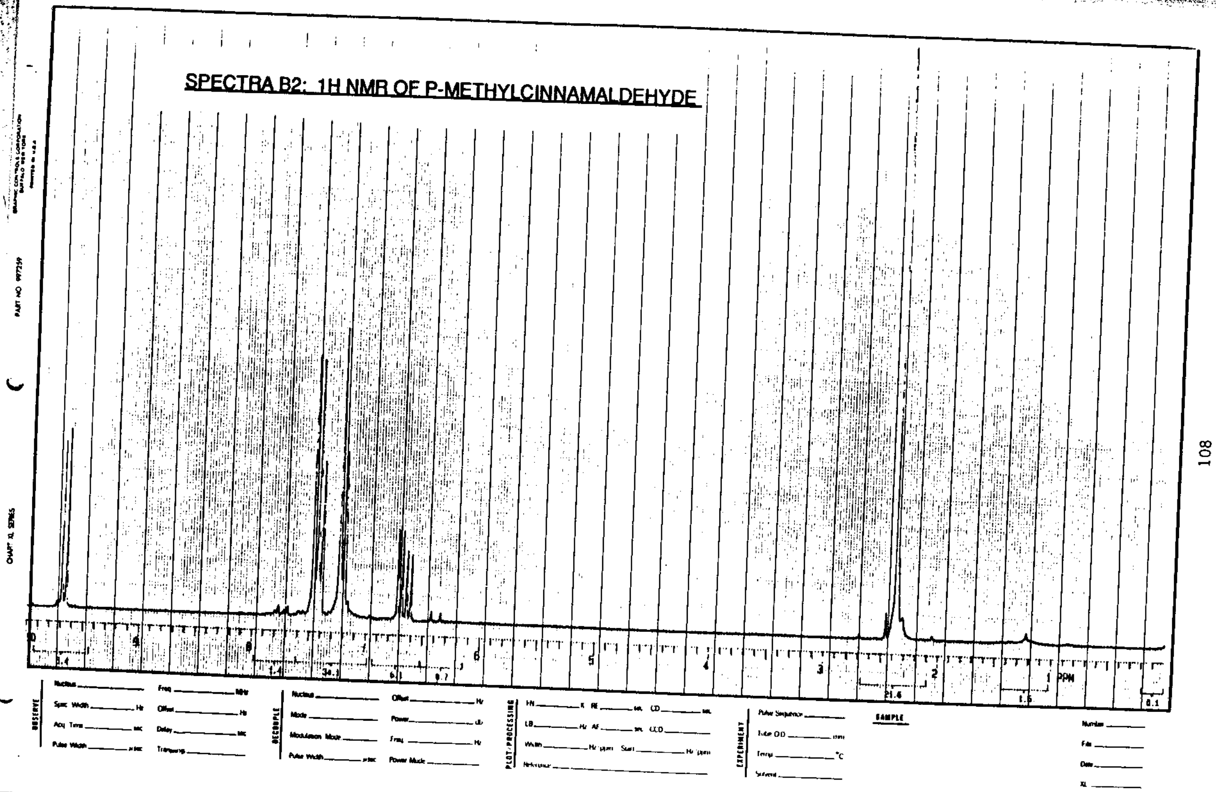

SPECTRA B3: 1H NMR OF *TRANS*-CINNAMALDEHYDE

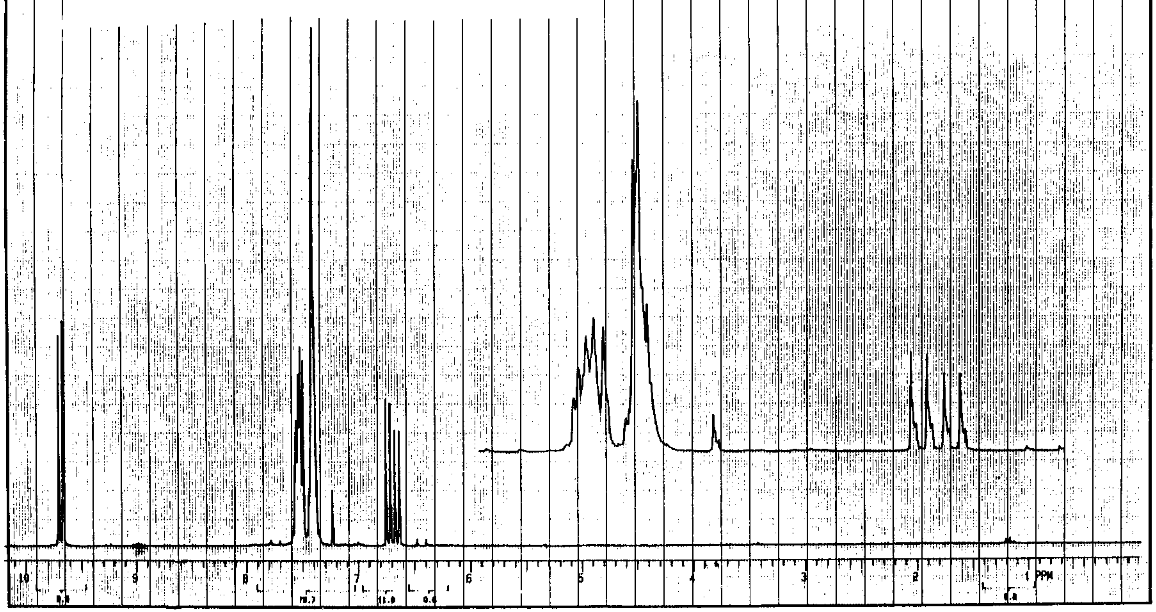

OBSERVE
Nucleus 1.000
Spec Width 3000.3 Hz
Acq Time 2.000 sec
Pulse Width 14.2 µsec
Freq 200 MHz
Offset 0 Hz
Delay 0 sec
Transients 16

DECOUPLE
Nucleus 1.000
Mode [illegible]
Modulation Mode C
Pulse Width µsec
Offset -200.0 Hz
Power 28.0 db
Freq 200 Hz
Power Mode 1.0

PLOT·PROCESSING
FN 16 K
LB Hz
Width 2030.0 Hz/ppm
Reference
RE sec
AF sec
Start 0 Hz/ppm
CD sec
CCD

EXPERIMENT
Pulse Sequence S2PUL
Tube O.D. mm
Temp °C
Solvent CDCL3

SAMPLE
TRANS-CINNAMALDEHYDE
(35N6/CDCL3)

Number
File 1CD00A
Date [illegible]-27-[illegible]
16:00:05
XL [illegible] 200

SPECTRA B4: 1H NMR OF O-NITROCINNAMALDEHYDE

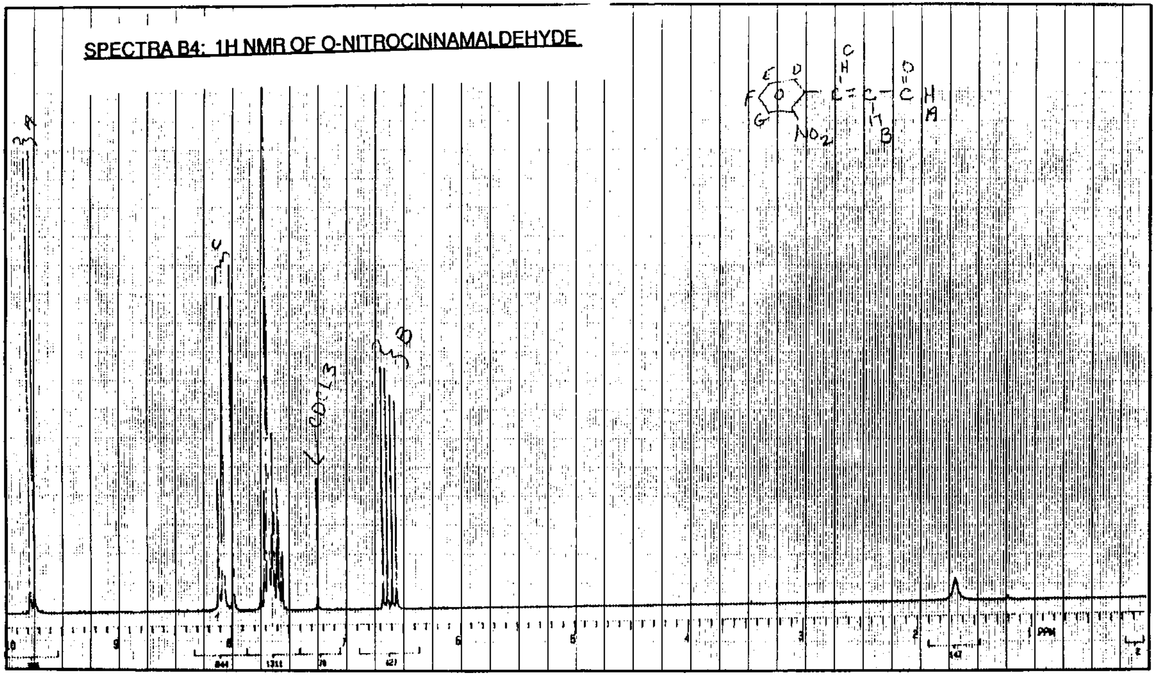

OBSERVE
Nucleus 1.000
Spec. Width 3000.3 Hz
Acq. Time 2.000 sec
Pulse Width 14.2 μsec
Freq. 200 MHz
Offset 0 Hz
Delay 0 sec
Transients 16

DECOUPLE
Nucleus 1.000
Mode NNN
Modulation Mode C
Pulse Width μsec
Offset 300.0 Hz
Power 20.0 db
Freq. 200 Hz
Power Mode 1.0

PLOT/PROCESSING
FN 16 K
LB Hz
W 3000.0 Hz/ppm
Reference
Start 0 Hz/ppm
CD --- sec
CCD ---

EXPERIMENT
Pulse Sequence S2PUL
Tube O.D. mm
Temp --- °C
Solvent CDCL3

SAMPLE
O-NITROCINNAMALDEHYDE
(20MG/CDCL3)

Number
File H
Date 09-21-88 13:43:21
XL GEM 200

SPECTRA B5: 1H NMR OF P-NITROCINNAMALDEHYDE

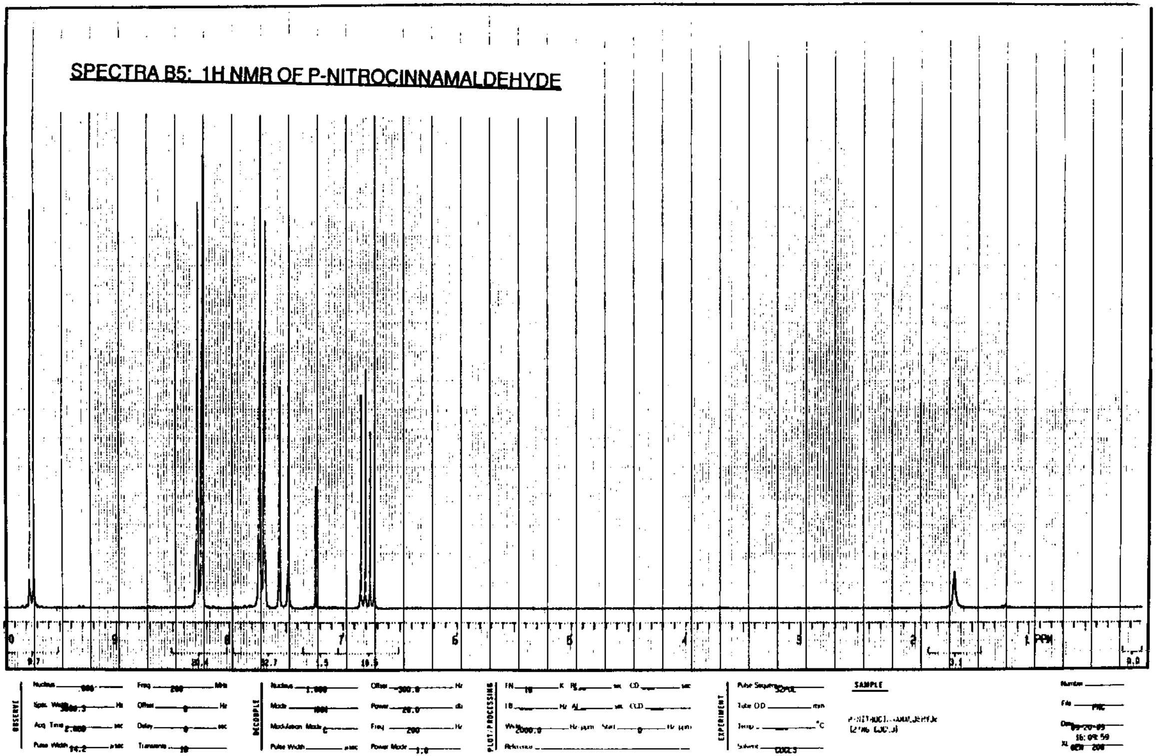

SPECTRA B6: 1H NMR OF P-CHLOROCINNAMALDEHYDE

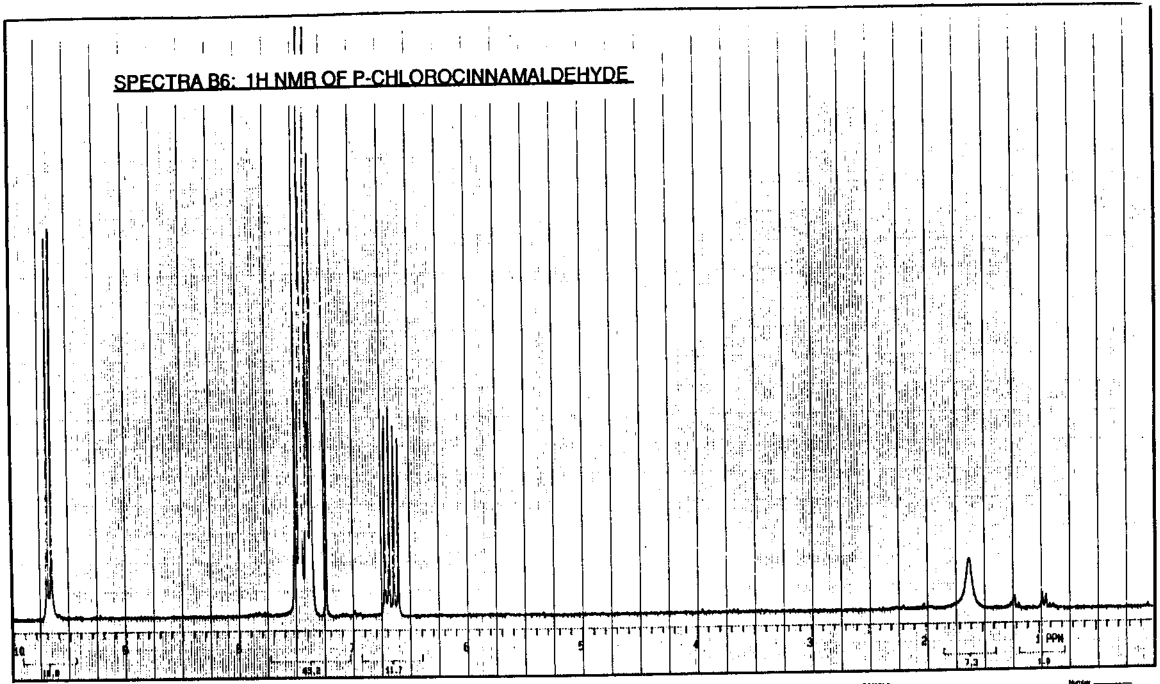

OBSERVE
Nucleus ______ Freq ______ MHz
Spec Width ______ Hz Offset ______ Hz
Acq Time ______ sec Delay ______ sec
Pulse Width ______ μsec Transients ______

DECOUPLE
Nucleus ______ Offset ______ Hz
Mode ______ Power ______ db
Modulation Mode ______ Freq ______ Hz
Pulse Width ______ μsec Power Mode ______

PLOT/PROCESSING
FN ______ K FB ______ sec CD ______ sec
LB ______ Hz AF ______ sec CCD ______
Width ______ Hz/ppm Start ______ Hz/ppm
Reference ______

EXPERIMENT
Pulse Sequence ______
Tube O.D. ______ mm
Temp ______ °C
Solvent ______

SAMPLE

Number ______
File ______
Date ______
XL ______

CHART XL SERIES PART NO 997259

SPECTRA B7: 1H NMR OF M-BROMOCINNAMALDEHYDE

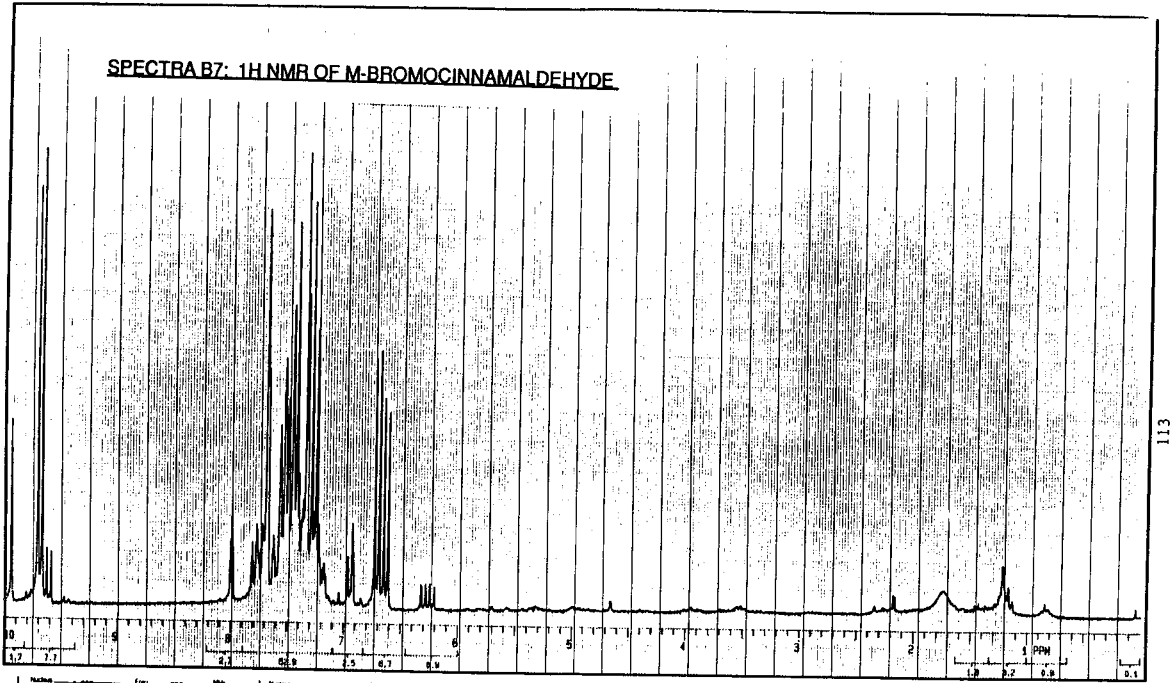

OBSERVE

Nucleus 1.000 Freq 200 MHz
Spec Width 3000.3 Hz Offset 0 Hz
Acq Time 2.000 sec Delay 0 sec
Pulse Width 19.5 μsec Transients 16

DECOUPLE

Nucleus 1.000 Offset -300.0 Hz
Mode 1000 Power 20.0 db
Modulation Mode C Freq 200 Hz
Pulse Width ____ μsec Power Mult 1.0

PLOT PROCESSING

FN 16 K Rt ____ sec CD ____ sec
LB ____ Hz AF ____ sec CCD ____
Width 2000.0 Hz ppm Start 0 Hz ppm
Reference ____

EXPERIMENT

Pulse Sequence S2PUL
Tube OD ____ mm
Temp ____ °C
Solvent CDCl3

SAMPLE

~~[illegible]~~
m-bromocinn
crude
4/26/90

Number ____
File H
Date 04-26-90
16:26:40
Id GEM 200

SPECTRA B8: 1H NMR OF P-BROMOCINNAMALDEHYDE

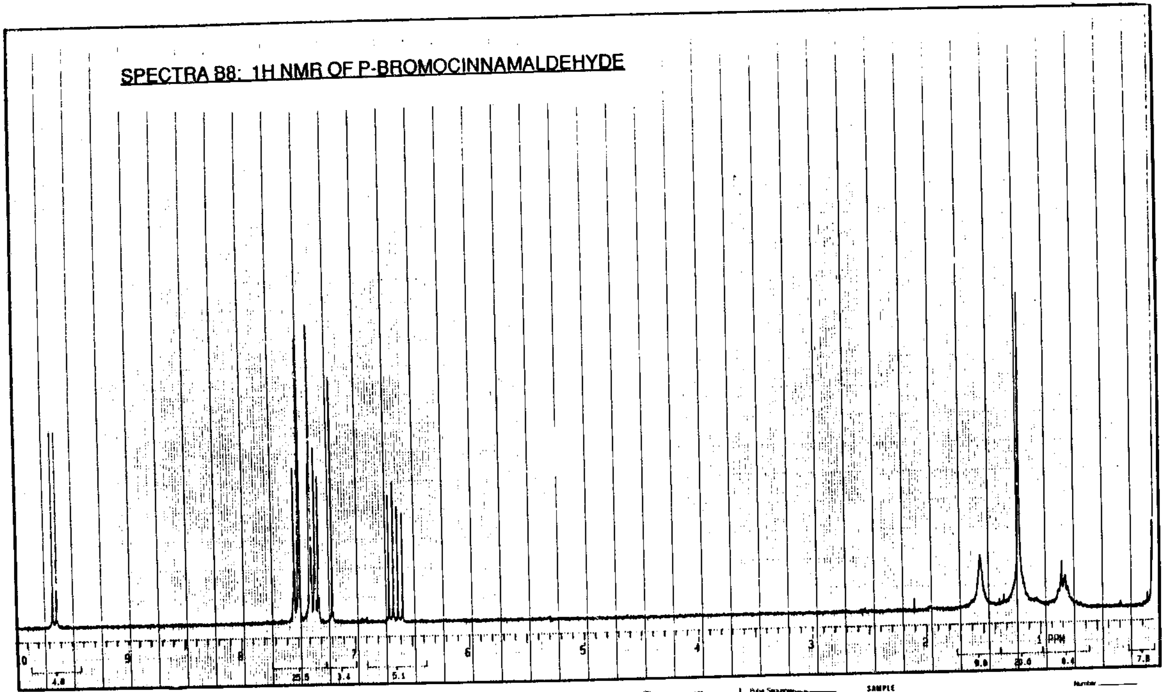

OBSERVE

Nucleus 1.000
Spec. Width 3000.3 Hz
Acq. Time 2.000 sec
Pulse Width 14.2 μsec
Freq 200 MHz
Offset 0 Hz
Delay 0 sec
Transients 10

DECOUPLE

Nucleus 1.000
Mode 1000
Modulation Mode C
Pulse Width μsec
Offset 300.0 Hz
Power 20.0 db
Freq 200 Hz
Power Mode 1.0

PLOT · PROCESSING

FN 16 K
LB Hz
Width 2000.0 Hz/ppm
Reference
NL sec
AI sec
Start 0 Hz/ppm
CD sec
CCD

EXPERIMENT

Pulse Sequence S2PUL
Tube O.D. mm
Temp °C
Solvent CDCL3

SAMPLE

P-BROMOCINNAMALDEHYDE
SECOND RECRYSTALLIZATION
(10MG, CDCL3)

Number
File NMBC2
Date 10-20-89
10:54:05
XL GEM 200

P -

SPECTRA B9: ^{13}C NMR OF P-DIMETHYLAMINOCINNAMALDEHYDE

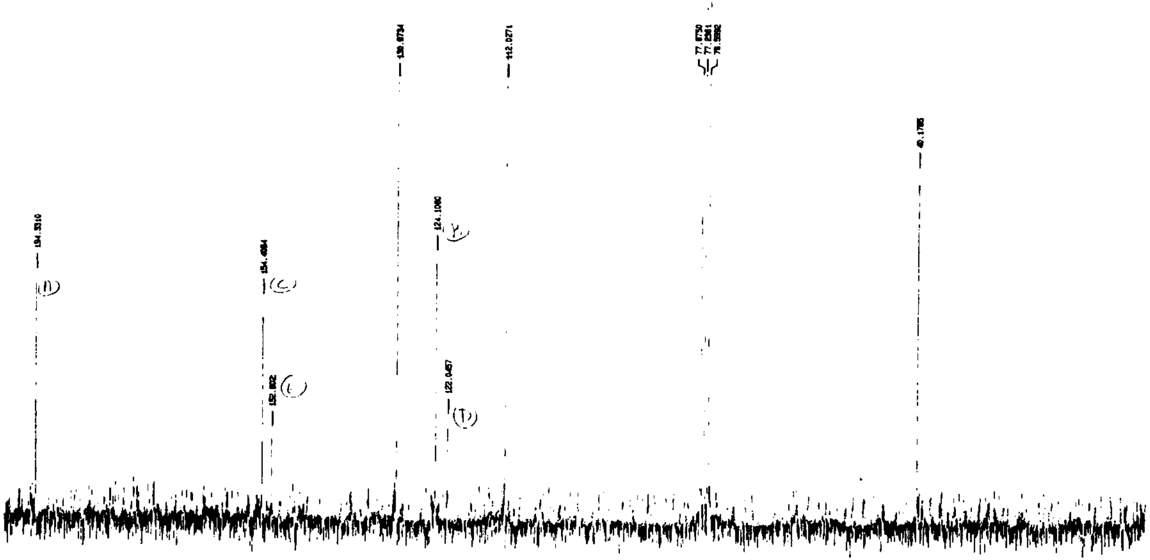

SPECTRA B10: ^{13}C NMR OF P-METHOXYCINNAMALDEHYDE

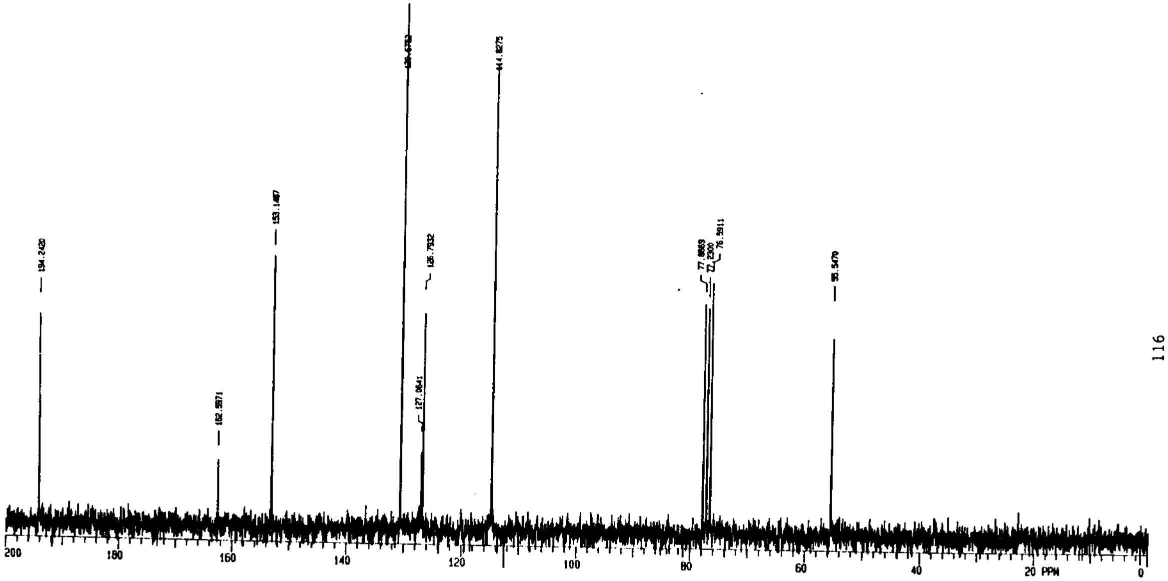

P-MEO

SPECTRA B11: ^{13}C NMR OF P-METHYLCINNAMALDEHYDE

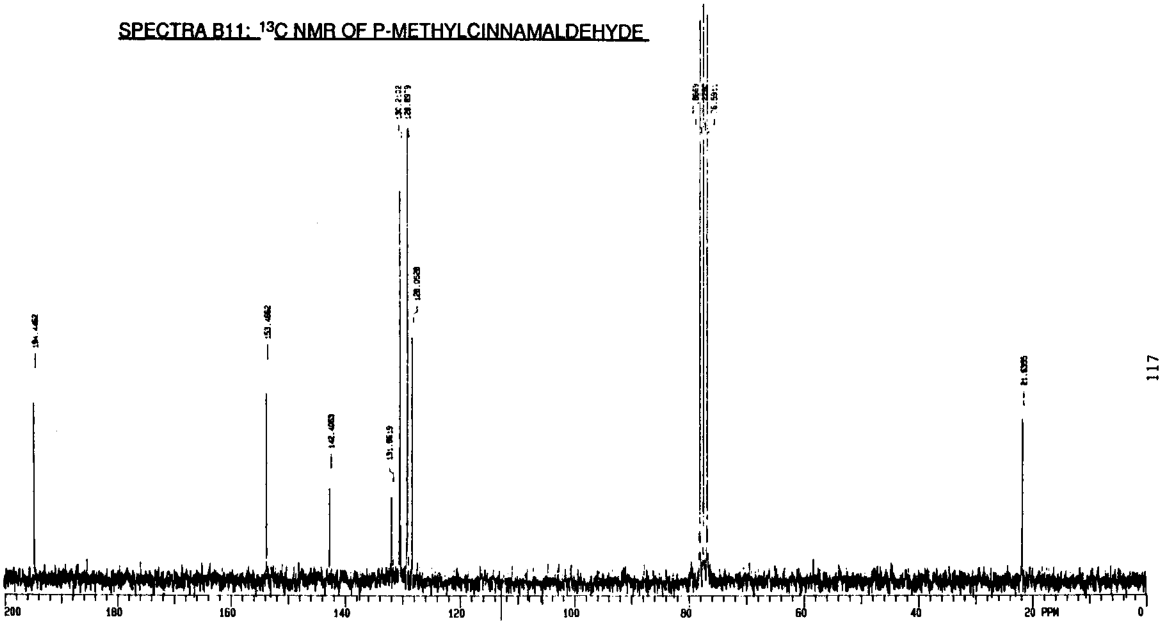

p-~~bromo~~cinnamaldehyde
methyl

SPECTRA B12: ^{13}C NMR OF P-*TRANS*-CINNAMALDEHYDE

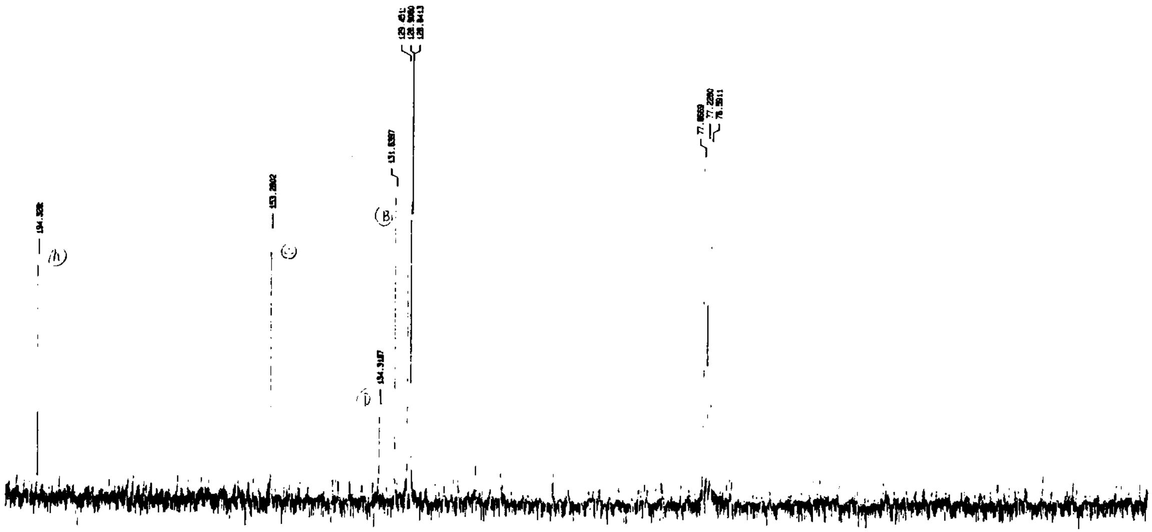

SPECTRA B13: ^{13}C NMR OF O-NITROCINNAMALDEHYDE

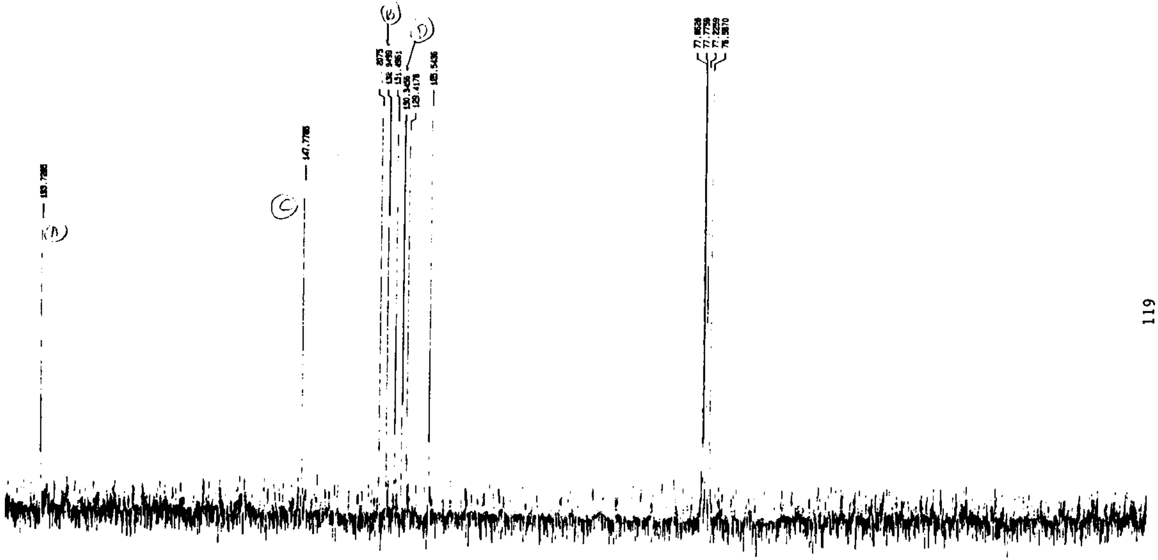

SPECTRA B14: ^{13}C NMR OF P-NITROCINNAMALDEHYDE

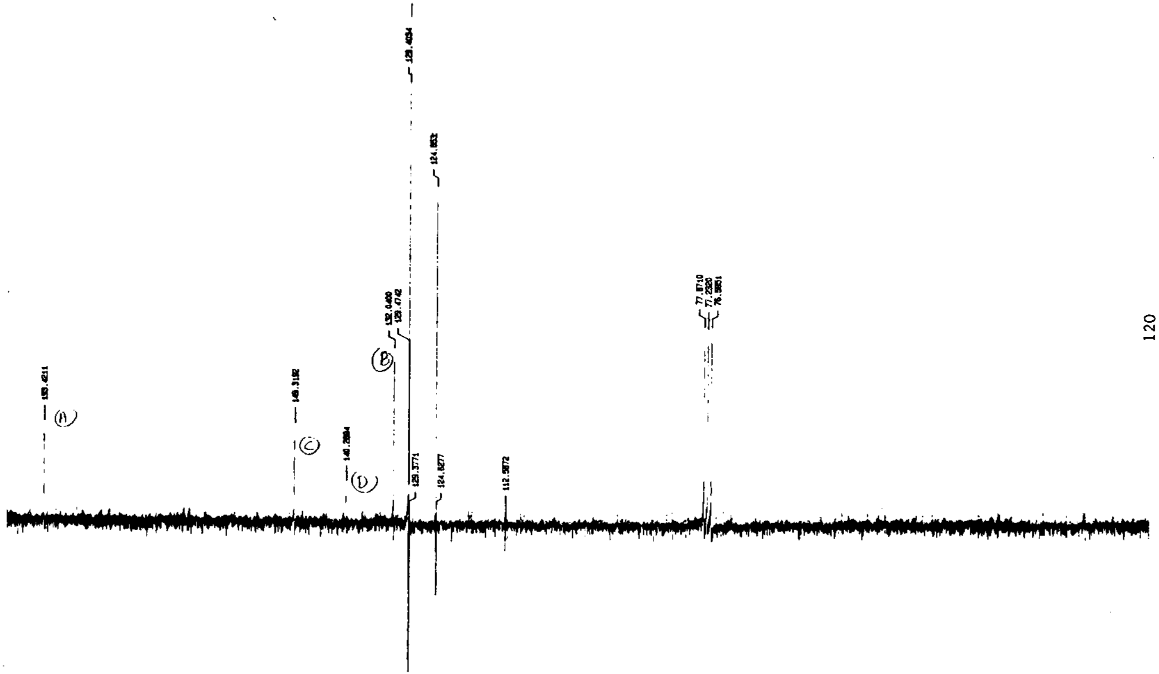

SPECTRA B15: ^{13}C NMR OF P-CHLOROCINNAMALDEHYDE

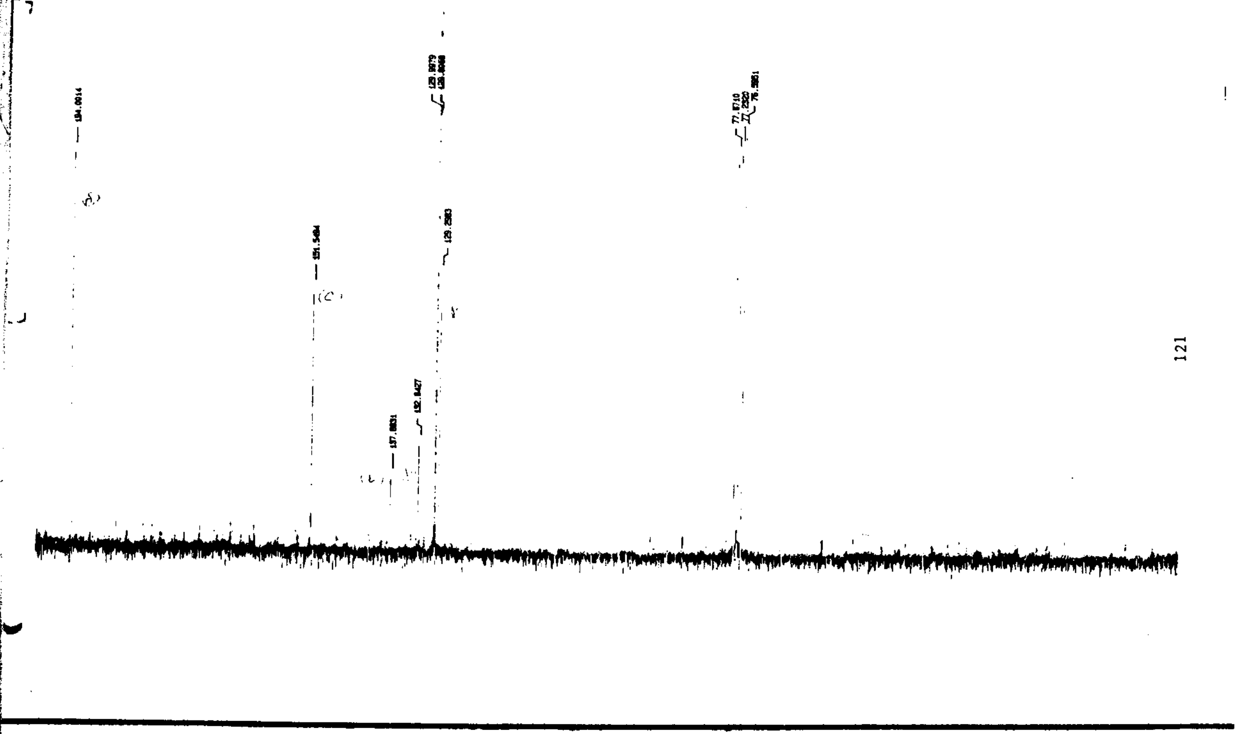

SPECTRA B16: ^{13}C NMR OF O-METHOXYCINNAMALDEHYDE

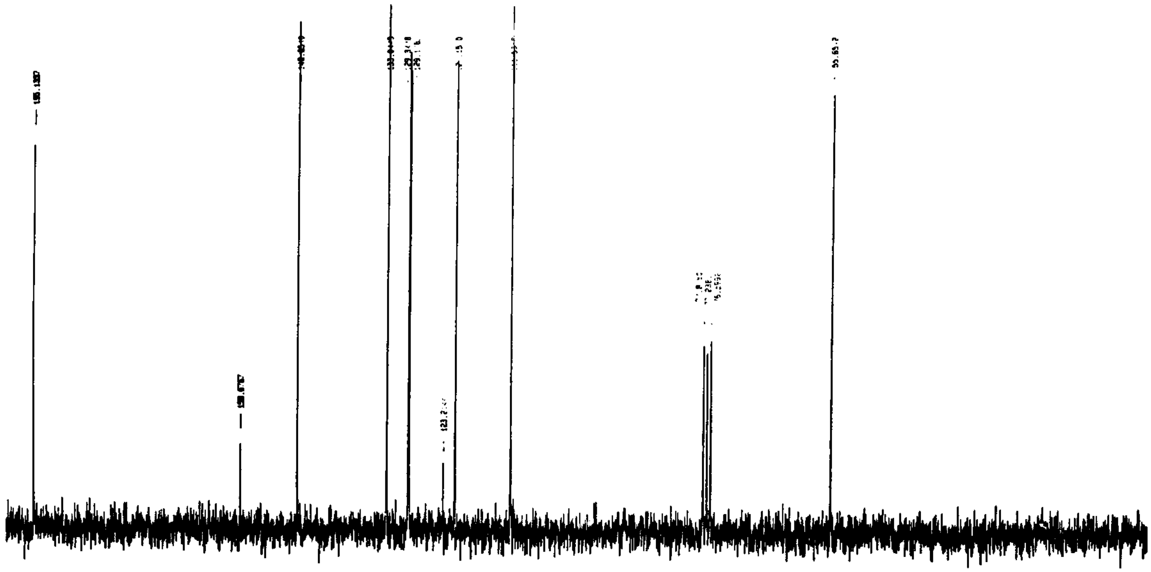

SPECTRA B17: ^{13}C NMR OF M-BROMOCINNAMALDEHYDE

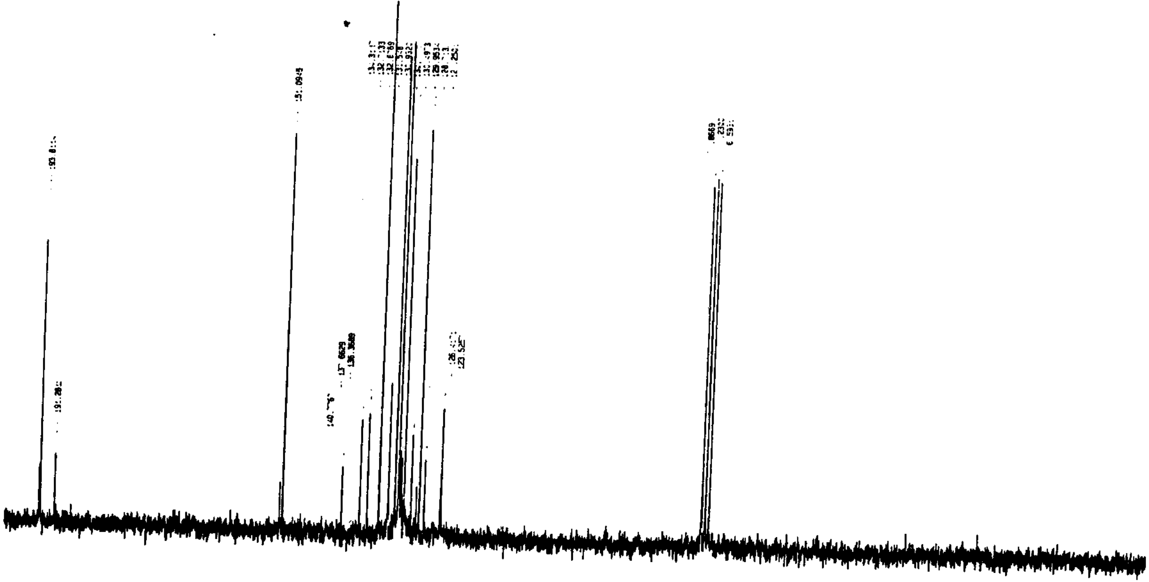

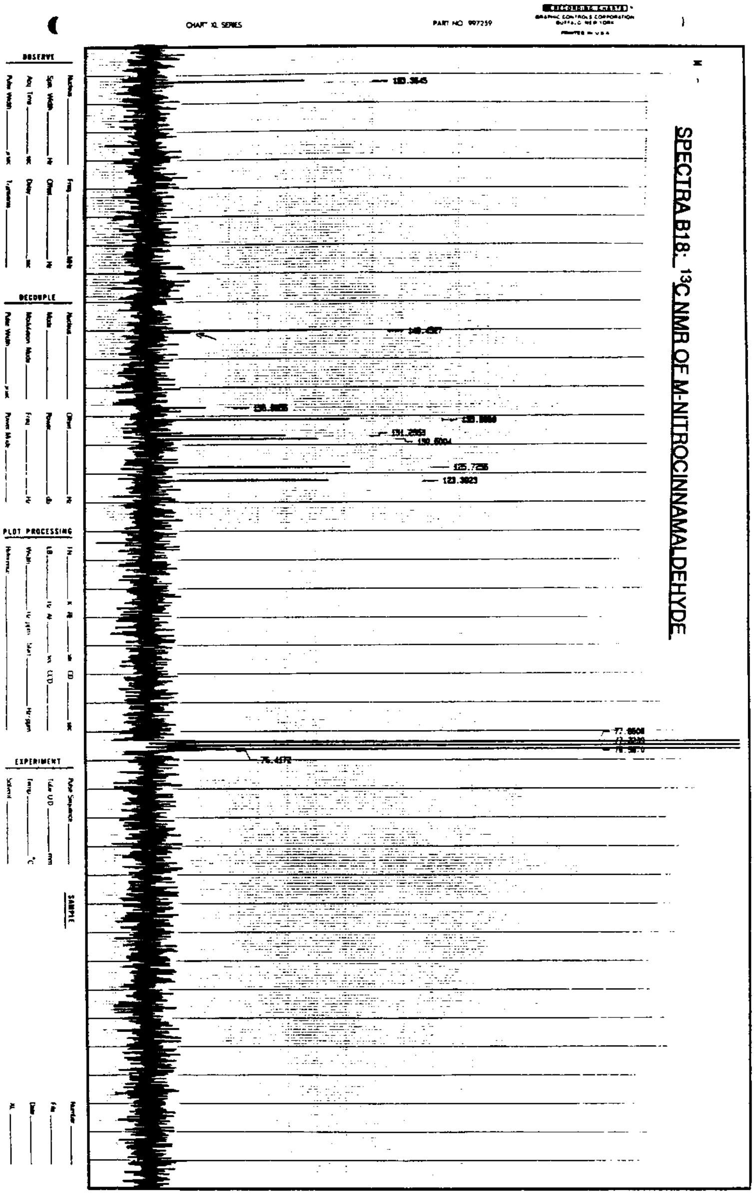

SPECTRA B18. ^{13}C NMR OF M-NITROCINNAMALDEHYDE p - 1

6 / 9 0 1

SPECTRA B19: ^{13}C NMR OF P-BROMOCINNAMALDEHYDE

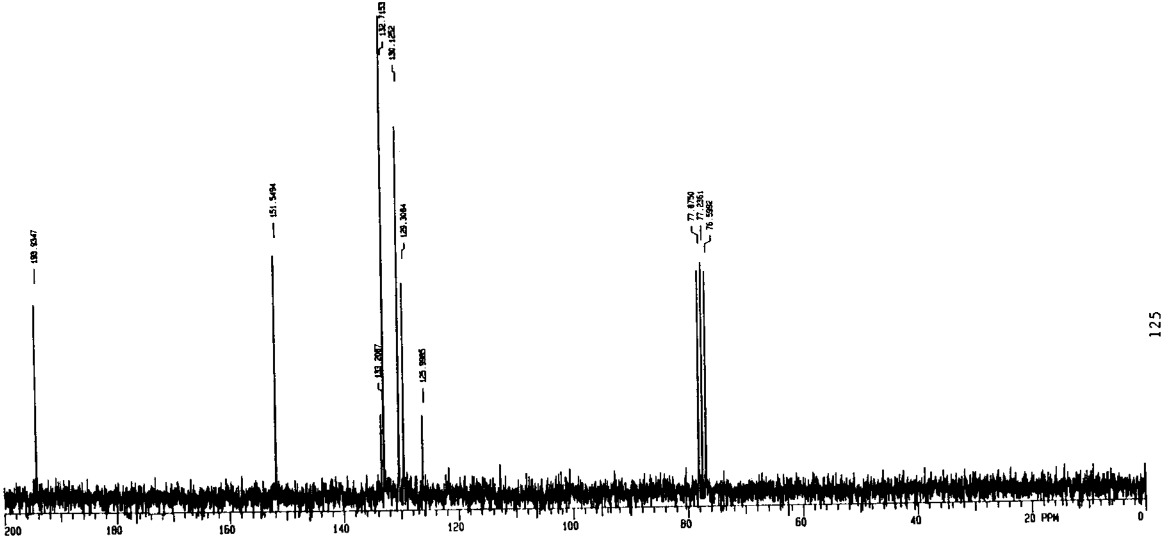

SPECTRA B20: APT OF M-BROMOCINNAMALDEHYDE

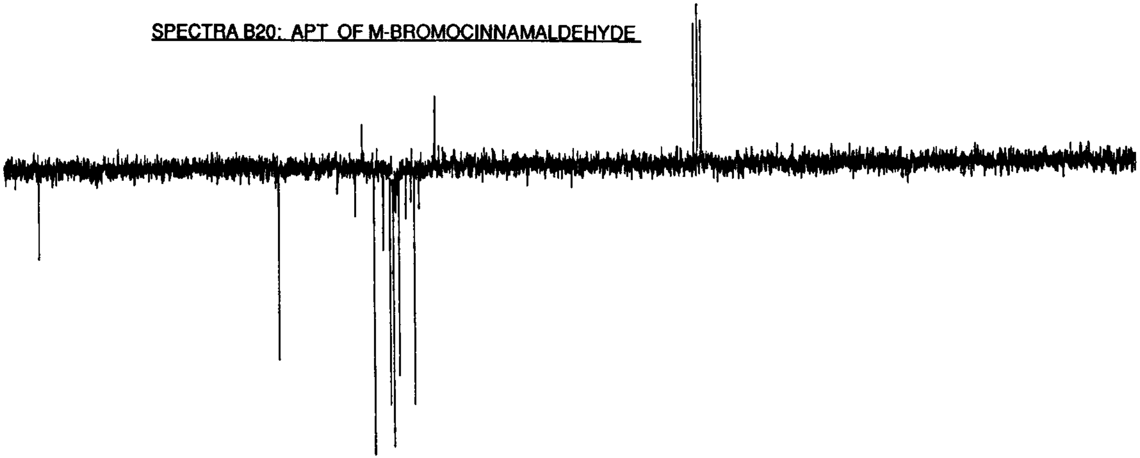

SPECTRA B21: HETCOR OF P-DIMETHYLAMINOCINNAMALDEHYDE

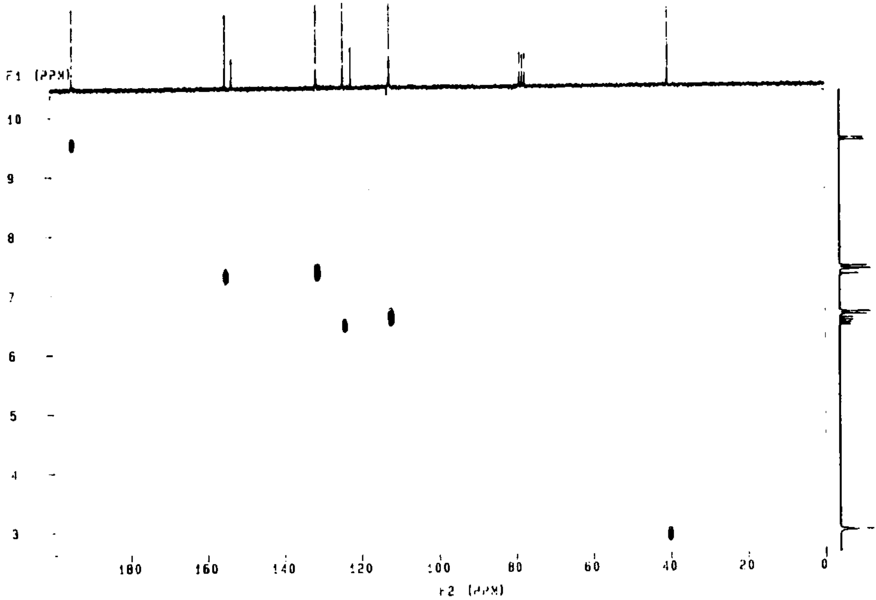

DIMETHYLAMINO-
EXP4 PULSE SEQUENCE: HETCOR
DATE 01-03-00
SOLVENT CDCL3
FILE HETCOR

HETCOR PULSE SEQUENCE
OBSERVE CARBON
FREQUENCY 90.200 MHZ
1D SPECTRAL WIDTH (F2) 14982.6 HZ
2D SPECTRAL WIDTH (F1) 1540.0 HZ
ACQ. TIME 68.3 MSEC
RELAXATION DELAY 1.0 SEC
PULSE WIDTH 90 DEGREES
AMBIENT TEMPERATURE
NO. REPETITIONS 16
NO. INCREMENTS 128
DECOUPLE PROTON
LOW POWER 20 DB
BROADBAND MODULATED
DATA PROCESSING
PSEUDO-ECHO SHAPED
FT SIZE 2K X 256
TOTAL TIME 40.4 MINUTES

UN82 HOFF, S.M. LINEAR FREE ENERGY CORRELATIONS OF THE EFFECT OF SUBSTITUENTS, etc
H6981/1990 CHEMISTRY HRS. 6/90 3 of 3

SPECTRA B22: HETCOR OF P-METHOXYCINNAMALDEHYDE

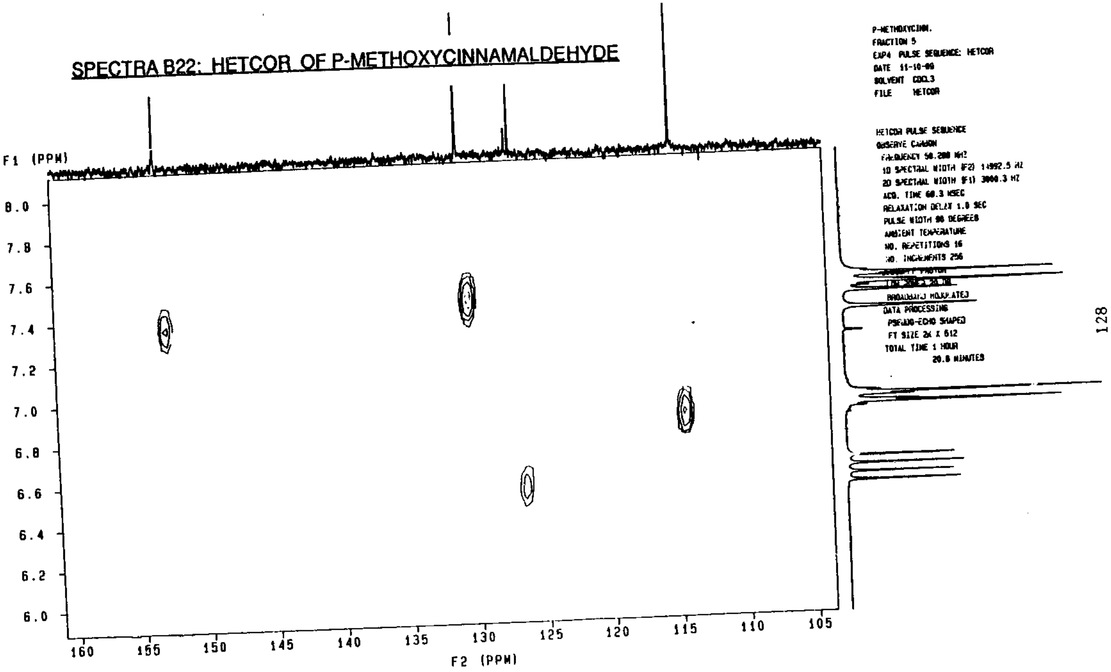

P-METHOXYCINN.
FRACTION 5
EXP4 PULSE SEQUENCE: HETCOR
DATE 11-10-90
SOLVENT CDCL3
FILE HETCOR

HETCOR PULSE SEQUENCE
OBSERVE CARBON
FREQUENCY 50.288 MHZ
1D SPECTRAL WIDTH (F2) 14992.5 HZ
2D SPECTRAL WIDTH (F1) 3000.3 HZ
ACQ. TIME 60.3 MSEC
RELAXATION DELAY 1.0 SEC
PULSE WIDTH 90 DEGREES
AMBIENT TEMPERATURE
NO. REPETITIONS 16
NO. INCREMENTS 256
[illegible] PROTON
[illegible]
BROADBAND MODULATED
DATA PROCESSING
PSEUDO-ECHO SHAPED
FT SIZE 2K X 512
TOTAL TIME 1 HOUR
20.0 MINUTES

SPECTRA B23: HETCOR OF P-METHYLCINNAMALDEHYDE

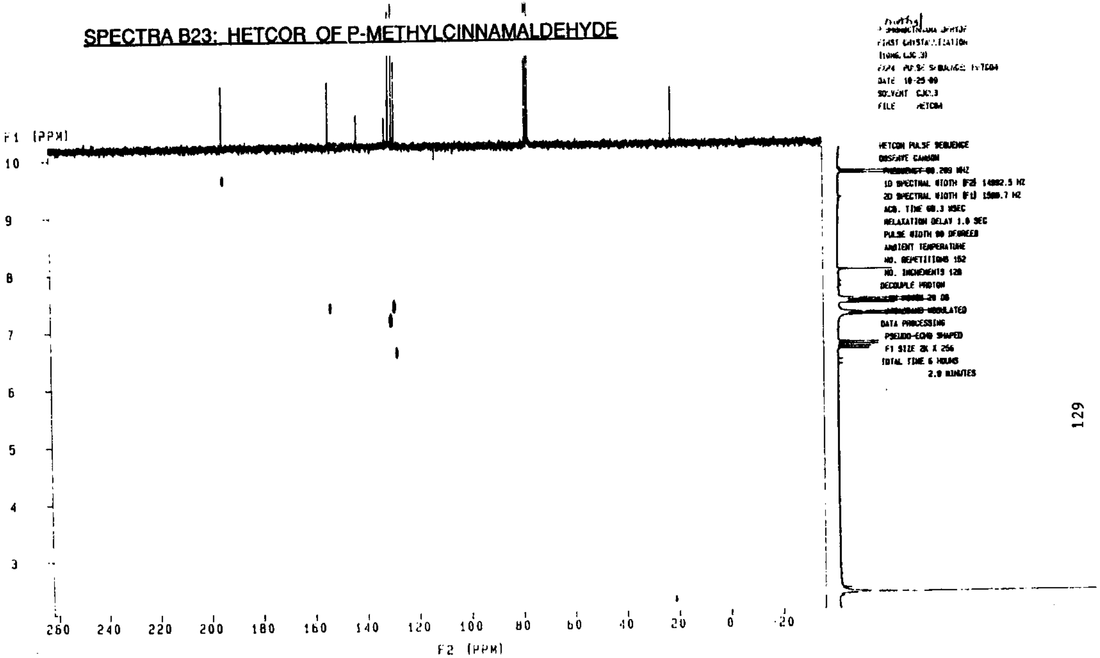

```
methyl
P-[illegible]CINNAMALDEHYDE
FIRST CRYSTALLIZATION
(TONG, LJC 3)
[illegible] PULSE SEQUENCE: HETCOR
DATE 10-25-90
SOLVENT CDCL3
FILE HETCOR

HETCOR PULSE SEQUENCE
OBSERVE CARBON
 FREQUENCY 50.289 MHZ
 1D SPECTRAL WIDTH (F2) 14992.5 HZ
 2D SPECTRAL WIDTH (F1) 1500.7 HZ
 ACQ. TIME 68.3 MSEC
 RELAXATION DELAY 1.0 SEC
 PULSE WIDTH 90 DEGREES
 AMBIENT TEMPERATURE
 NO. REPETITIONS 152
 NO. INCREMENTS 128
DECOUPLE PROTON
 [illegible]-20 DB
 [illegible] MODULATED
DATA PROCESSING
 PSEUDO-ECHO SHAPED
 F1 SIZE 2K X 256
TOTAL TIME 6 HOURS
        2.0 MINUTES
```

SPECTRA B24: HETCOR OF O-NITROCINNAMALDEHYDE

O-NITROCINN
SAT'D IN CDCL3
EXP4 PULSE SEQUENCE: HETCOR
DATE 01-00-00
SOLVENT CDCL3
FILE HETCOR

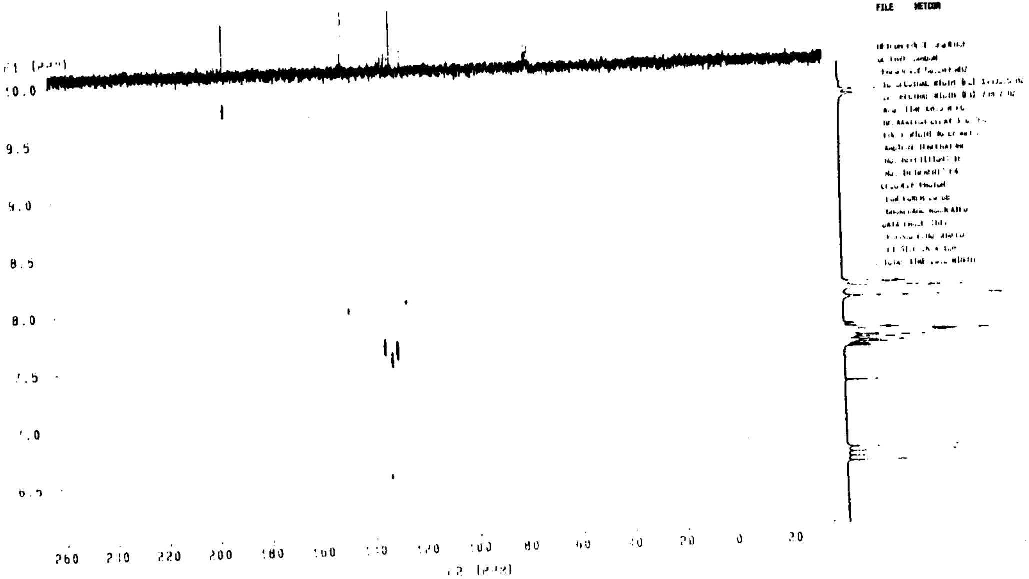

SPECTRA B25: HETCOR OF P-NITROCINNAMALDEHYDE

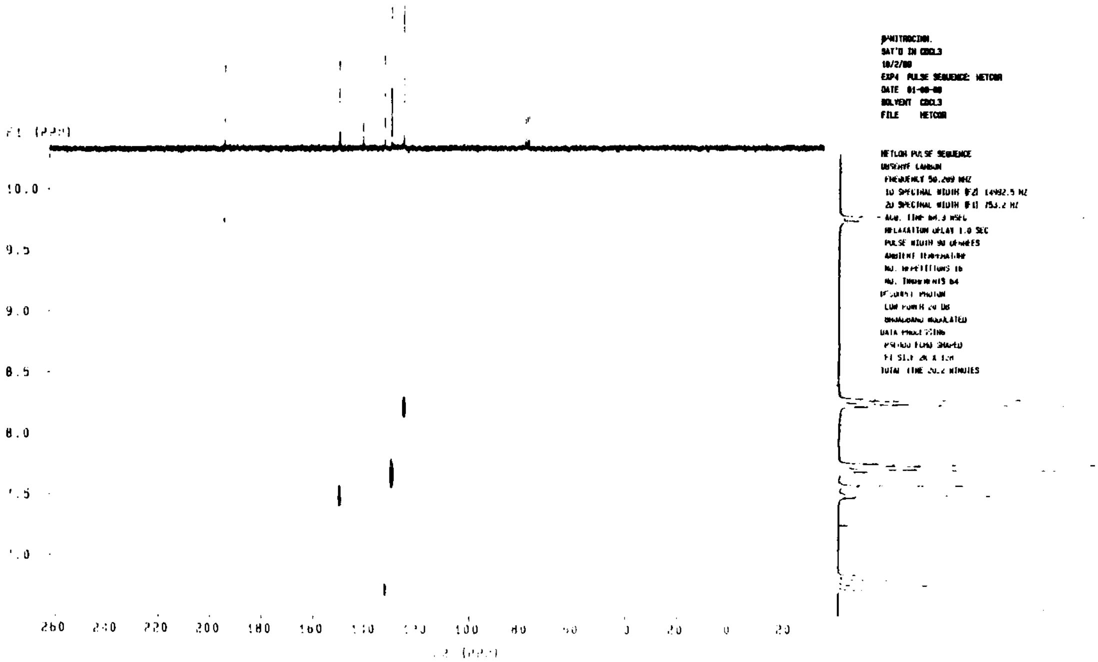

SPECTRA B26: HETCOR OF M-BROMOCINNAMALDEHYDE

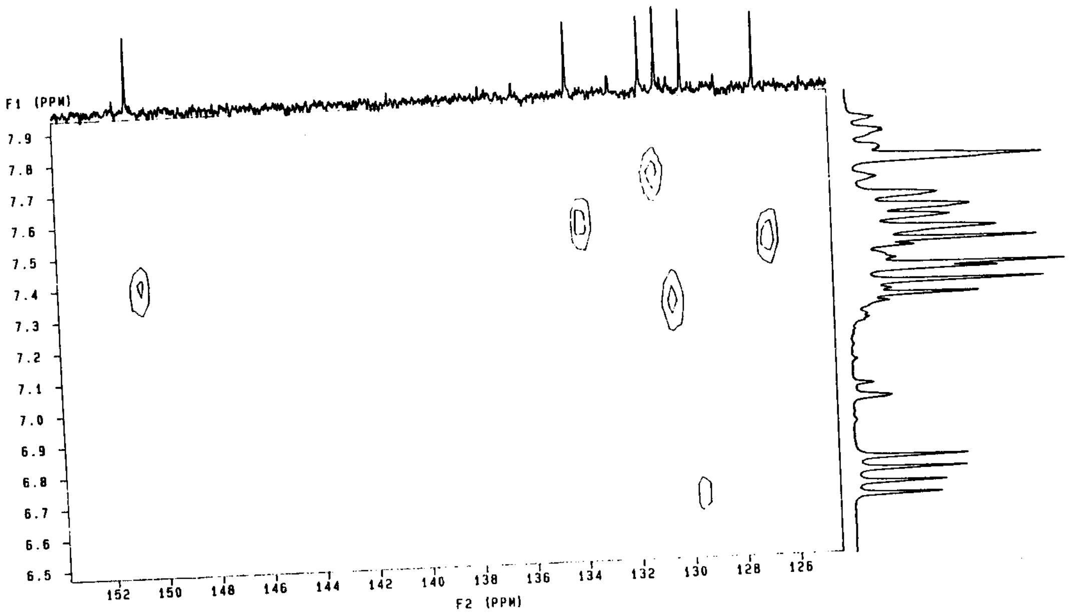

SPECTRA B27: HETCOR OF O-METHOXYCINNAMALDEHYDE

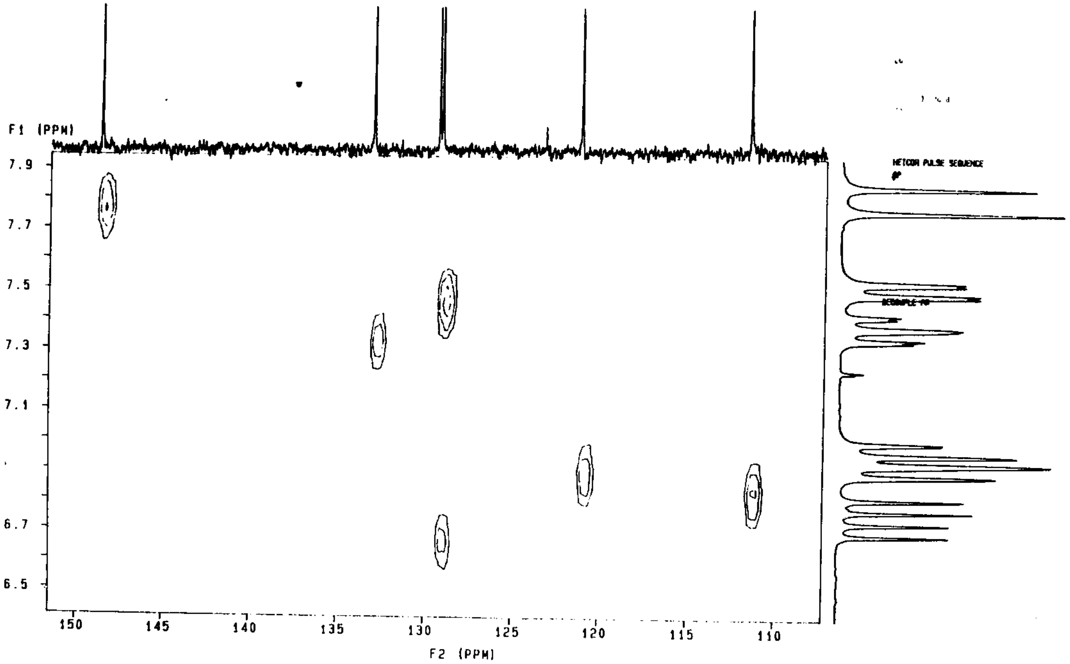

SPECTRA B28: HETCOR OF M-NITROCINNAMALDEHYDE

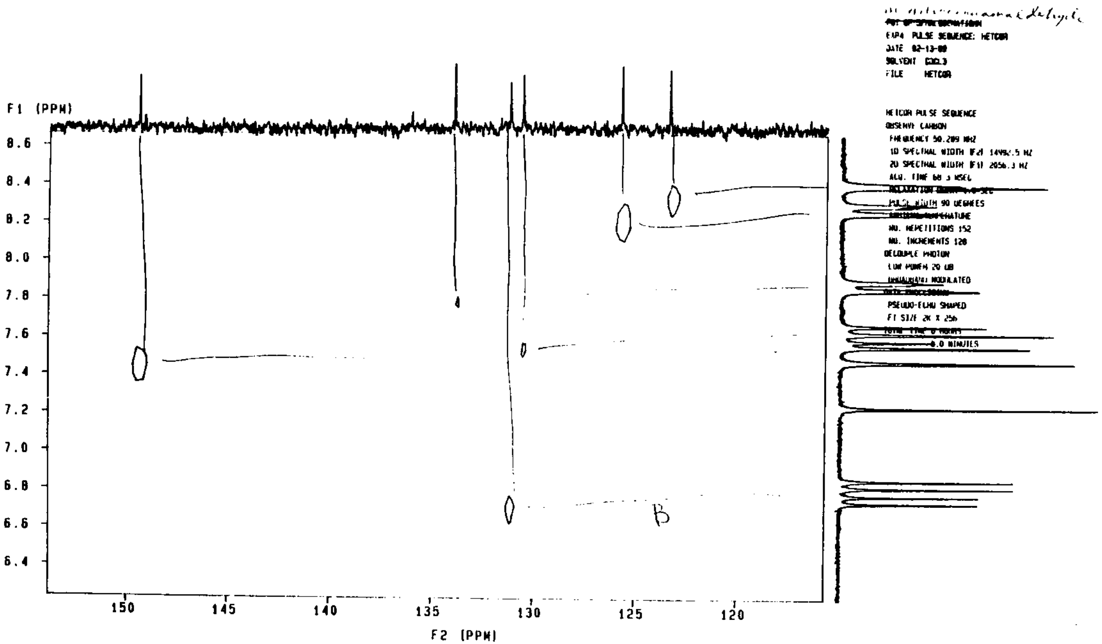

SPECTRA B29: HETCOR OF P-BROMOCINNAMALDEHYDE

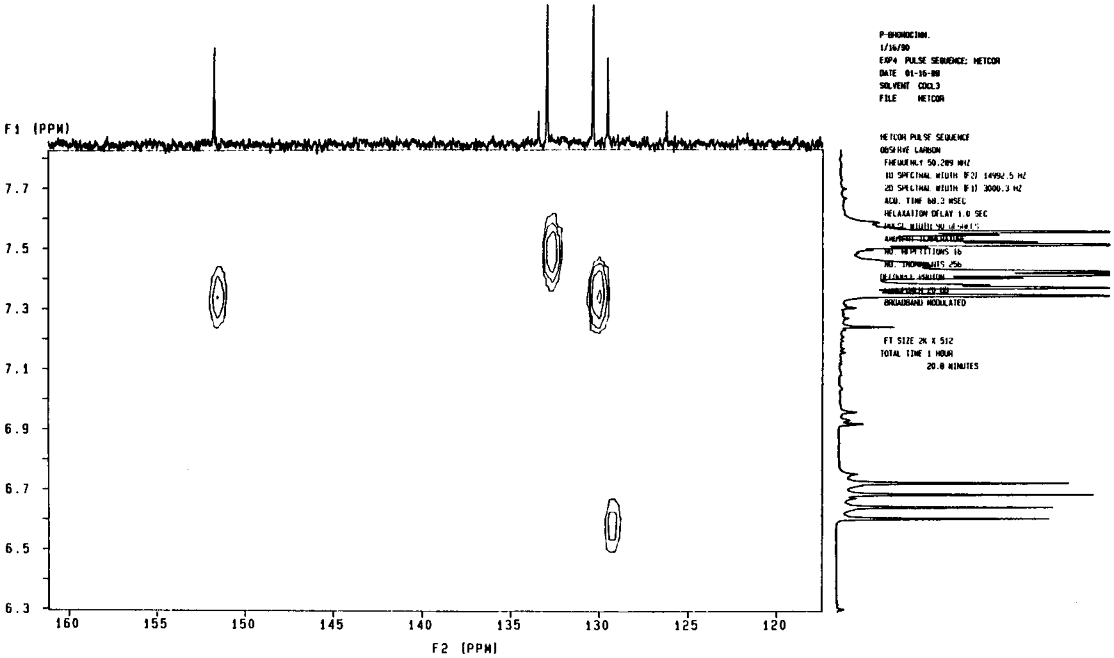

Appendix C

UV-Visible Absorption Spectra

SPECTRA C1: UV-VIS SPECTRA OF O-NITROCINNAMALDHEYDE

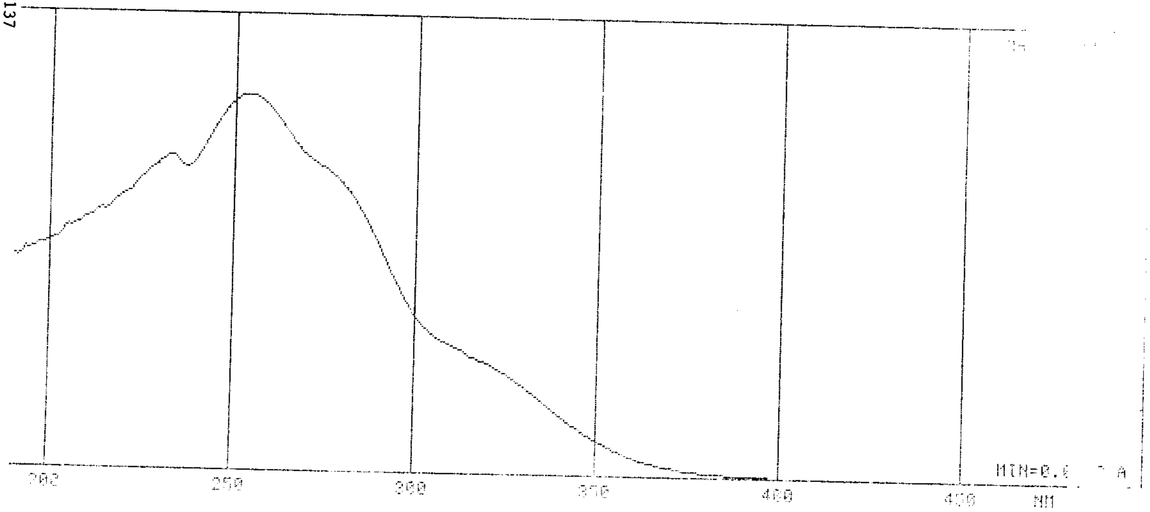

SPECTRA C2: UV-VIS SPECTRA OF O-METHOXYCINNAMALDHEYDE.

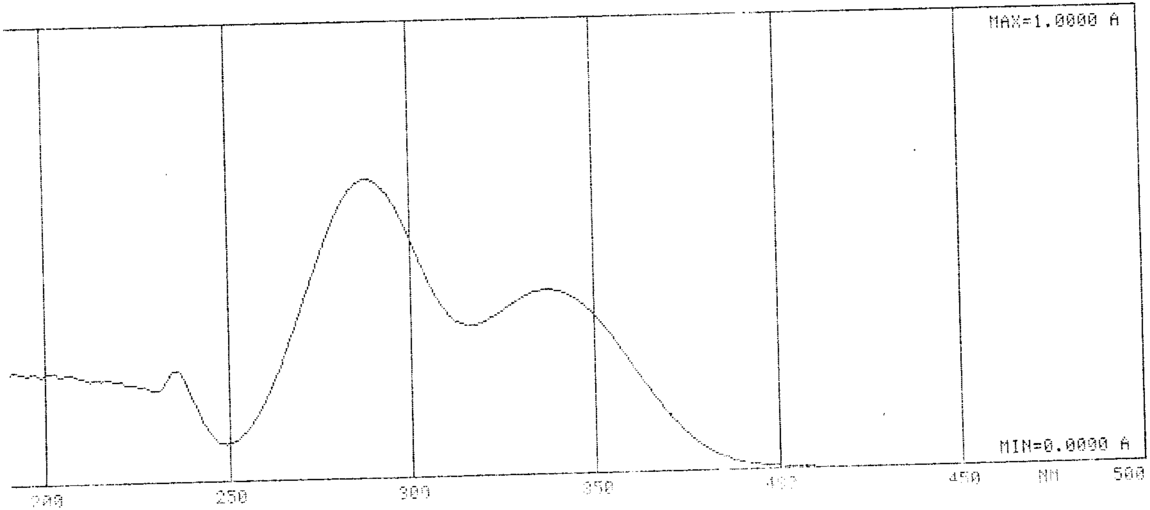

SPECTRA C3: UV-VIS SPECTRA OF P-BROMOCINNAMALDHEYDE

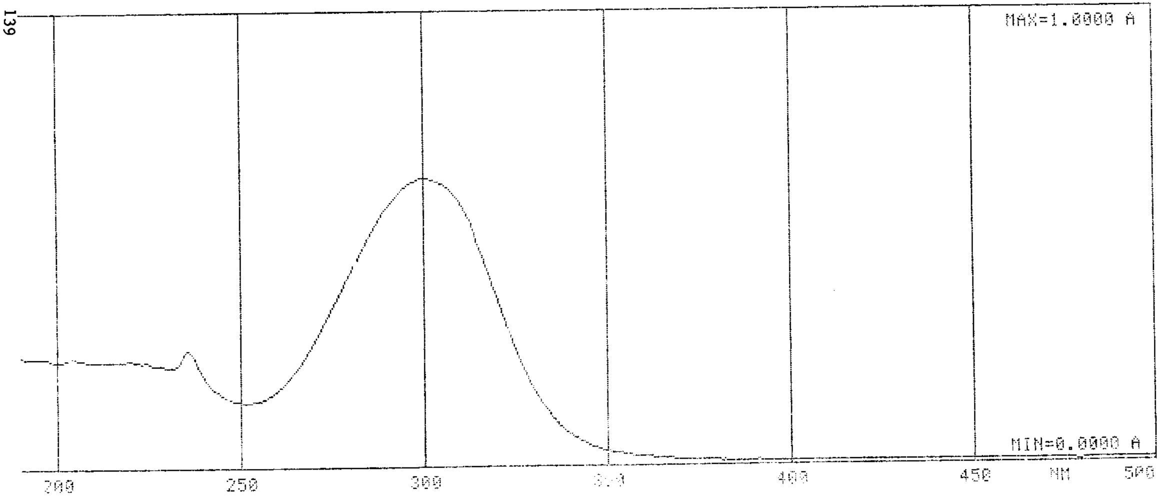

SPECTRA C4: UV-VIS SPECTRA OF M-NITROCINNAMALDHEYDE

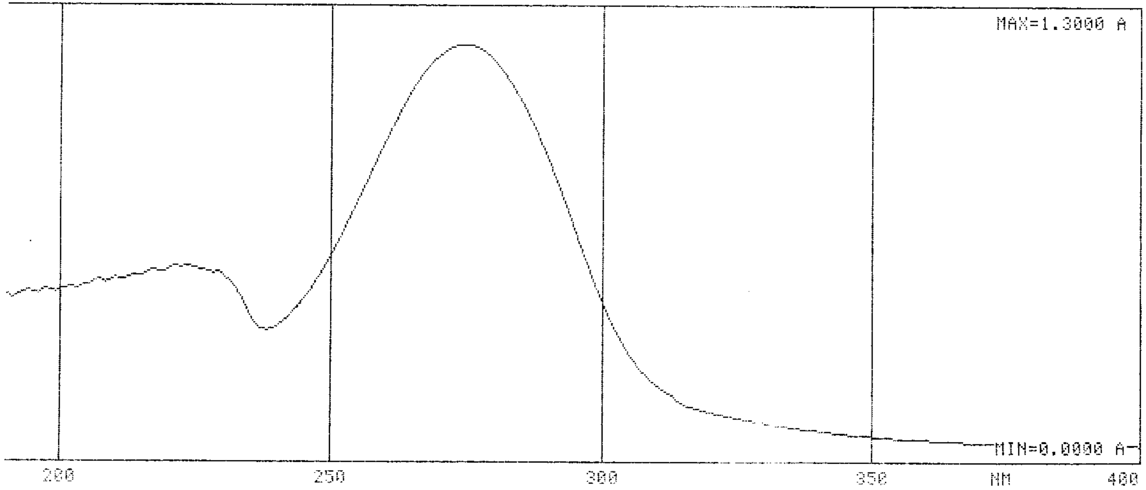

SPECTRA C5: UV-VIS SPECTRA OF P-NITROCINNAMALDHEYDE

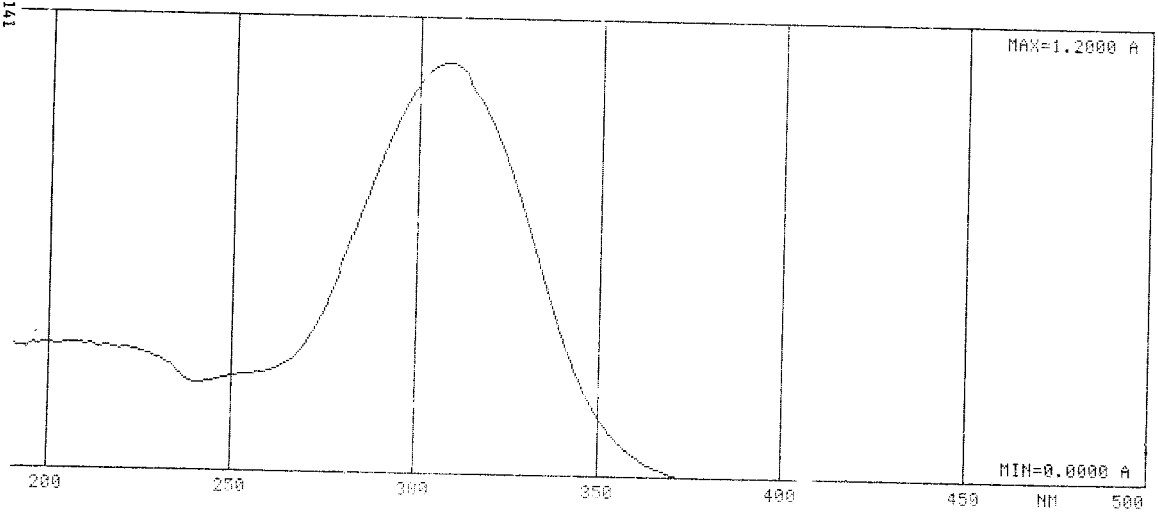

SPECTRA C6: UV-VIS SPECTRA OF P-METHOXYCINNAMALDHEYDE

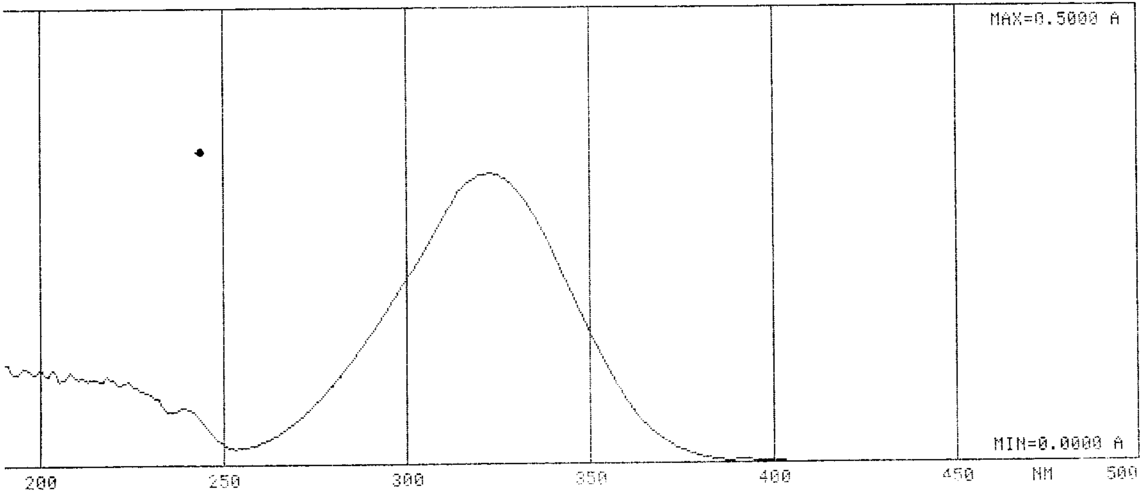

SPECTRA C7: UV-VIS SPECTRA OF M-BROMOCINNAMALDHEYDE

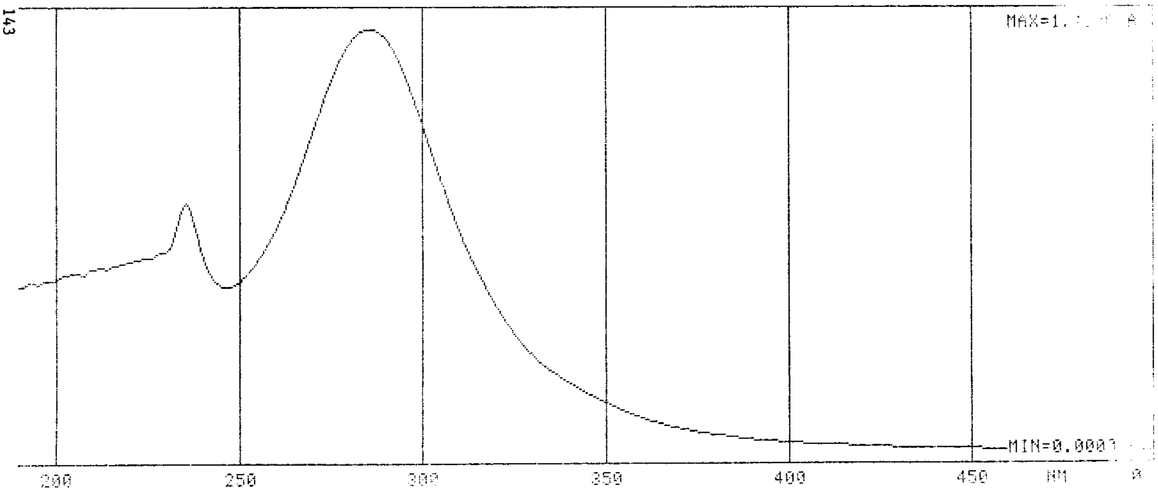

SPECTRA C8: UV-VIS SPECTRA OF P-METHYLCINNAMALDHEYDE

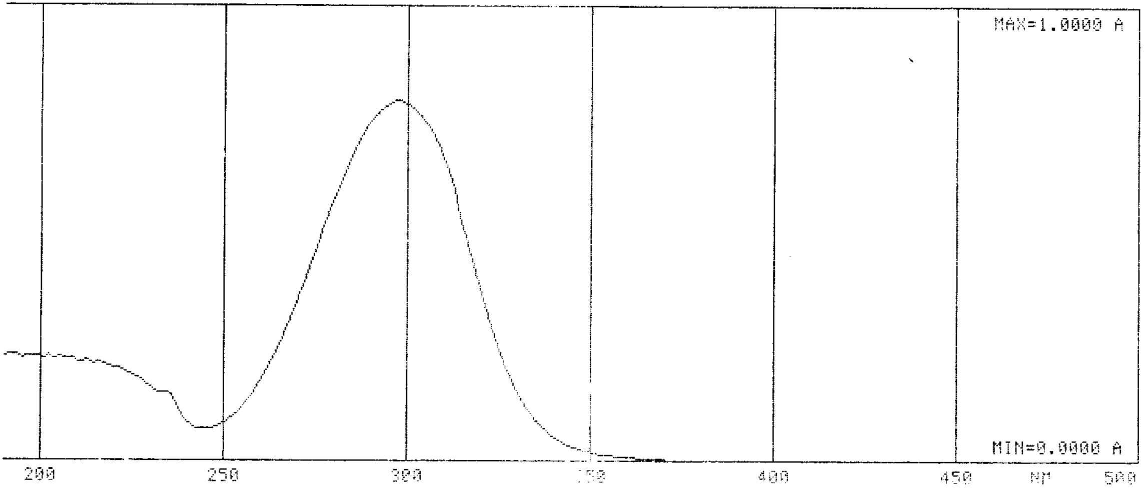

SPECTRA C9: UV-VIS SPECTRA OF P-CHLOROCINNAMALDHEYDE

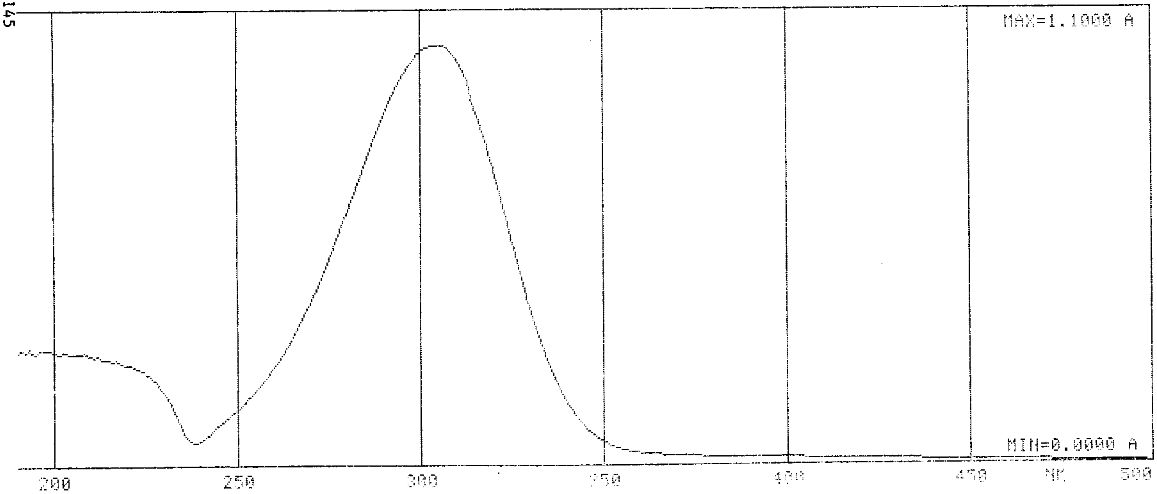

PREVIOUS DOCUMENTS IN POOR ORIGINAL CONDITION